

# Stratigraphy, paleontology, and depositional setting of the Late Eocene (Priabonian) lower Pagat Member, Tanjung Formation, in the Asem Asem Basin, South Kalimantan, Indonesia

John-Paul Zonneveld,<sup>1\*</sup> Nabilah Adani,<sup>2</sup> Aswan,<sup>2</sup> Jonathan I. Bloch,<sup>3</sup> Antonino Briguglio,<sup>4</sup> Russell L. Ciochon,<sup>5</sup> Laura J. Cotton,<sup>6</sup> Agus T. Hascaryo,<sup>2</sup> Jason Head,<sup>7</sup> Javier Luque,<sup>7</sup> Yan Rizal,<sup>2</sup> Nadia Santodomingo,<sup>8,9</sup> Thierry Smith,<sup>10</sup> Jonathan Todd,<sup>8</sup> Peter Wilf,<sup>11</sup> and Yahdi Zaim<sup>2,12</sup>

<sup>1</sup>Department of Earth and Atmospheric Sciences, University of Alberta, Edmonton, Alberta, Canada, <[zonnevel@ualberta.ca](mailto:zonnevel@ualberta.ca)>

<sup>2</sup>Faculty of Earth Science and Technology, Bandung Institute of Technology, Indonesia, <[Nadani2@slb.com](mailto:Nadani2@slb.com)>, <[aswan@itb.ac.id](mailto:aswan@itb.ac.id)>, <[agusgeoar@yahoo.com](mailto:agusgeoar@yahoo.com)>, <[yan@gl.itb.ac.id](mailto:yan@gl.itb.ac.id)>, <[zaim@office.itb.ac.id](mailto:zaim@office.itb.ac.id)>

<sup>3</sup>Florida Museum of Natural History, University of Florida, Gainesville, Florida, USA, <[jbloch@flmnh.ufl.edu](mailto:jbloch@flmnh.ufl.edu)>

<sup>4</sup>Dipartimento di Scienze della Terra, dell'Ambiente e della Vita Università degli Studi di Genova Corso Europa, 26 - 16132 Genova, Italy, <[antonino.briguglio@unige.it](mailto:antonino.briguglio@unige.it)>

<sup>5</sup>Department of Anthropology, University of Iowa, Iowa City, Iowa, USA, <[russell-ciochon@uiowa.edu](mailto:russell-ciochon@uiowa.edu)>

<sup>6</sup>Natural History Museum of Denmark, Øster Voldgade 5, 7, 1350 København K, Denmark, <[laura.cotton@snm.ku.dk](mailto:laura.cotton@snm.ku.dk)>

<sup>7</sup>Department of Zoology and University Museum of Zoology, University of Cambridge, Cambridge, United Kingdom, <[jjh71@cam.ac.uk](mailto:jjh71@cam.ac.uk)>, <[jl2351@cam.ac.uk](mailto:jl2351@cam.ac.uk)>

<sup>8</sup>Natural History Museum, London, United Kingdom, <[n.santodomingo@nhm.ac.uk](mailto:n.santodomingo@nhm.ac.uk)>, <[j.todd@nhm.ac.uk](mailto:j.todd@nhm.ac.uk)>

<sup>9</sup>Institute of Earth Sciences (ISTE), University of Lausanne, Switzerland

<sup>10</sup>Royal Belgian Institute of Natural Sciences, Brussels, Belgium, <[tsmith@naturalsciences.be](mailto:tsmith@naturalsciences.be)>

<sup>11</sup>Department of Geosciences, Pennsylvania State University, University Park, Pennsylvania, USA, <[pwilf@psu.edu](mailto:pwilf@psu.edu)>

<sup>12</sup>Department of Geology, Institut Teknologi Sumatera - ITERA, Indonesia, <[jahdi.zaim@gl.itera.ac.id](mailto:jahdi.zaim@gl.itera.ac.id)>

**Non-technical Summary.**—The Eocene Pagat Member of the Tanjung Formation records the transition from marginal-marine to shallow-marine deposition on the southern coast of Indonesian Borneo. This unit contains a diverse tropical marine invertebrate assemblage that includes foraminifera, snails, bivalves, crabs, sea urchins, solitary corals, and bryozoans. These fossils occur in bioclast-rich limestone beds that were deposited in low-relief biostromes on a mud-dominated coast. A diverse trace-fossil assemblage indicates the occurrence of many other invertebrates, including sponges, worms, and other marine arthropods that were not preserved as body fossils. This diverse biota suggests that the Central Indo-Pacific marine biodiversity hotspot may have originated as early as the late Eocene (about 34 million years ago).

**Abstract.**—Marine sedimentary rocks of the late Eocene Pagat Member of the Tanjung Formation in the Asem Asem Basin near Satui, Kalimantan, provide an important geological archive for understanding the paleontological evolution of southern Kalimantan (Indonesian Borneo) in the interval leading up to the development of the Central Indo-Pacific marine biodiversity hotspot. In this paper, we describe a moderately diverse assemblage of marine invertebrates within a sedimentological and stratigraphical context. In the studied section, the Pagat Member of the Tanjung Formation records an interval of overall marine transgression and chronicles a transition from the marginal marine and continental siliciclastic succession in the underlying Tambak Member to the carbonate platform succession in the overlying Berau Formation.

The lower part of the Pagat Member contains heterolithic interbedded siliciclastic sandstone and glauconitic shale, with thin bioclastic floatstone and bioclastic rudstone beds. This segues into a calcareous shale succession with common foraminiferal packstone/rudstone lenses interpreted as low-relief biostromes. A diverse trace fossil assemblage occurs primarily in a muddy/glauconitic sandstone, sandy mudstone, and bioclastic packstone/rudstone succession, constraining the depositional setting to a mid-ramp/mid to distal continental shelf setting below fair-weather wave base but above storm wave base.

Each biostrome rests upon a storm-generated ravinement surface characterized by a low-diversity *Glossifungites* or *Trypanites* trace fossil assemblage. The erosional surfaces were colonized by organisms that preferred stable substrates, including larger benthic foraminifera, solitary corals, oysters, and serpulid annelid worms.

The biostromes comprised islands of high marine biodiversity on the mud-dominated Pagat coastline. Together, the biostromes analyzed in this study contained 13 genera of symbiont-bearing larger benthic foraminifera, ~40 mollusk taxa, at least 5 brachyuran decapod genera, and 6 coral genera (*Anthemiphyllia*, *Balanophyllia*, *Caryophyllia*, *Cycloseris*,

\*Corresponding author

*Trachyphyllia*, and *Trochocyathus*), as well as a variety of bryozoans, serpulids, echinoids, and asterozoans. High foraminiferal and molluscan diversity, coupled with modest coral diversity, supports the hypothesis that the origin of the diverse tropical invertebrate faunas that characterize the modern Indo-Australian region may have occurred in the latest Eocene/earliest Oligocene.

## Introduction

The well-described Neogene marine successions in Island Southeast Asia are characterized by diverse invertebrate fossil assemblages (e.g., Wilson et al., 1999; Satyana, 2002; Wilson and Lokier, 2002; Johnson et al., 2014, 2015a, b; Kusworo et al., 2015; Marshall et al., 2015; Renema et al., 2015; Rosler et al., 2015; Santodomingo et al., 2015a, b; Wilson, 2015). In comparison, few publications discussing Paleogene marine strata in this area are available, despite the importance of this interval in the evolution of tropical marine invertebrate faunas, particularly corals and coral reefs (Adams, 1965; Wilson and Rosen, 1998; Renema, 2007; Cotton et al., 2014; Mihaljević et al., 2014, 2017; Johnson et al., 2015a, b; Kessler and Jong, 2017). Following the middle Eocene inundation of the Sunda Shelf (Lutetian, ca. 45 mya), marine successions became widespread in Sulawesi and Borneo (Kalimantan and Sarawak); however, late middle and late Eocene strata are poorly fossiliferous or difficult to access in most of these sections (Adams, 1965; Renema et al., 2002).

Latest Eocene (Priabonian) strata are prevalent in the Asem Asem Basin on the southern coast of Kalimantan on the island of Borneo; however, these strata are very poorly exposed due to low topography and dense vegetation. Within the Satui area (Fig. 1), the large opencast Wahana Baratama coal mine provides exposure of the Eocene to early Oligocene Tanjung Formation (Fig. 2). The uppermost part of this formation (Pagat Member) consists of a thick succession of gray calcareous shale with subordinate glauconitic, bioclastic rudstone and bioclastic floatstone and minor glauconitic sandstone.

The Pagat Member in the Satui area is very fossiliferous, including abundant gastropods, bivalves, echinoids, bryozoans, scleractinian corals, foraminiferans, and crustaceans. This assemblage is one of the most diverse Paleogene marine fossil assemblages yet reported from Island Southeast Asia (e.g., Wilson and Rosen, 1998). The present contribution provides an assessment of the age, stratigraphic architecture, and depositional environments of the Pagat Member, Tanjung Formation, in the Satui area of South Kalimantan in order to provide a framework for subsequent paleontological analyses.

## Geological setting

**Structural setting.**—Eocene to early Oligocene strata of the Tanjung Formation occur, at present, in the Barito and Asem Asem basins in South Kalimantan, Indonesia (Kusuma and Darin, 1989; Panggabean, 1991; Satyana and Silitonga, 1994; Sapiie et al., 2011; Witts et al., 2012a, b; 2014). The study area is within the Asem Asem Basin on the Java Sea coast of South Kalimantan (Fig. 1). The Asem Asem Basin is separated from the much larger Barito Basin by bands of ophiolitic and metamorphic rocks that record a mid-Cretaceous collision and

terrane accretion along the eastern margin of Sundaland (Sikumbang, 1986; Wakita et al., 1998; Wakita, 2000; Witts et al., 2012a, b, 2014).

The similarity of sedimentary strata among the Barito, Asem Asem, and Kutai basins indicates that, during the Eocene, the three basins formed a single depocenter (van Bemmelen, 1949; van de Weerd and Armin, 1992; Witts et al., 2012a, b), referred to as the proto-Barito Basin (sensu Witts et al., 2012a, b). The Kutai Basin separated from the Barito and Asem Asem basins in the early Oligocene due to movement on the Paternoster fault system (Moss and Chambers, 1999; Satyana and Armandita, 2008; Witts et al., 2012a, b, 2014). The Asem Asem and Barito basins remained a single depocenter until uplift of the Meratus complex separated them during the Late Miocene (Satyana and Armandita, 2008; Witts et al., 2012a, b, 2014).

The Asem Asem Basin includes a thin, onshore western margin on the southeastern edge of the Meratus Range and a much larger subsea portion under the northern Java Sea, northwest of Pulau Laut Ridge (Kusuma and Darin, 1989; Panggabean, 1991; Sapiie et al., 2011; Werdaya et al., 2013). The present study area is in the northwestern, onshore portion of the Asem Asem Basin in exposures created during mining of the lower Tanjung Formation coal resources (Fig. 1).

**Stratigraphic setting.**—The Eocene to earliest Oligocene Tanjung Formation consists of a thick succession of primarily siliciclastic strata (Witts et al., 2012b, 2014). The basal two-thirds of the Tanjung Formation record the earliest siliciclastic input into the basin and are represented by comparably coarse-grained strata of the Eocene Mankook and Tambak members (Fig. 2). These units reflect a transition from alluvial fan and braided fluvial deposition to meandering fluvial channel, broad interfluvial, and coastal lagoon/marsh (Witts et al., 2012b). At Wahana, the Mankook Member is not exposed. The base of the exposure in the study area occurs in heterolithic claystone, siltstone, fine- to very fine-grained sandstone, and coal of the late Eocene lower Tambak Member (Zonneveld et al., 2024). The Tambak is an overall fining-upwards succession, with thicker and more abundant sandstone and coal beds towards its base (Zonneveld et al., 2024). The upper Tambak Member is dominated by claystone and siltstone intercalated with thin coal horizons and contains significant plant fossils (Spagnuolo et al., 2024; Zonneveld et al., 2024).

Conformably overlying the Tambak Member sits a mixed siliciclastic–carbonate succession consisting of calcareous shale with interbeds of muddy glauconitic sandstone and sandy bioclastic rudstone to grainstone assigned to the Pagat Member (Fig. 2). The Pagat Member straddles the Eocene–Oligocene boundary (Fig. 2). In most areas, the Tanjung Formation records an overall deepening upwards (transgressive) succession with basal alluvial fan and braided fluvial deposits of the Mankook Member segueing upwards into meandering fluvial and

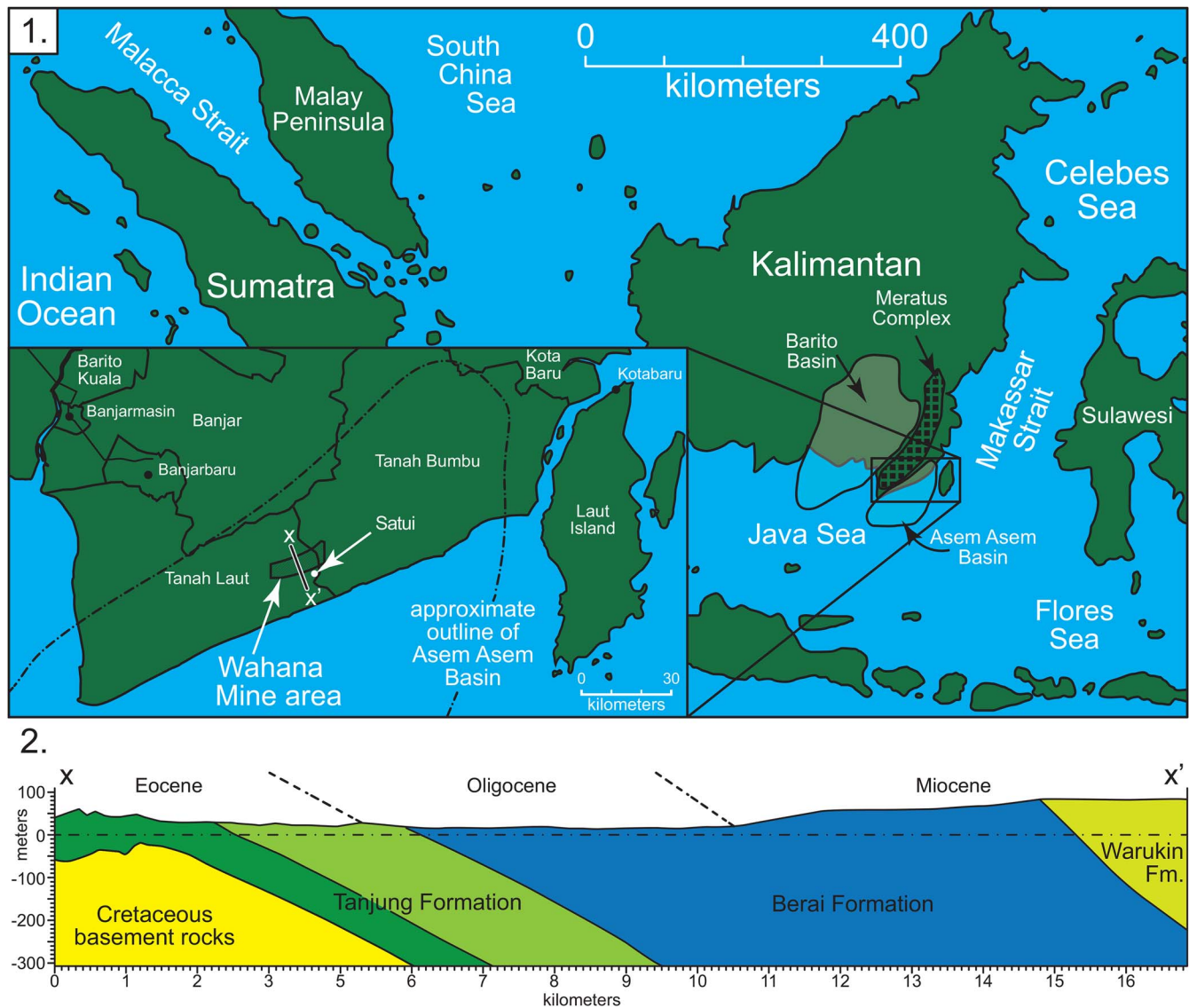


**Figure 1.** The Asem Asem Basin, Kalimantan, Indonesia. (1) Location of the Asem Asem Basin on the southern margin of the Meratus uplift complex, southern coast of Kalimantan, Indonesia. Inset map shows the location of the Hanuman Superpit coal mine on the boundary between the Tanah Laut and Tanah Bumbu provinces. (2) Cross-section through the northern part of the Asem Asem Basin, from the Meratus complex to the north to the Java Sea coast. The Pagat Member is shown in light green.

estuarine deposits of the Tambak Member and finally into shallow marine coastal deposits (shoreface, shelf, deltaic, and foraminiferal ramp) of the Pagat Member (Kusuma and Darin, 1989; Satyana, 1995; Moss and Chambers, 1999; Witts et al., 2012b, 2014; this study). The Pagat Member of the Tanjung Formation is overlain by the Berai Formation in the Asem Asem Basin (Fig. 2). The Berai limestone has been dated as late Oligocene using planktonic foraminifera and is dominated by calcareous shale and bioclastic rudstone to grainstone (Moss and Chambers, 1999; Saller and Vijaya, 2002; Hidayat et al., 2012; Werdaya et al., 2013).

The Tanjung and Berai formations generally are poorly exposed in the Asem Asem Basin due to extensive vegetation and agriculture. Outcrops of the Tanjung Formation are best exposed in rare coastal exposures on and near Laut Island and in coal mines that occur on several linear trends on the margins

of the Asem Asem and Barito basins. The Berai Formation is best known from limited outcrops and from offshore petroleum exploration wells in the northern Java Sea (e.g., Satyana, 2002).

## Materials and methods

This study focuses on outcrop exposures of the Pagat Member of the Tanjung Formation associated with the Wahana Baratama Mining operation near the village of Satui, Kabupaten Tanah Bumbu, Kalimantan Selatan, Indonesia (Fig. 1). This quarry exposes a thick succession through much of the Tambak and Pagat members of the Tanjung Formation (Figs. 1, 2). We sampled and described the Tambak and lower Pagat members in August 2014, with particular attention paid to fossiliferous intervals. In December 2019, we sampled and described the middle/upper Pagat Member (as high as was safely accessible

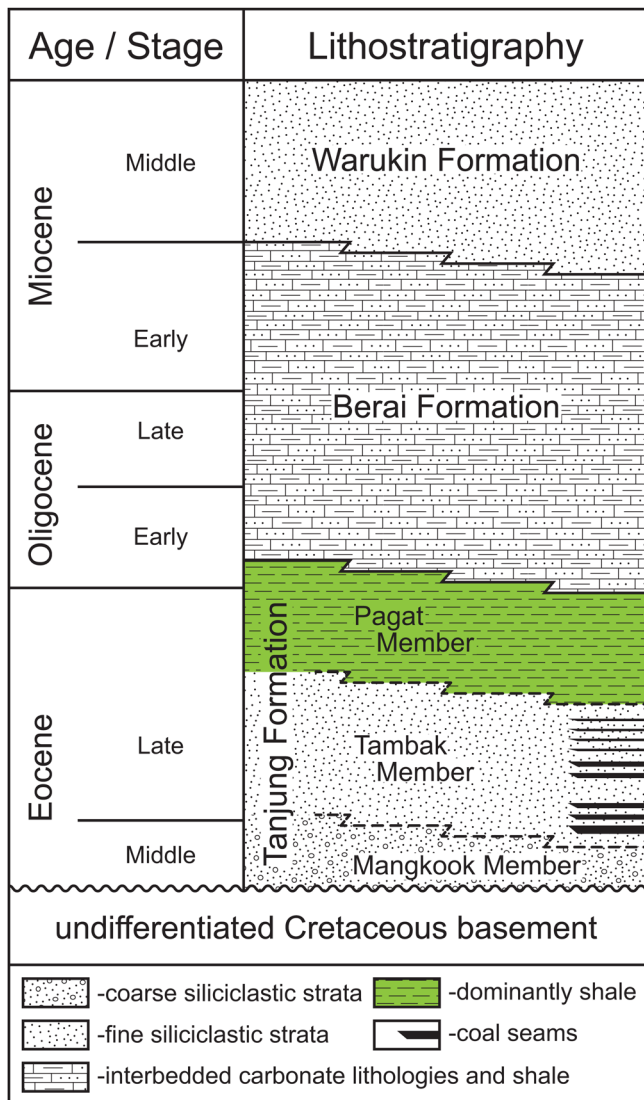


**Figure 2.** Paleogene and Neogene stratigraphy, southern Kalimantan, Indonesia. Only the Tambak and Pagat members crop out in the study area.

at the time). The present contribution focuses solely on the Pagat Member. The zero datum of the measured section included herein occurs on an inferred marine flooding surface that approximates the contact of the Tambak and Pagat members.

Exposures were logged, sampled, and photographed. Depositional units and lithofacies were described in detail (Fig. 3) and samples obtained for petrographic and biostratigraphic analyses. Physical structures and biogenic structures were noted, and bed- and unit-bounding surfaces were described. Trace fossils were examined in both horizontal and vertical aspects to ensure accurate identification.

The occurrence, position, and orientation of fossils were recorded and photographed in the field. Census samples were obtained from fossiliferous beds to aid in paleontological analyses. Fossil collections were made primarily from six main fossiliferous bioclastic rudstone beds/bedsets (15.7–17.65 m; 71.4–71.9 m; 80.0–80.35 m; 87.8–88.1 m; 93.3–93.6 m, 97.2–97.6 m; Fig. 3). Fossils were photographed using an Olympus OM-D E-M1 Mark II digital camera with 20.4

megapixel resolution using either an Olympus 12–40 mm zoom lens or an Olympus 60 mm macro lens. The built-in bracketed focus-stacking option was used to ensure that the entire surface of 3-dimensional fossils was in focus. Each image consists of nine stacked images, which were automatically amalgamated by onboard software into a single image in real time. Direct, low- to moderate-angle incident lighting, using 1150 Lux LED flood lamps set at ~0.5 meters, was used in all fossil photographs. Small fossils were imaged using a scanning electron microscope.

Twenty-five standard thin sections, obtained from 12 floatstone and rudstone beds throughout the study interval, were analyzed, described, and used to assess the presence, abundance, and taxonomy of larger benthic foraminifera in the samples. Each thin-section was point-counted, and all included fossil material was identified. Photographs were obtained to aid in taxonomic identification.

*Repository and institutional abbreviation.*—All fossils, lithological samples, and thin-sections are housed in the paleontology collection of the Department of Earth and Atmospheric Sciences at the University of Alberta (UA-P).

## Results

*Larger foraminifera biostratigraphy.*—The study interval is characterized by numerous muddy glauconitic sandstone and bioclastic floatstone to rudstone beds (Figs. 4–7). Of the 12 floatstone and rudstone beds analyzed, 10 contained identifiable larger benthic foraminifera (LBF; Fig. 4–6, Table 1). The lowermost two beds sampled (samples 14-1 and 14-2) produced no identifiable foraminiferal taxa. The next eight beds above these (14-3 to 14-6 and 19-2A–D) were each characterized by 4–12 taxa. The uppermost two beds (19-2A and 19-2B) produced the highest generic richness. The assemblage remains relatively consistent throughout the section. Thirteen genera were identified, with nummulitids and orthophragmines dominating the assemblage, alongside pellatispirids and, frequently, small miliolids. Identifications have been kept largely generic because the petrological thin sections produced only randomly oriented cuts of LBF and, therefore, did not allow for detailed measurement of species-level characters. Nonetheless, some stratigraphic range control is possible. We used the East Indian letter classification, the regional scheme for the Indo-West Pacific, following Adams (1970), with updates by Lunt (2003) and Lunt and Luan (2022), with comparison to the Tethyan Shallow Benthic Zones of Serra Kiel et al. (1998).

The first biostratigraphic constraint is provided by the occurrence of members of the orthophragminid group (e.g., *Discocyclina* and *Asterocyclina*), which are found at approximately 31.5–87.5 m in the section (Figs. 4, 5). Within the Indo-Pacific, both have a range from the late Paleocene to their global extinction at the Eocene/Oligocene boundary (Ta1 to Tb; Cotton and Pearson, 2011; Lunt and Luan, 2022; Molina et al., 2016). *Nummulites*, *Palaeonnummulites*, *Heterostegina*, and *Operculina* are also long-ranging genera—from Paleocene to Oligocene in the case of *Nummulites* and all the way to the present day for the latter three genera. However, true reticulate *Nummulites* only occur

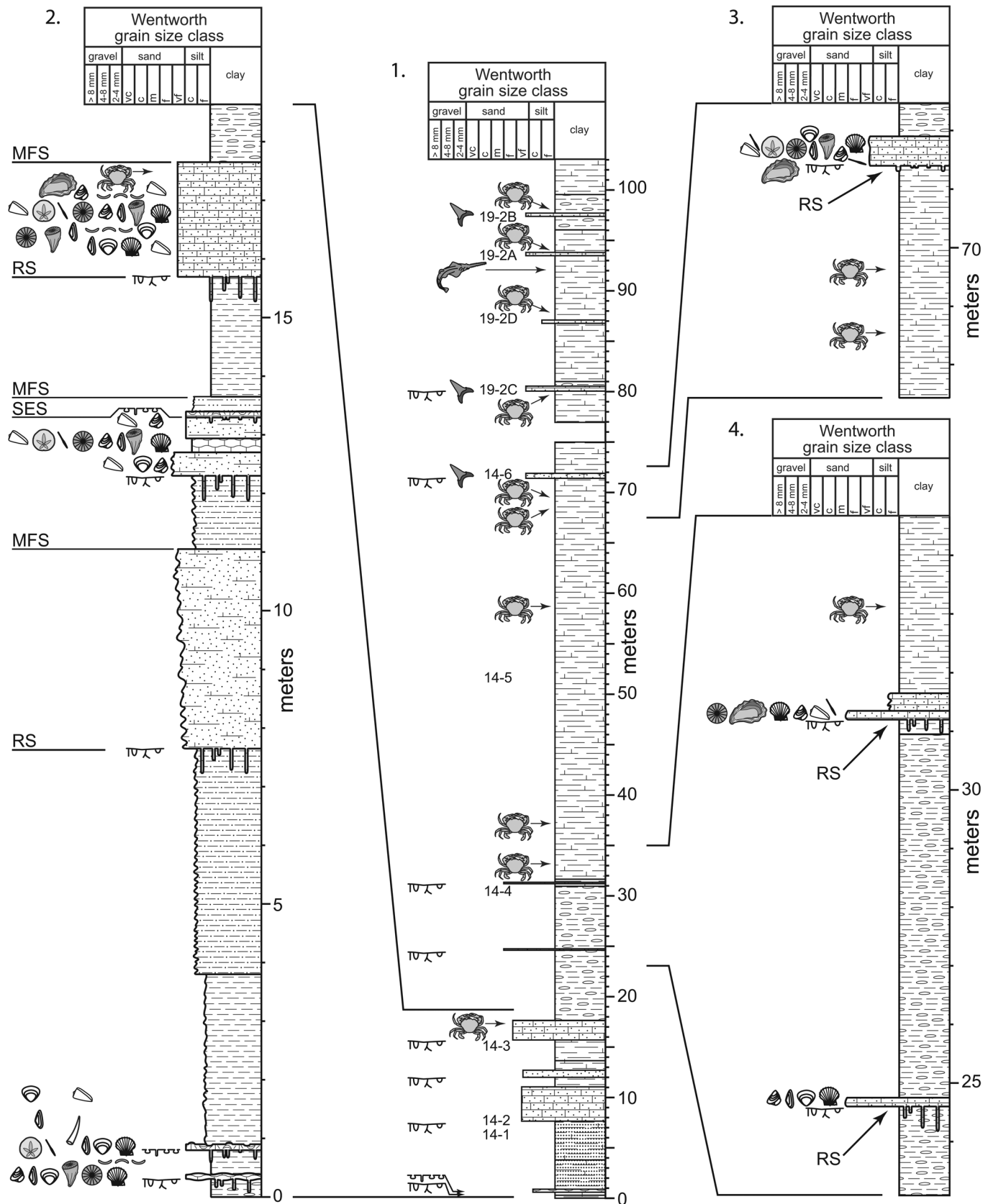


**Figure 3.** Vertical distribution of lithofacies in the study interval. (1) The study interval begins at the base of the Pagat Member and includes all safely accessible exposures of the Pagat Member in the Hanuman Superpit coal mine. (2) Detail of the basal 18.5 meters of the study interval. (3) Detail of the 67.5–62.5 m interval. (4) Detail of the 23–32.5 meter interval. Key for symbols and lithology patterns provided in Figure 10. MFS = marine flooding surface; SES = subaerial exposure surface; RS = ravinement surface.

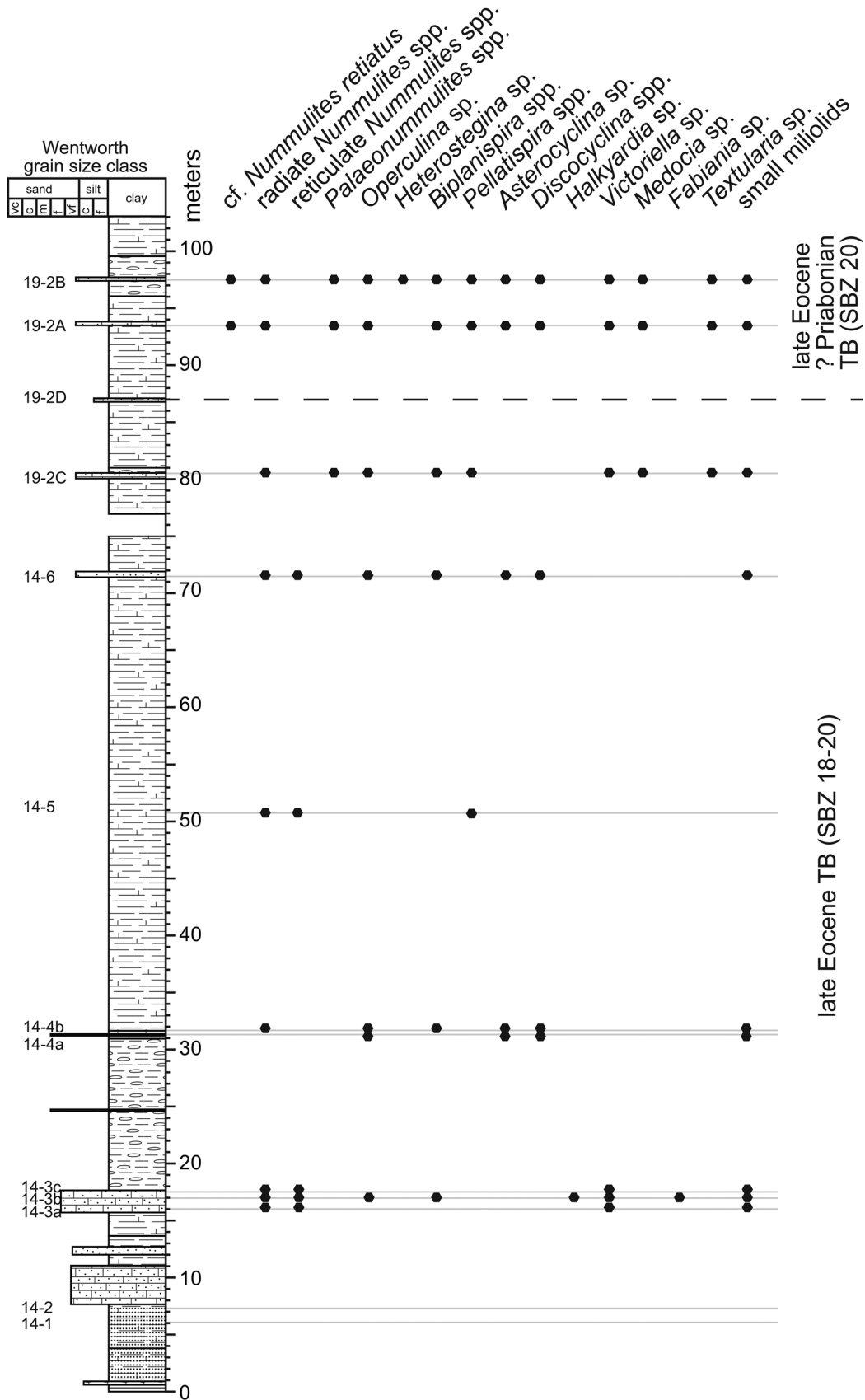


**Figure 4.** Vertical distribution of foraminifera in the study interval. Most of the Pagat Member accessed in the study interval was deposited during the late Eocene planktonic foraminiferal zones P15b, with the uppermost beds reflecting deposition during the latest Eocene planktonic foraminiferal zones P16–P17. Lithology patterns identified in Figure 10.

**Table 1.** Foraminifera identified from the Pagat Member, Tanjung Formation in the Asem Asem Basin, near Satui.

Foraminifera	
Class Globthalamia	
Subclass Rotalia	
Order Rotaliida	
Family Nummulitidae	
	<i>Heterostegina</i> sp.
	<i>Nummulites retius</i>
	Reticulate <i>Nummulites</i>
	Radiate <i>Nummulites</i> spp.
	<i>Palaeonummulites</i> spp.
	<i>Operculina</i> sp.
	<i>Halykardia</i> sp.
Family Pellatispiridae	
	<i>Biplanospira</i> spp.
	<i>Pellatispira</i> spp.
Family Asterocyclinidae	
	<i>Asterocyclina</i> sp.
Family Discocyclinidae	
	<i>Discocyclina</i> spp.
Family Victoriellidae	
	<i>Victoriella</i> sp.
Family Rotaliidae	
	<i>Medocia</i> sp.
Family Cymbaloporidae	
	<i>Fabiania</i> sp.
Order Textulariida	
Family Textulariidae	
	<i>Textularia</i> sp.
Class Tubothalamia	
Order Miliolida	
	miliolid spp.

from mid-Tb to Te (SBZ19–22; Lunt, 2003; Lunt and Luan, 2022). Several of the *Nummulites* Lamarck, 1801, are tentatively assigned to *N. retius* Roveda, 1959, which points toward a late Eocene, Priabonian age. One reticulate *Nummulites* was found in the succession at 51 m (level 14-5; Fig. 3), indicating a late Eocene age. This specimen shows clear reticulation in a sub-axial section, but the proloculus is not visible, therefore no species-level identification can be made. *Halykardia* also was identified in a single horizon at 17 m, indicating mid Ta3 (ca. SBZ 14) to Te1 (mid SBZ 22), middle Eocene to early late Oligocene. *Fabiania* was also found only within the 17-m bed and ranges from mid-middle Eocene (mid Ta3; SBZ 14) to the Eocene/Oligocene boundary (top of Tb; SBZ 20). The pellatispirid genera *Biplanospira* and *Pellatispira* occur in six and four of the twelve levels, respectively, particularly toward the upper part of the section (Fig. 5). *Pellatispira* has a first regional occurrence in the Indo-West Pacific within the uppermost middle Eocene (Ta3; SBZ 17), while *Biplanospira* first occurs within the late Eocene (Tb; SBZ 18). Both have a last occurrence at the Eocene/Oligocene boundary.

The overall assemblage, particularly the presence of pellatispirids, supports an overall late Eocene Tb age (SBZ 18–20), with *N. retius* indicating a likely Priabonian age, definitely prior to the Eocene/Oligocene boundary. The absence of typical Ta taxa, including *Alveolina*, *Assilina*, *Linderina*, and *Orbitolites*, which go extinct at the Ta/Tb boundary, additionally lends support to this interpretation.

**Lithofacies.**—The Pagat Member in the Satui area consists of laminated and nodular calcareous shale, glauconitic siliciclastic sandstone, muddy/silty sandstone, bioclastic floatstone, and bioclastic rudstone/grainstone (Table 2).

Proportionately, the Pagat Member is dominated by laminated to massive gray calcareous shale (Figs. 7–9). Interbeds of nodular calcareous mudstone as well as common thin (mm- to cm-scale) and rare thick (dm- to m-scale) interbeds of bioclastic rudstone also occur (Figs. 3 and 7). Thin-section analyses indicate that the Pagat Member comprises a true mixed siliciclastic–carbonate succession (Fig. 10). Many beds, particularly near the base of the Pagat Member, contain glauconite as well as abundant detrital quartz grains (Fig. 10). Beds containing appreciable proportions of quartz and chert grains are most common in the basal 20 m of the study interval but occur higher up as well (Fig. 10).

In the basalmost 17 m of the study interval, glauconitic siliciclastic sandstone, silty sandstone, and sandy bioclastic rudstone beds occur interstratified with glauconitic calcareous shale (Figs. 3, 8, and 9). These beds are characterized by high degrees of bioturbation. Siliciclastic sandstone beds are limited to this basal interval (i.e., are absent higher in the section). Bioclastic floatstone, coarser-grained rudstone, and grainstone dominated by foraminifera also are more common lower in the section but do occur as beds and lenses in the upper part of the study interval as well (Fig. 11). Rudstone/sandstone to shale ratios range from between 1:1 and 1:4 in the basal part of the study interval to 1:75 in the upper three-quarters of the upper part (Fig. 3). Glauconite is most common in heterolithic silty shale and muddy sandstone successions in the basal half of the study interval, but also occurs in some of the bioclastic rudstone beds, particularly lower in the section (Fig. 10). In heterolithic calcareous silty shale and muddy sandstone units, glauconite occurs primarily as minute (0.1–0.75 mm) ovoid pellets or peloids. In bioclastic rudstone beds, the glauconite occurs in the form of both pellets/peloids and as biomoldic void-fill.

Laminated shale-dominated intervals are characterized by thick intervals dominated by fissile planar laminae with several thin (decimeter-scale) massive (unbedded) horizons and several minor, convolute-bedded horizons (Table 2, Figs. 3 and 7). Shale-dominated intervals become increasingly calcareous towards the top of the study interval but have a significant argillaceous component throughout.

Invertebrate macrofossils are rare in shale-dominated intervals and consist primarily of scattered gastropods, bivalves, foraminifera, and articulated arthropods (crabs). Nodular shale successions have numerous horizontal, dendritic networks of siderite concretions/nodules, commonly containing crabs and other fossils (Fig. 8.2). The nodular mudstone facies invariably occurs laterally and vertically adjacent to foraminiferal grainstone/rudstone beds.

Coarser-grained intervals (sandstone and packstone/grainstone/rudstone intervals) are most common lower in the study interval but occur throughout. These include numerous normally graded beds, commonly characterized by sharp bases and asymmetrical (current) ripples (Table 2). Small-scale (decimeter-scale) convolute beds were observed in several horizons. Several of the upper rudstone/grainstone beds exhibited broad hummocked internal surfaces and/or a cliniform morphology with moderately complex downlapping bed contacts (Fig. 7).

Foraminiferal grainstone/rudstone successions are a few centimeters up to over a meter in thickness and are typically

**Table 2.** Lithofacies characteristics, Pagat Member, Tanjung Formation in the Asem Asem Basin, near Satui.

Acronym	Lithofacies	Description	Biogenic Sedimentary Structures	Fossils Noted
<b>SHI</b>	Laminated calcareous shale	Planar-laminated calcareous shale and silty shale; glauconitic in lower Pagat; mm-scale silt horizons with low-relief asymmetrical ripples; bioturbation index 0–1	<i>Chondrites</i> , <i>Planolites</i> , <i>Schaubcylichnus</i>	Rare crabs, bivalves, gastropods; single pristinid rostrum
<b>SHnc</b>	Nodular calcareous shale	Planar-laminated calcareous shale with common rust-red ironstone (hematite) nodules/concretions; mm-to cm scale silt horizons with low-relief asymmetrical ripples; bioturbation index 1–2	<i>Chondrites</i> , <i>Macanopsis</i> , <i>Planolites</i> , <i>Psilonichnus</i> , <i>Schaubcylichnus</i> , <i>Thalassinoides</i> ,	Very common crabs, bivalves, gastropods; rare shark teeth
<b>SSm</b>	Muddy/silty sandstone	Planar laminae, wavy laminae, symmetrical ripples, asymmetrical ripples, bioturbation index 3–5	<i>Arenicolites</i> , <i>Asterosoma</i> , <i>Chondrites</i> , <i>Gyrolithes</i> , <i>Planolites</i> , <i>Palaeophycus</i> , <i>Phycosiphon</i> , <i>Rhizocorallium</i> , <i>Scalarituba</i> , <i>Scolicia</i> , <i>Skolithos</i> , <i>Schaubcylichnus</i> , <i>Teichichnus</i> , <i>Thalassinoides</i> , <i>fugichnia</i>	Rare, scattered gastropods and bivalves
<b>SSg</b>	Glauconitic sandstone	Wavy and hummocky cross-strata, symmetrical ripples, asymmetrical ripples; bioturbation index 3–5	<i>Lockeia</i> , <i>Macanopsis</i> , <i>Palaeophycus</i> , <i>Planolites</i> , <i>Psilonichnus</i> , <i>Rhizocorallium</i> , <i>Scolicia</i> , <i>Siphonichnus</i> , <i>Skolithos</i> , <i>Teichichnus</i> , <i>Thalassinoides</i> , <i>fugichnia</i>	Rare, scattered gastropods and bivalves; scattered foraminifera
<b>LSbw</b>	Bioclastic wackestone/floatstone	Massive in appearance; bioturbation index 0–1	<i>Gastrochaenolites</i> , <i>Rogerella</i> , <i>Trypanites</i>	Scattered foraminifera, bivalves, and gastropods; rare corals, rare bryozoans
<b>LSbpr</b>	Bioclastic packstone/rudstone	Wavy-bedded; onlapping, downlapping, and offlapping clinofolds; bioturbation index variable (1–5)	<i>Macanopsis</i> , <i>Palaeophycus</i> , <i>Planolites</i> , <i>Psilonichnus</i> , <i>Rhizocorallium</i> , <i>Scolicia</i> , <i>Skolithos</i> , <i>Thalassinoides</i> , <i>Gastrochaenolites</i> , <i>Rogerella</i> , <i>Trypanites</i>	Densely abundant foraminifera; very common gastropods, bivalves, bryozoans, corals, crabs, echinoid spines and plates; rare shark teeth
<b>LSmbl</b>	Mudstone/wackestone	Rounded carbonate mudstone and wackestone pebbles	<i>Gastrochaenolites</i> , <i>Rogerella</i> , <i>Trypanites</i>	none

laterally continuous on a scale of tens to hundreds of meters, often downlapping on other foraminiferal rudstone beds (Fig. 8) or interfingering with and pinching out laminated or nodular calcareous shale successions (Figs. 8.2, 8.3, and 9). Whole, unabraded, and articulated fossils, as well as disarticulated and fragmentary fossils, are common in the foraminiferal grainstone/rudstone facies. Bioclastic detritus in these units commonly occurs concordant to bedding, but in many cases, the detritus occurs in random orientations oblique to bedding as well. Although specific trace fossil taxa can be difficult to differentiate in the bioclastic rudstone/grainstone facies, localized disruptions in bioclast orientation are consistent with the passage of infaunal bioturbators. Most bivalves occur as paired, articulated valves, although isolated single valves also occur. Gastropods and articulated bivalves exhibit sediment infill that is both similar and dissimilar to the host matrix.

Trace fossils are diverse and abundant, particularly in sandy shale and sandy bioclastic rudstone/grainstone beds in the lower part of the study interval (Fig. 11). Many beds are thoroughly bioturbated (Figs. 11–14), commonly with physical structures completely obscured by infaunal activity.

Fossils are common and diverse, particularly in rudstone beds. Taxa identified include benthic and planktonic foraminifera, gastropods, bivalves, arthropods (brachyuran decapods), echinoids (cidaroids and spatangoids), corals, annelids (serpulids), bryozoans, and marine vertebrates (Figs. 3 and 7). The latter comprise several chondrichthyan teeth collected from bioclastic rudstone beds and a pristinid (sawfish) rostrum collected from laminated mudstone near the top of the study interval (Fig. 3).

*Trace fossil distribution.*—Trace fossil assemblages in the Pagat Member occur in all lithologies in the study interval (Fig. 11).

They are subdivided herein as follows: (1) soft-bottom assemblages that were emplaced in unlithified, uncompacted sediment regardless of grain size; (2) substrate-controlled assemblages that were emplaced in firm or hard substrates; and (3) traces on mobile substrates that were emplaced in firm or hard intraclasts and bioclasts.

Trace fossil assemblages in shale-dominated successions are of low diversity (*Chondrites*, *Planolites*, and *Schaubcylichnus*) and overall low population density compared with coarser-grained and heterolithic soft-bottom settings (Fig. 11). The siderite nodules in the nodular mudstone facies (Fig. 12.1) include what are interpreted to be three-dimensionally preserved burrow networks (*Psilonichnus* and *Thalassinoides*), which commonly contain brachyuran decapods (crabs) preserved in situ.

Soft-bottom trace fossil assemblages are much more prevalent in glauconitic sandstone and sandy bioclastic rudstone/grainstone units than in calcareous/argillaceous shale successions (Figs. 12–14). Most traces were observed in vertical aspect, although bedding plane assemblages also occur. Ichnotaxa observed include traces purportedly made by marine worms (*Arenicolites*, *Asterosoma*, *Chondrites*, *Gyrolithes*, *Palaeophycus*, *Planolites*, *Phycosiphon*, *Rhizocorallium*, *Scalarituba*, *Skolithos*, *Schaubcylichnus*, *Teichichnus*), bivalves (*Lockeia*, *Siphonichnus*), echinoids (*Scolicia*), and arthropods (*Palaeophycus*, *Psilonichnus*, *Rhizocorallium*, *Thalassinoides*) (Figs. 12–14, Table 3).

Substrate-controlled trace fossil assemblages occur at several horizons within the study interval (Figs. 11 and 14.1). These include firmground surfaces (*Glossifungites*-demarcated discontinuity surfaces) and hardground surfaces (*Trypanites*-demarcated discontinuity surfaces). The occurrence of a *Glossifungites*-demarcated discontinuity surface implies the

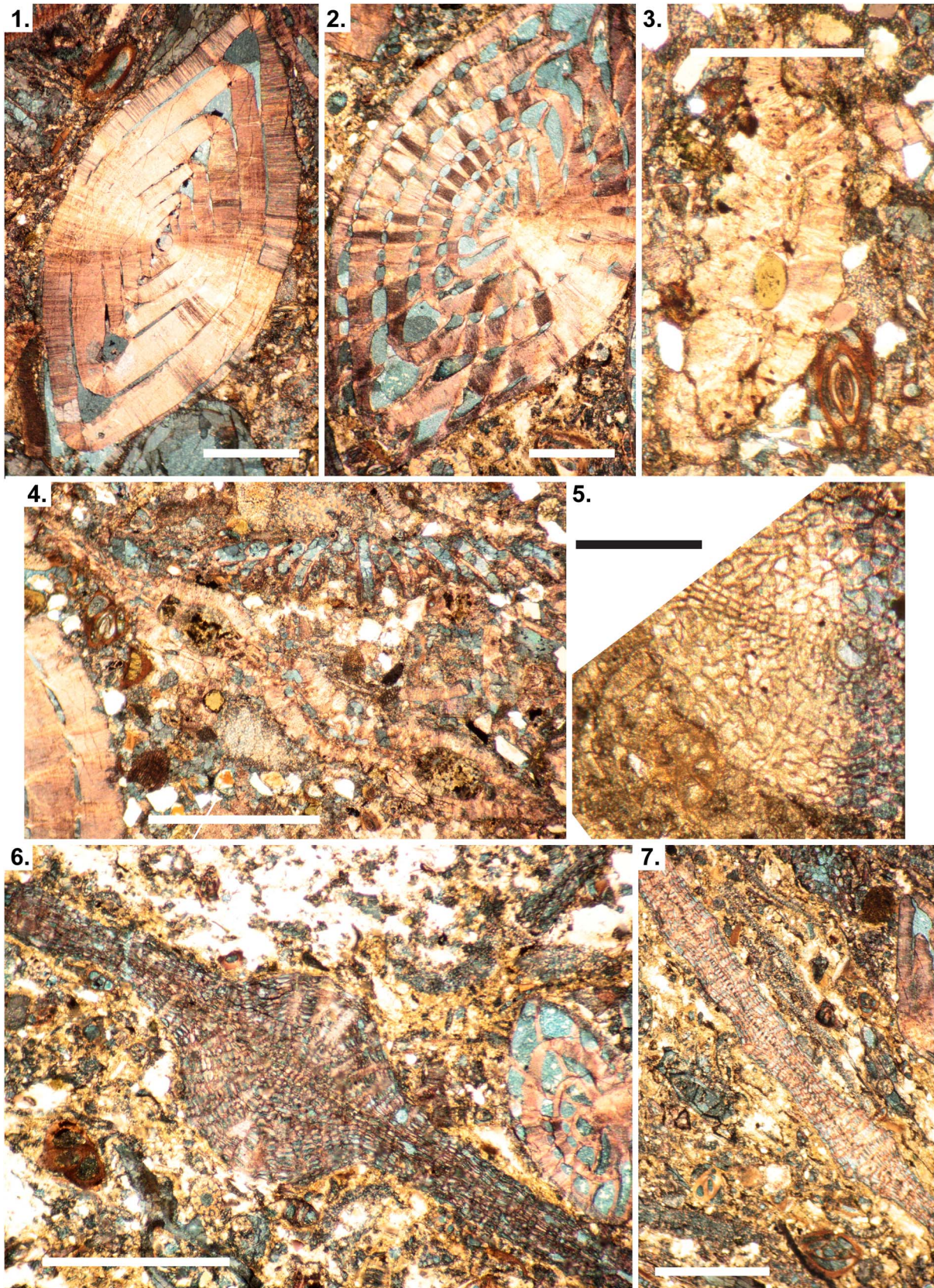


**Figure 5.** Foraminifera from the basal part of the study interval, Pagat Member, Tanjung Formation. Layers identified in Figure 4. All scale bars are 1 mm. (1) Radiate *Nummulites* – cf. *N. striatus* (Bruguière, 1792), sample SM-14-31.5, layer 14-4b; (2) reticulate *Nummulites*, sample SM-14-50.8, layer 14-5; (3) *Pellatispira* sp., sample SM-14-50.8, layer 14-5. (4) *Biplanispira* sp., sample SM-14-17.05, layer 14-3c. (5) *Discocyclina* sp. in oblique equatorial section, sample SM-14-31.5, layer 14-4b. (6) *Discocyclina* sp. in axial section, sample 71.5, layer 14-6. (7) *Discocyclina* sp., microspheric section, sample SM-14-31.5, layer 14-4b.

occurrence of either an omission surface or a horizon that was deposited, buried, and compacted (and thus made firm), subsequently exhumed, and finally tunneled into by organisms capable of penetrating firm but unlithified substrates (Seilacher 1964; Frey and Seilacher, 1980; Pemberton and Frey, 1984; MacEachern et al., 1992, 2012). *Trypanites*-demarcated discontinuity surfaces are formed when a substrate is lithified and the

tracemakers bore into a hard substrate (Pemberton et al., 1980, 1992; Taylor and Wilson, 2003; Zonneveld et al., 2012; Furlong et al., 2015, 2016; Schultz et al., 2016).

*Glossifungites*-demarcated discontinuity surfaces occur at the bases of thicker bioclastic rudstone and bioclastic sandstone beds in the study interval (0.30 m, 7.65 m, 12.70 m, 15.70 m, 24.60 m, 31.20 m, 71.40 m, 80 m; Figs. 11, 14.1, and 14.2).

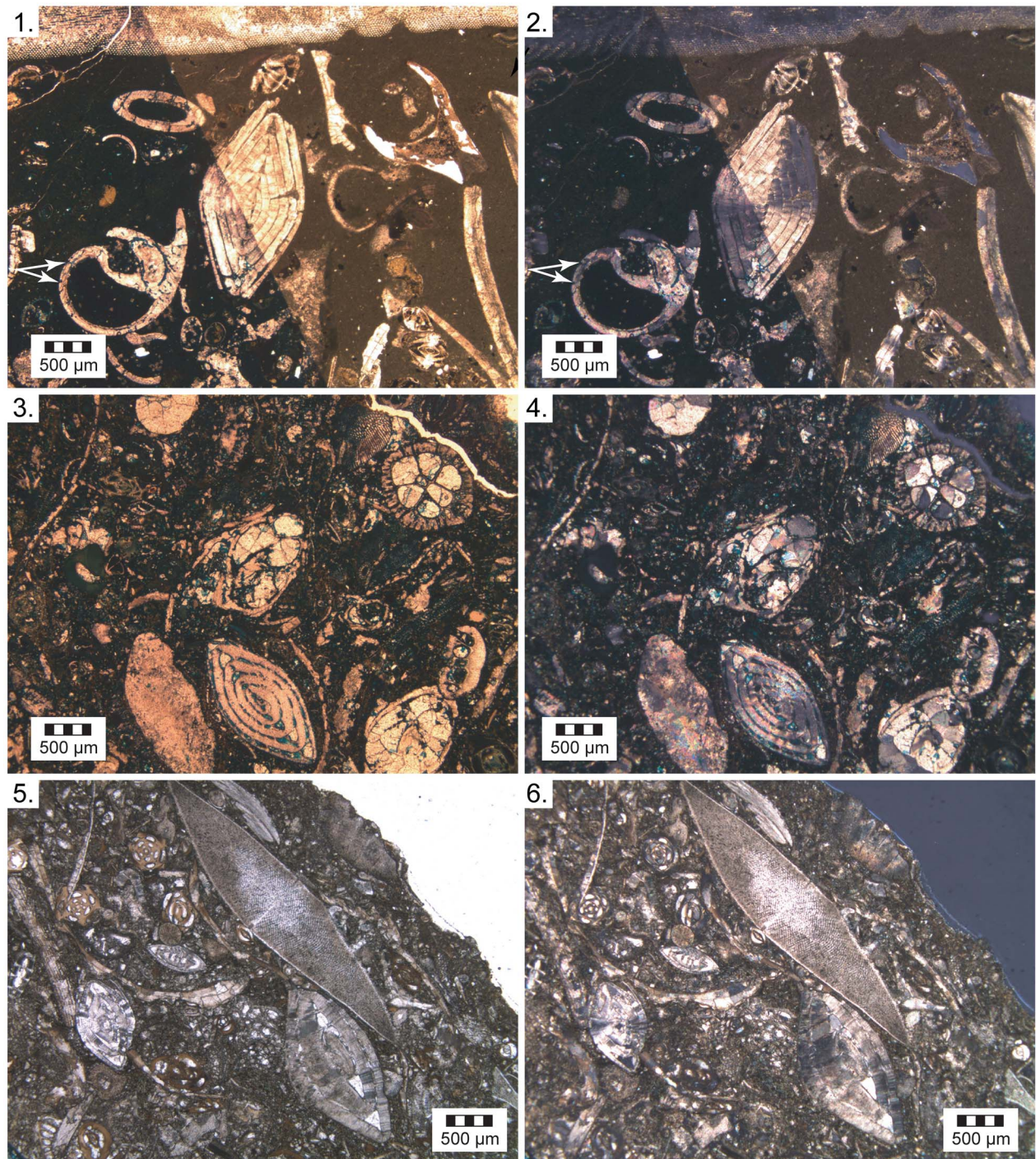


**Figure 6.** Thin-section micrographs illustrating foraminifera and other fossils from the upper part of the study interval, Pagat Member, Tanjung Formation. All thin-section micrographs shown in pairs with the image at the left in plane-polarized light and the image at the right in cross-polarized light. (1, 2) *Nummulites* sp. at center, with a gastropod to the left. Note the microborings in the gastropod wall (arrows), level 19-2C, 80.5 m. (3, 4) Bioclastic rudstone, level 19-2A, 93.5 m. (5, 6) Bioclastic rudstone, level 19-2B, 97.5 m.

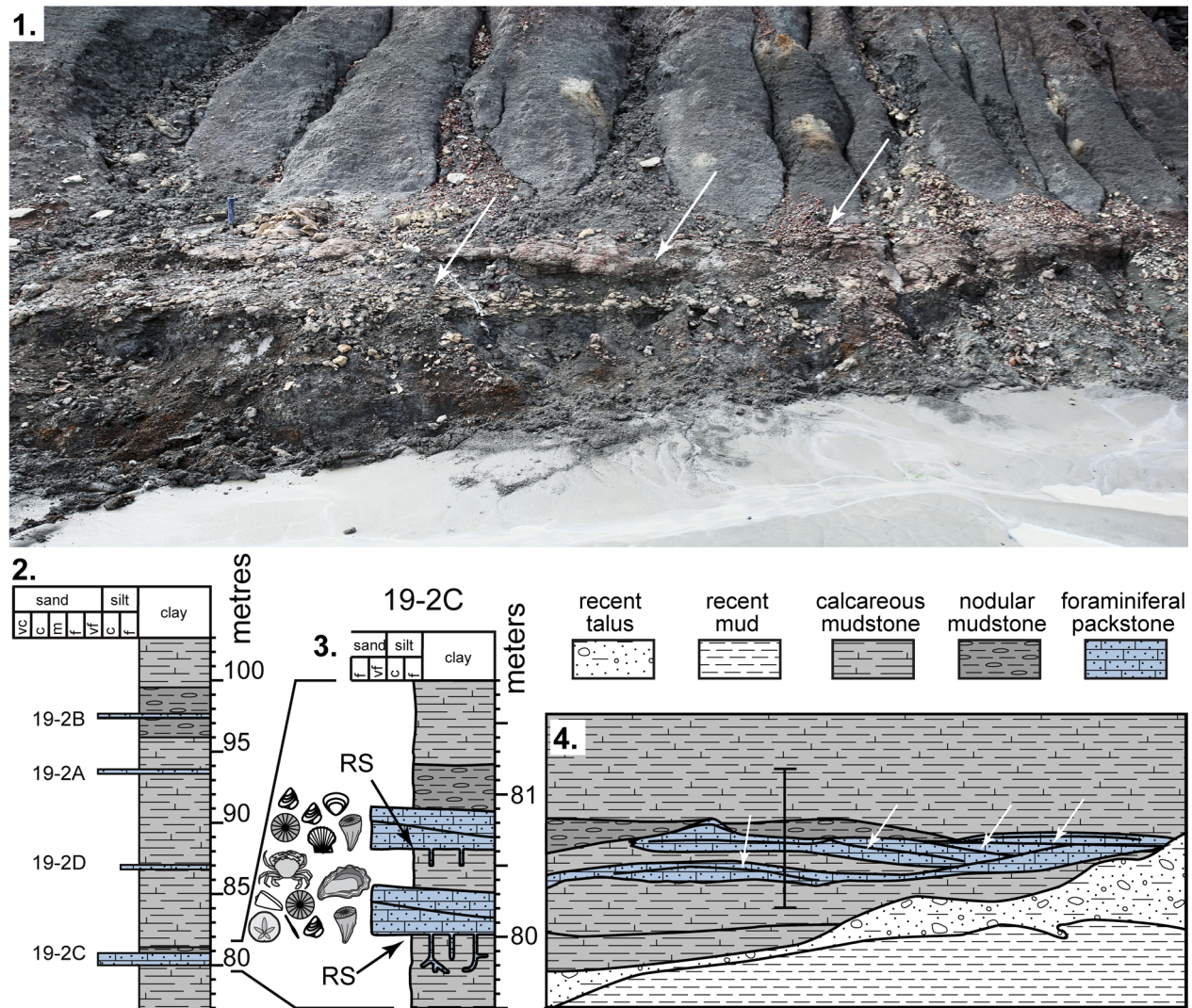


**Figure 7.** Foraminiferal packstone beds in the upper Pagat Member. (1) Bedset 19-2C in the upper Pagat Member. Note the off-lapping clinoform-like surfaces that denote mound tops (white arrows). (2) Measured section through the uppermost beds in the study interval. (3) Detailed section through the 19-2C bedset interval. (4) Sketch of the photograph in (1) showing lithofacies distribution; vertical line indicates approximate position of (3). Key for symbols in Figure 10.

These horizons range from monotypic assemblages of *Thalassinoides* to low-diversity assemblages of two or all of *Arenicolites*, *Planolites*, *Rhizocorallium*, *Skolithos*, and *Thalassinoides*. These sharp-walled burrows typically pipe bioclastic detritus, clastic sand, and glauconite deep into underlying strata. Maximum depths of penetration range from one to eight decimeters.

Only a single, discrete *Trypanites*-demarcated discontinuity surface was observed within the study area. This surface occurs near the base (0.90 m) and is characterized by numerous bored intraclasts that were eroded from a lithified substrate and bored on all sides before becoming incorporated into the bed that was subsequently lithified into the 0.90 m hardground. Ichnotaxa include *Gastrochaenolites*, *Rogerella*, and *Trypanites* (Table 3), with traces that penetrate 1–25 mm into the lithified surface.

In addition to the discrete *Trypanites* surface, abundant bored and encrusted bioclasts and intraclasts occur in most bioclastic floatstone and rudstone beds and in several of the bioclastic sandstone horizons in the study area. Many of these are also

characterized by encrusting organisms (serpulids, ostreids, and bryozoans). Bored and encrusted bioclasts and lithoclasts are common in the study area, but neither is dominant in any horizon. Most intraclasts and bioclasts are devoid of macroscopic borings. Those that do have macroscopic borings generally have low epizoan diversity, rarely exceeding one or two taxa per clast. Five ichnotaxa were identified: *Entobia*, *Gastrochaenolites*, *Oichnus* (= *Sedilichnus*), *Rogerella*, and *Trypanites* (Table 3). Microscopic borings were commonly observed in bivalve and gastropod shells in thin section.

*Entobia* in the study interval consist of closely spaced networks of interconnected subspherical chambers, which were observed penetrating the outer surface of bivalve and gastropod shells. *Oichnus* (= *Sedilichnus*) were observed on pectinid shells, rare corals, and the tests of LBF. Those on mollusk shells (*O. paraboloides*) are 1.5–3 mm in diameter. *Oichnus* on LBF are tiny (0.1–0.5 mm in diameter) and include *O. paraboloides* Bromley, 1981, *O. spongiophilus* Müller, 1977, and *O. simplex* Bromley, 1981. *Gastrochaenolites*, *Rogerella*, and *Trypanites*

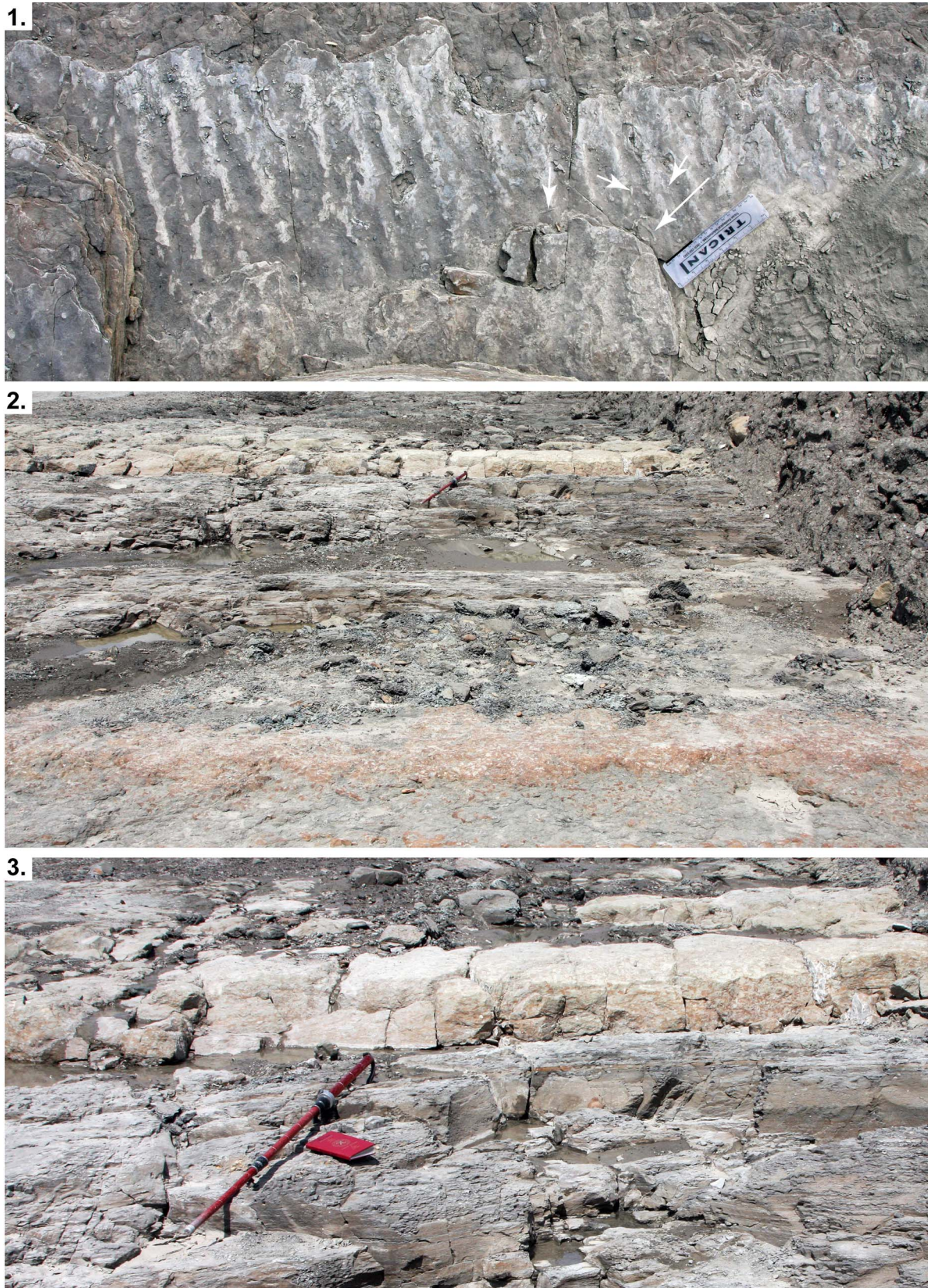


**Figure 8.** Lithofacies in the Pagat Member. (1) Bedding plane of glauconitic calcareous siltstone with linear, low-relief, symmetrical ripples. Ripple wave lengths are 5–7 cm and wave heights are 0.5–0.75 cm. Note the numerous trace fossils on this bedding plane (arrows). Scale bar is 15 cm. Photograph taken at 31.0 m above base of section. (2) Silty, calcareous mudstone with bioclastic packstone interbeds (reddish and rusty yellow beds). Note the nodular mudstone at the base, which consists of bioclastic packstone piped into burrows that penetrate into the underlying calcareous mudstone interval. Jacob staff is 1.5 m in length and is placed at the 24.75–24.95 m bioclastic packstone bed. (3) Close-up of the uppermost packstone bed in (2). Note the sharp base of the bed and the pronounced red-green burrow mottling indicating both abundant iron carbonate and abundant glauconite.

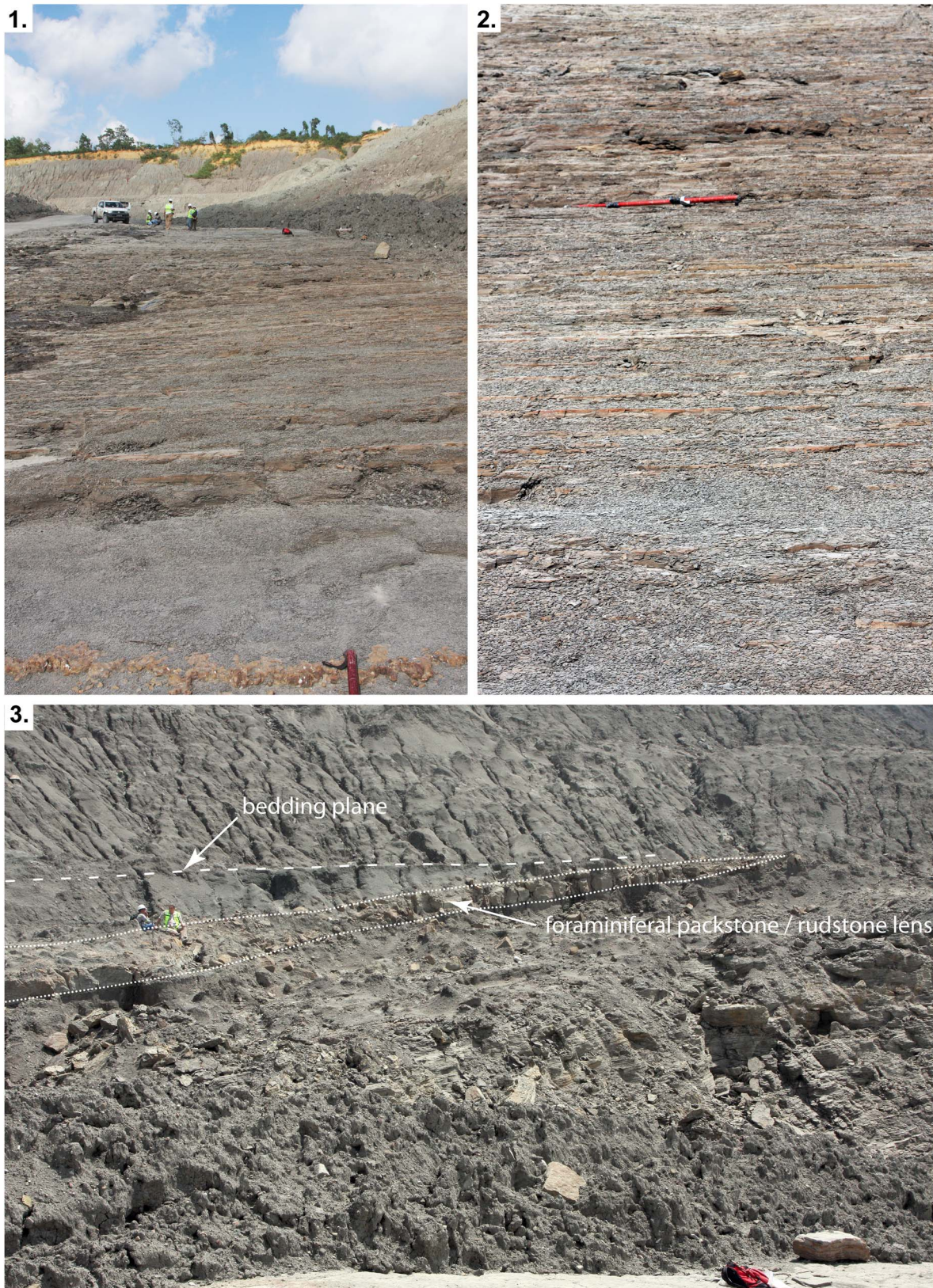


**Figure 9.** Lithofacies in the Pagat Member. (1) Heterolithic interval with intercalated foraminiferal wackestone/packstone and calcareous mudstone. The nodular packstone bed at the base of the image occurs at 0.9 m in the section. (2) Heterolithic mudstone–packstone interval, 5–10 meters above the base of the section. This part of the succession is characterized by cm-scale interlaminae grading from a ratio of packstone to mudstone beds of  $\sim 1:3$  at the base of the image to a ratio of  $\sim 3:1$  at the top of the image. (3) Mudstone-dominated succession from  $\sim 8$  m to  $\sim 25$  m in the section. The two people (left arrow) are sitting on the 15.7–17.65 fossiliferous packstone bed. This bed forms a lens on a clinoform emplaced obliquely to bedding.

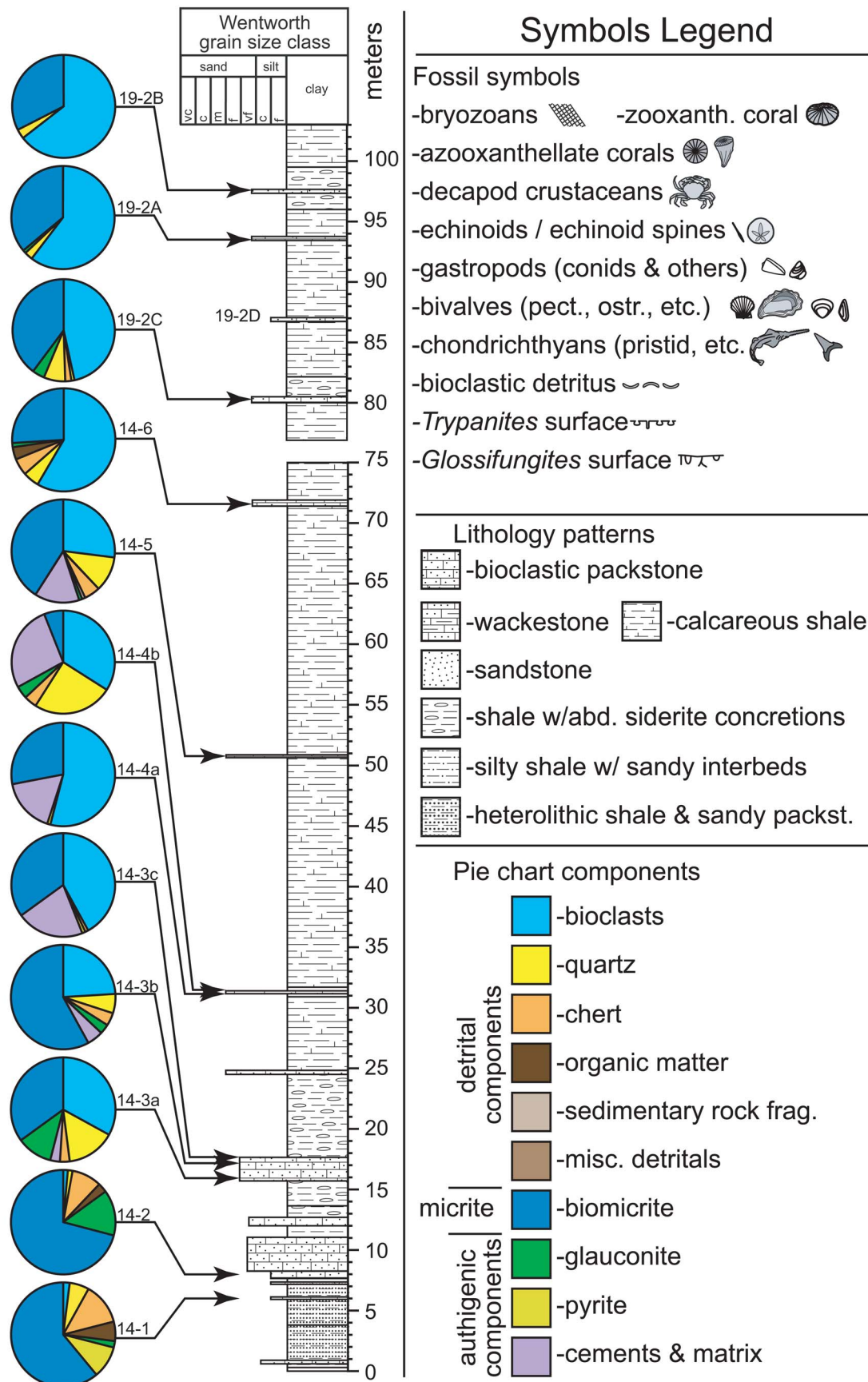


**Figure 10.** Petrography of wackestone and packstone beds in the Pagat Member. The pie diagrams show the relative proportions of carbonate (shown in shades of blue) and non-carbonate/siliciclastic components (shown in other colors).

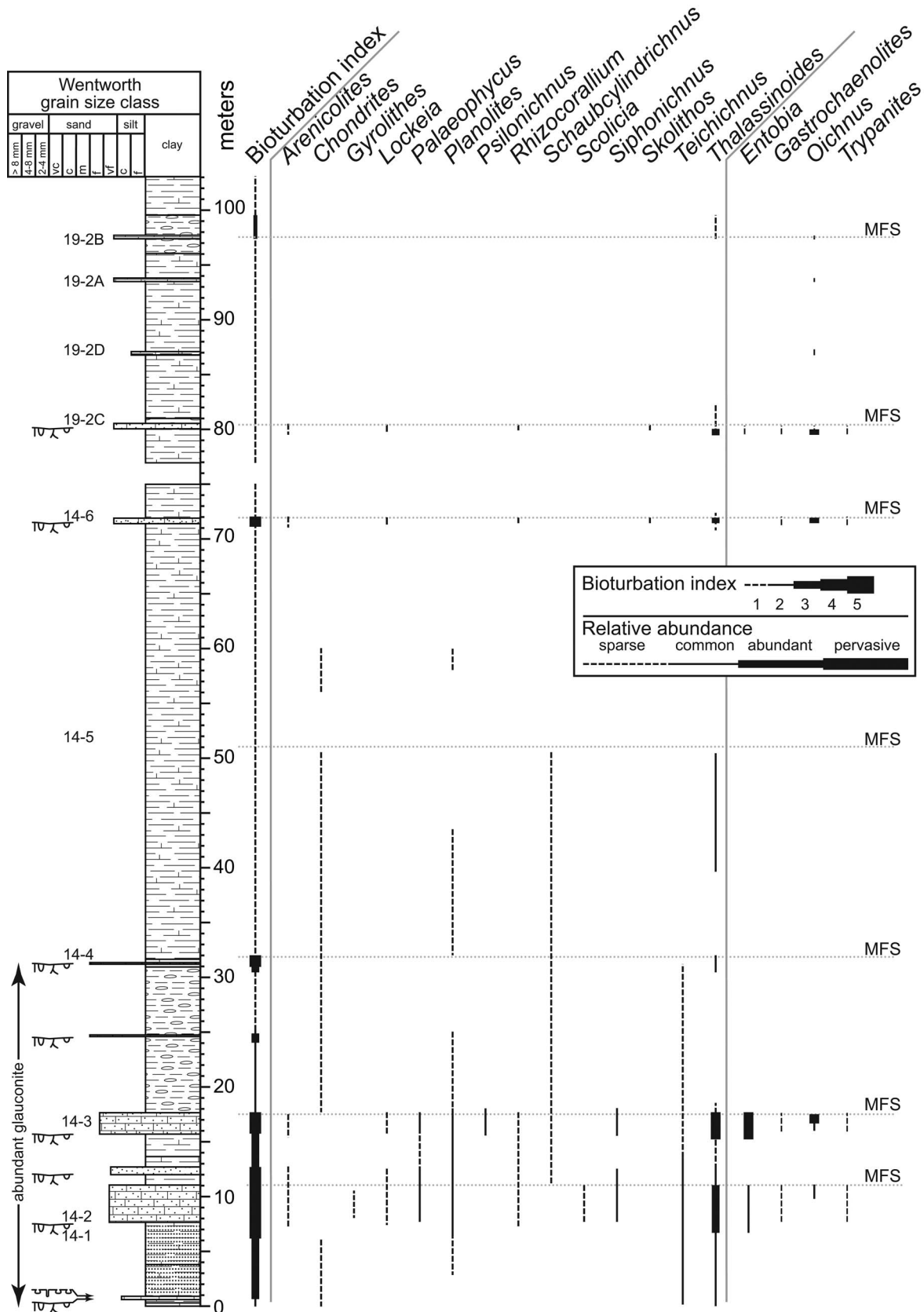


**Figure 11.** Distribution of trace fossils in the Pagat Member. The thickness of the line denotes relative abundances of individual ichnotaxa. Dashed lines indicate taxa that are present but sparsely distributed. The column on the left side of the taxonomic chart shows the bioturbation index. Note that trace fossils are, in general, much more common near the base of the section, as well as within and beneath bioclastic packstone beds, than in other lithologies. Lithology patterns and symbols identified in Figure 10. MFS = marine flooding surface.

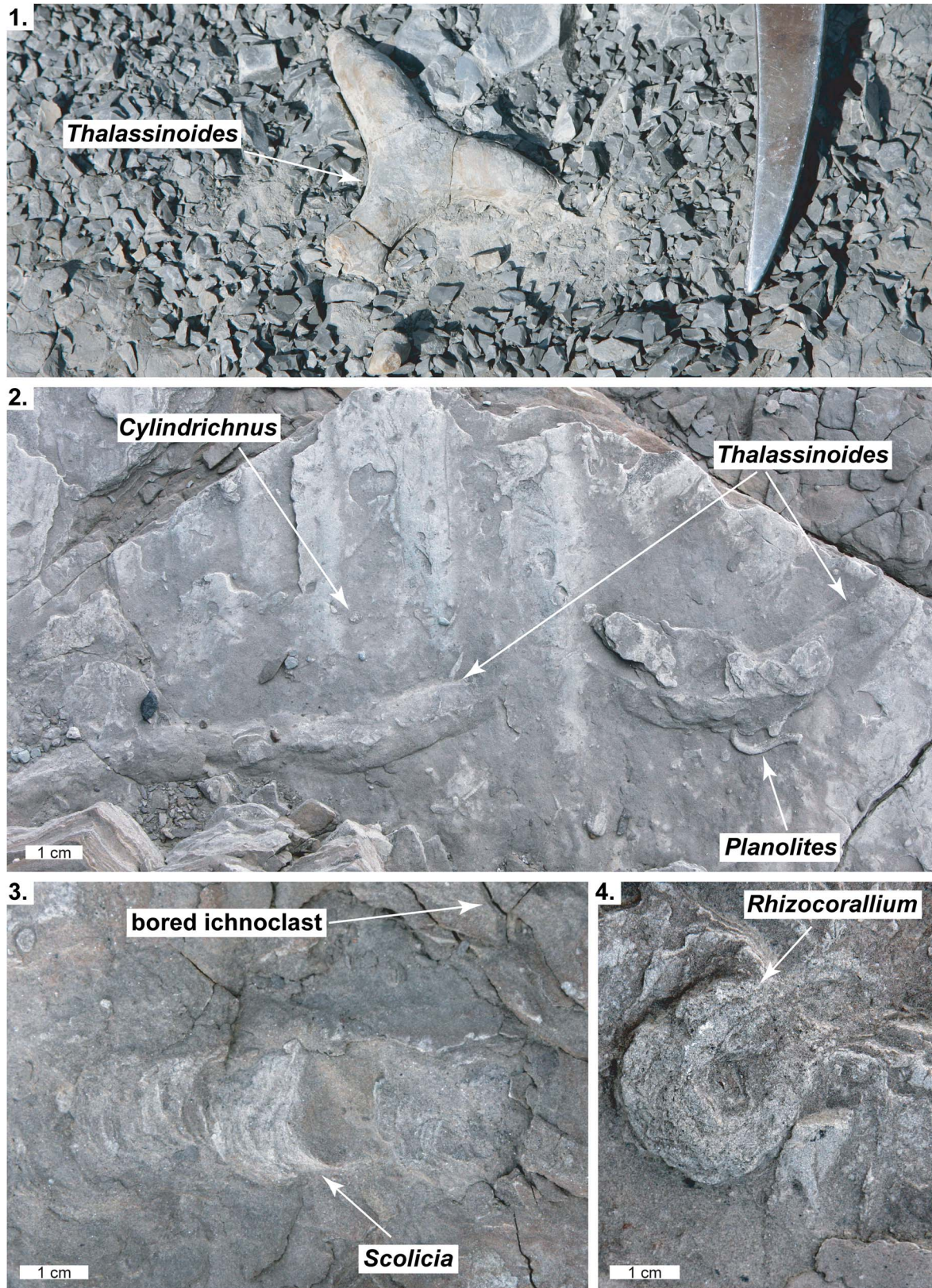


**Figure 12.** Ichnotaxa of the Pagat Formation. (1) A short section showing a branch in the trace fossil *Thalassinoides* preserved as a siderite concretion. The host sediment is calcareous mudstone whereas the burrow fill is bioclastic wackestone (0.75 m). (2) A large, elongate, unbranched horizontal tube attributed to *Thalassinoides* on a rippled bedding plane. Note other traces on this bedding plane including *Planolites* and *Cylindrichnus* (11.0 m). (3) A large *Scolicia* on a bedding plane. The clast at top revealed several boring ichnotaxa (not illustrated here) when extricated from the outcrop and cleaned (12.0 m). (4) Obliquely oriented *Rhizocorallium* isp. on a bedding plane (12.5 m). All measurements from base of section.

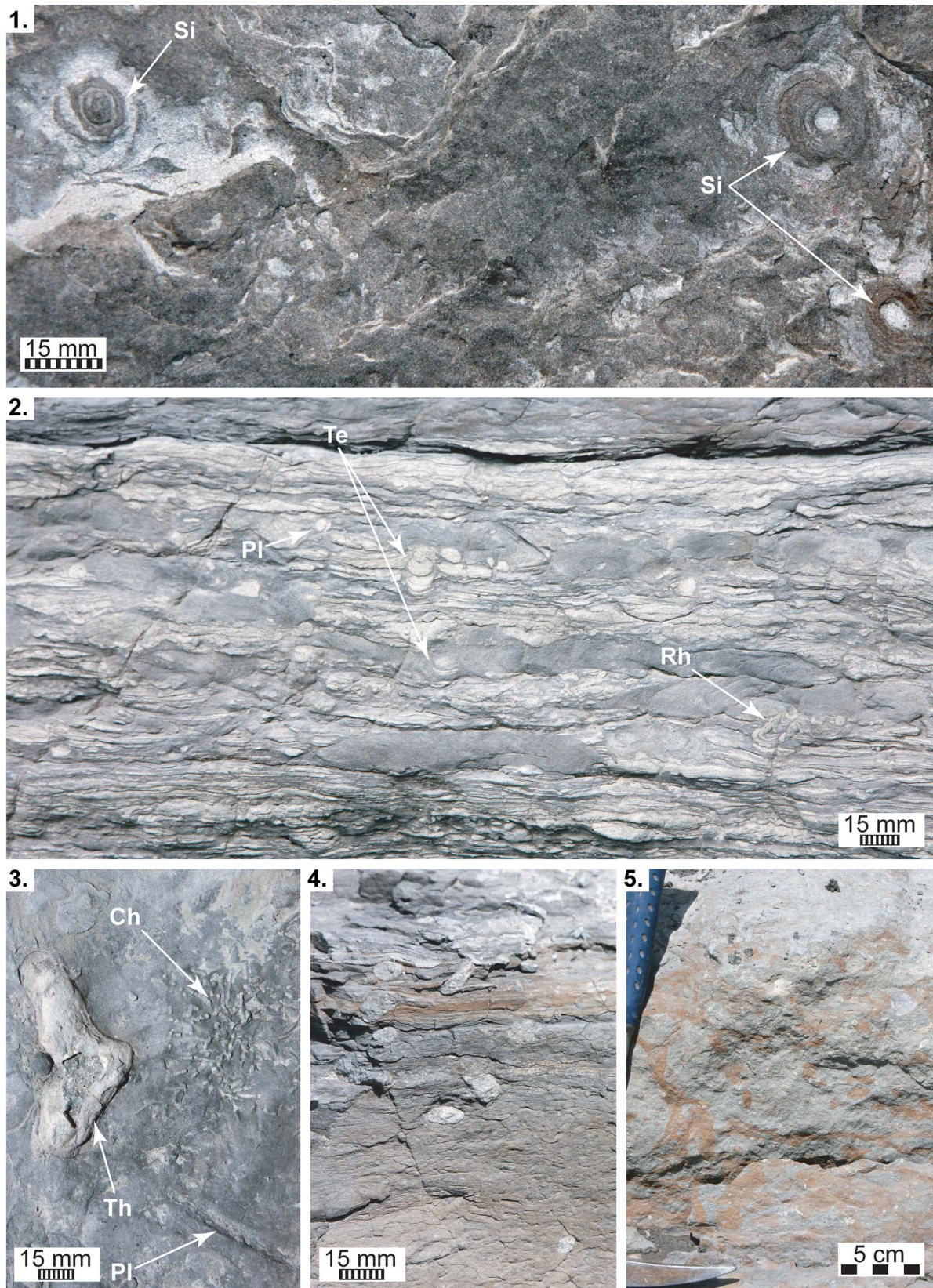


**Figure 13.** Ichnotaxa of the Pagat Formation. (1) Bedding plane illustrating several moderate-sized *Siphonichnus* (Si). Note the single siphon hole at the center of each trace indicating that these burrows were made by a bivalve with a mantled siphon (12.5 m). (2) A vertical section showing interlaminated glauconitic silty mudstone and bioturbated glauconitic sandstone (12.6 m). Illustrated are *Rhizocorallium* (Rh), *Teichichnus* (Te), and *Planolites* (Pl). (3) Bedding plane in silty mudstone showing *Chondrites* (Ch), *Planolites* (Pl), and wackestone-filled *Thalassinoides* (Th) (26.4 m). (4) Glauconitic sand-filled *Thalassinoides* tubes in a bioclastic silty sandstone succession (15.7 m). (5) Glauconitic bioclastic wackestone with rust-red-colored *Thalassinoides* tubes (71.5 m).

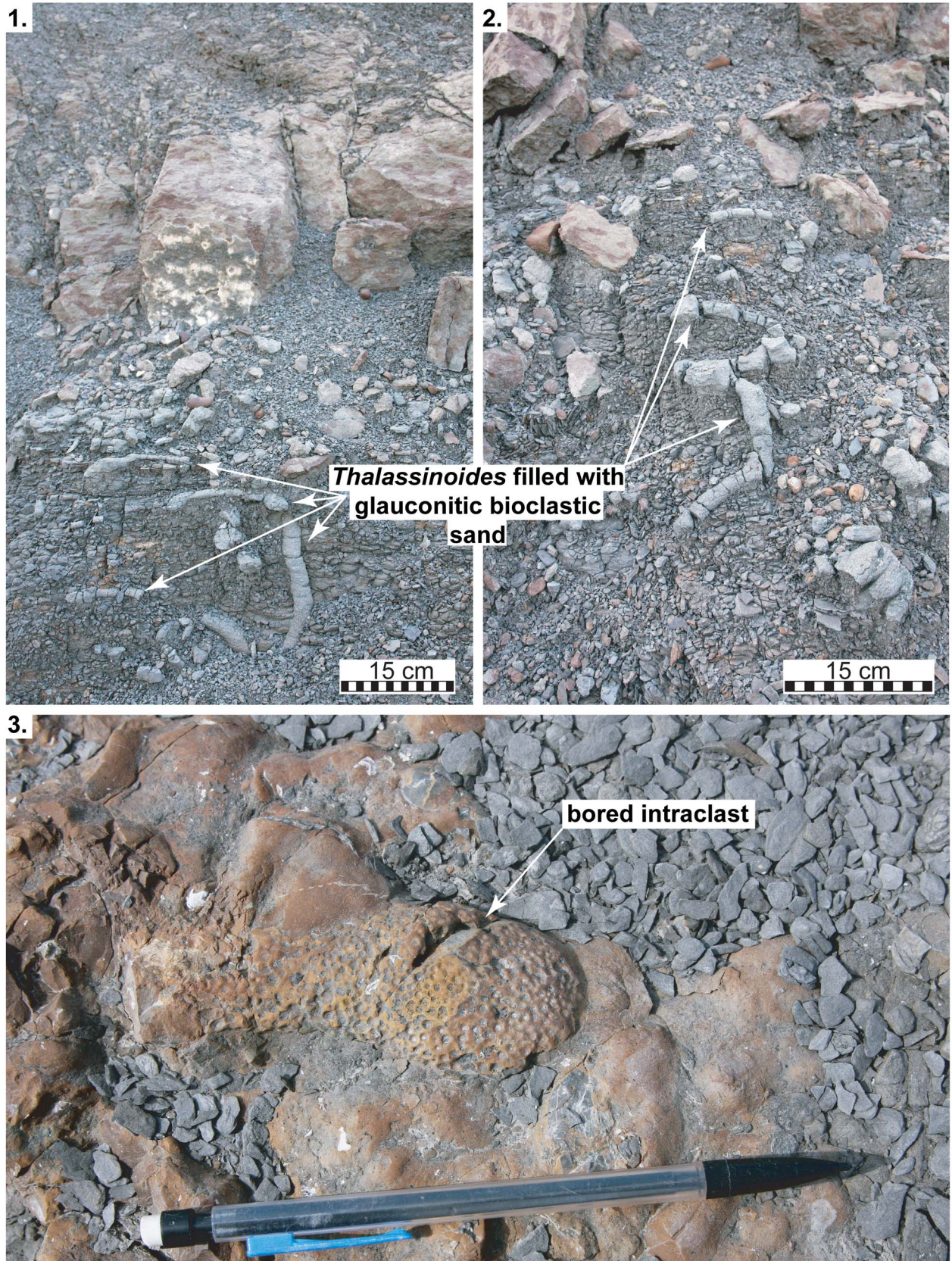


**Figure 14.** Ichnotaxa of the Pagat Formation. (1, 2) Deeply penetrating three-dimensional burrow network (*Thalassinoides*) penetrating down from the base of a foraminiferal packstone bed. Sharp-walled burrows with fill that differs sharply from the host strata indicate that these beds comprise low-diversity *Glossifungites* communities (15–16 m). (3) Irregular surface at the top of a bioclastic packstone bed. The intraclast illustrated is characterized by numerous diminutive *Gastrochaenolites* (7.65 m).

**Table 3.** Trace fossil taxa, their lithofacies occurrence and behavioral inferences of the Pagat Member, Tanjung Formation in the Asem Asem Basin, near Satui. Acronyms identified in Table 2. Behavioral inferences based on previous work by numerous workers (Bromley and Asgaard, 1979; Bromley, 1981; Lambers and Boekschoten, 1986; Dworschak and Rodrigues, 1997; Gingras et al., 1999, 2000, 2008; Bromley and Uchman, 2003; Taylor, and Wilson, 2003; Knaust, 2004, 2013; Seike and Nara, 2007; Neto de Carvalho et al., 2010; Fernández and Pazos, 2012; Zonneveld and Gingras, 2014; Furlong et al., 2015, 2016; Hanken et al., 2016).

Ichnotaxon	Lithofacies occurrence	Inferred behavior	Inferred tracemaker
<b>Burrows</b>			
<i>Arenicolites</i>	SSm	Domichnia of infaunal suspension feeders	polychaetes, arthropods
<i>Asterosoma</i>	SSm	Fodinichnia	vermiform organisms
<i>Chondrites</i>	SHl, SHnc, SSm	Fodinichnia	vermiform organisms
<i>Gyrolithes</i>	SSm	Domicile of an infaunal suspension feeder	polychaete worms, arthropods
<i>Lockeia</i>	SSg	Cubichnia	bivalved mollusks
<i>Macanopsis</i>	SHnc, SSg, BIOR	Domichnia	decapod crustaceans
<i>Palaeophycus</i>	SSm, SSg, LSbpr	Domichnia/Fodinichnia/Praedichnia	polychaete worms, arthropods
<i>Phycosiphon</i>	SSm	Fodinichnia – deposit feeding	vermiform organisms
<i>Planolites</i>	SHl, SHnc, SSm, SSg, LSbpr	Domichnia/Fodinichnia	polychaetes, arthropods
<i>Pylonichnus</i>	SHnc, SSg, LSbpr	Domichnia	decapod crustaceans
<i>Rhizocorallium</i>	SSm, SSg, LSbpr	Domichnia/Fodinichnia	polychaetes, arthropods
<i>Scalartuba</i>	SSm	Fodinichnia	vermiform organisms
<i>Schaubcylindrichnus</i>	SHl, SHnc, SSm	Domichnia/Fodinichnia	vermiform organisms
<i>Scolicia</i>	SSm, SSg, LSbpr	Repichnia, fodinichnia	gastropods, echinoids
<i>Siphonichnus</i>	SSg	Domichnia of infaunal suspension and deposit feeders	bivalved mollusks
<i>Skolithos</i>	SSm, SSg, LSbpr	Domichnia of infaunal suspension feeders, praedichnia	polychaete worms, arthropods
<i>Teichichnus</i>	SSm, SSg	Domichnia, Fodinichnia, Equilibrichnia	polychaete worms
<i>Thalassinoides</i>	SHnc, SSm, SSg, LSbpr	Domichnia	decapod crustaceans
<i>Fugichnia</i>	SSm, SSg	Escape trace	a variety of infaunal taxa
<b>Borings</b>			
<i>Entobia</i>	bival., gastr.	Domichnia of filter feeder	sponges
<i>Gastrochaenolites</i>	LSbw, LSbpr	Domichnia	boring bivalves
<i>Oichnus</i>	bival., gastr., foram., coral	Praedichnia	gastropods, octopus
<i>Rogerella</i>	LSbw, LSbpr	Domichnia/Fodinichnia	arthropods (barnacles)
<i>Trypanites</i>	LSbw, LSbpr	Domichnia/Fodinichnia	vermiform organisms
Micro-borings	shells in LSbw, LSbpr thin-sect.	Fodinichnia	bacteria, algae

were also observed on micritic intraclasts. The microscopic borings in gastropod and bivalve shell material identified in thin-section consist of simple pit-like structures, clavate- or vase-shaped structures, and more complex meandering excavations that penetrate deeply into thicker shells. These traces are 10–25 µm across but were only observed in two-dimensional thin-section view; thus, no attempt was made to classify these micro-traces to ichnotaxon. Bored and encrusted bioclasts and lithoclasts are included within the *Trypanites* ichnofacies by some workers and separated into the *Gnathichnus* ichnofacies by others (e.g., Bromley and Asgaard, 1993; Mayoral and Muñiz, 1996; de Gibert et al., 2007, 2012; MacEachern et al., 2012).

**Invertebrate fossil distribution.**—The Pagat Member at Satui includes a moderately diverse assemblage of marine invertebrate fossils. Most fossils occur in highly fossiliferous bioclastic rudstone beds; however, some were also observed in bioclastic floatstone and bioclastic sandstone beds. Fossils occur in random orientations. Beds that occur at 15.7–17.65 m, 71.4–71.9 m, 80.0–80.35 m, 93.3–93.6 m, and 97.2–97.6 m are exceptionally fossiliferous. These beds have produced particularly rich and abundant faunas that include gastropods, bivalves, crabs, azooxanthellate corals, larger benthic foraminifera, bryozoans, and serpulids.

**Mollusca: Gastropoda and Bivalvia.**—Mollusk fossils are common in the study interval and include at least 55 morphotypes/species (Figs. 15–17, Tables 4 and 5). The recovered molluscan fauna is moderate sized, consisting of 465 specimens of gastropods and bivalves ranging from 4 to ~45 mm in size.

Specimens are preserved in three dimensions, but most aragonite has been dissolved or, at best, is present as fragmentary

chalky layers, sometimes underlying a diagenetic calcitic crust. Where present, the calcite component of shells is well preserved but apparently neomorphosed. As a result of this diagenesis, the dominantly aragonitic fauna is commonly represented by lithified mudstone, phosphatic steinkerns, or partial steinkerns. Often these have varying remnants of shell layers preserved, sometimes overlying a thin neomorphosed calcitic inner layer. A few centimetric light gray nodules were collected, one of which preserves a small and thin-shelled nuculanid valve otherwise absent from the collections, suggesting that the smaller and thinner-shelled components that might be expected to comprise a significant component of the original fauna were either not preserved or not recovered.

The overall poor state of mollusk preservation has restricted identifications mostly to family or superfamily level in the case of the gastropods (Table 4), where well-preserved protoconchs, external ornament, and growth lines, as well as critical details of the interior of the aperture, are mostly unavailable. Although many of the gastropods have a siphonate morphology, almost all have lost much of their rostrum. A small number of calcitic gastropods (epitoniids) are well preserved, and at least one could be identified at the species level with additional work. Although their ornament is preserved, the calcitic bivalves are mostly very fragmentary, which precludes detailed identification. Steinkerns of aragonitic bivalves are frequently of paired valves, preventing preservation of diagnostic interior morphology of hinge and muscle scars, but some have characteristic external morphologies (e.g., “*Carditamera*,” “*Apolymetis*”) that allow identification to genera in the broadest sense.

Distinct morphologies of ~40 different gastropods and 16 different bivalves were discriminated (Tables 4 and 5). Because of the limits imposed by preservation, these groupings should be

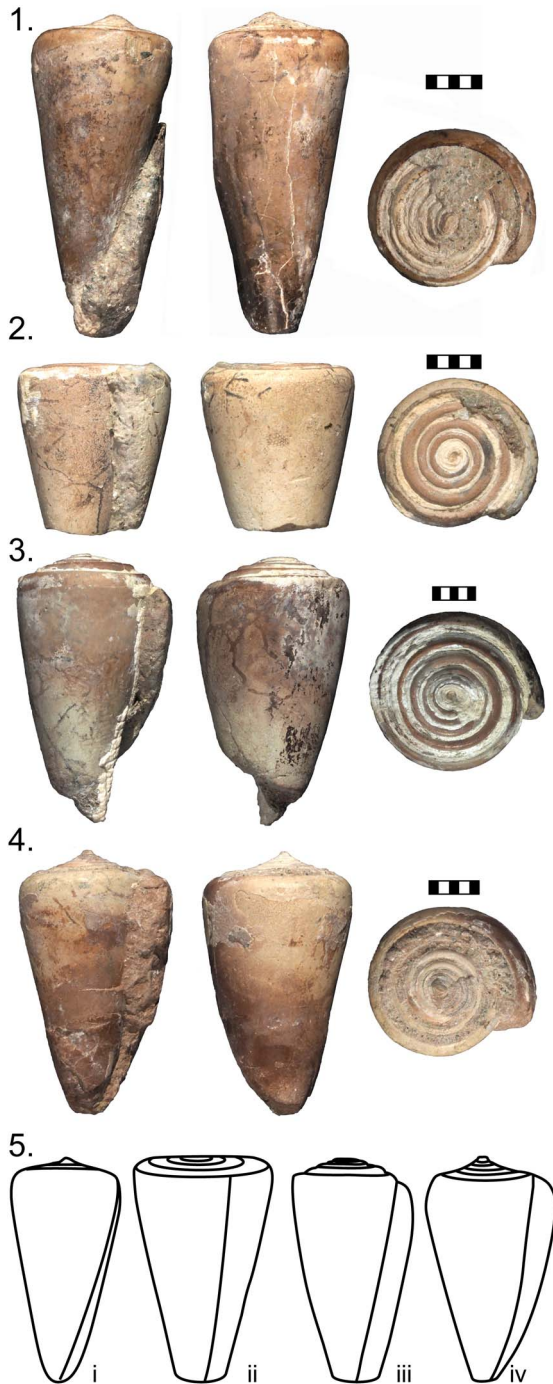


**Figure 15.** “*Conus*” species (morpho-groupings) of the Pagat Member, Satui region, Kalimantan, differentiated on the basis of length/width ratio, spire height and outline, shape of the shoulder, and presence of spiral ornament towards the base of the whorl. (1) *Conus* sp. 1, long and slender with narrow shoulders and a bi-concave spire and a pointed spire tip, UA-P1841. (2) *Conus* sp. 2, with broad shoulders and a flat spire, UA-P1837. (3) *Conus* sp. 3, obconical, exhibiting a low conical (bi-convex) spire and a cyrtocooid spire, UA-P1844. (4) *Conus* sp. 4, with a narrow base, broad shoulders, and a low turbinatate spire, UA-P1847. (5) Schematics of *Conus* sp. 1 to *Conus* sp. 4. Scale bars show millimeter increments.

regarded as morphotypes rather than morphospecies. For example, four broadly different groups of “*Conus*” could be discriminated based on size, length/width ratio, spire height and outline, shape of shoulder, and presence of spiral ornament

towards the base of the whorl (Fig. 15), but their preservation constrains interpretations on how this steinkern-dominated fauna relates to the species that occurred in the original mollusk fauna. Nonetheless, for consistency with identification of other taxa in the studied material, general rules of open nomenclature were followed (Bengtson, 1988).

The gastropod fauna comprises neogastropods and other caenogastropods, with a single heterobranch (architectonicid) present. At least five families of neogastropods, encompassing ~22 morphotypes (genera), occur in the study interval (Table 4), including Muricidae, Mitridae, Volutidae (Athletinae and Fulgorariinae), Conidae (several morphotypes of cf. *Conus* sp.), and Turridae (Figs. 15 and 16). Overall, neogastropods are much more common in the study interval, particularly in the 15.7–17.65 m, 71.4–71.9 m, 80.0–80.35 m, and 97.2–97.6 m beds. Volutids are particularly common in the 15.7–17.65 m, 71.4–71.9 m, and 97.2–97.6 m beds (45, 35, and 27, respectively). Seven buccinids occur in the 71.4–71.9 m bed. Conids are also common in the 15.7–17.65 m and 97.2–97.6 m beds. Several architectonicids were also collected from the study interval, primarily from the 15.7–17.65 m bed.

Nine families of other caenogastropods containing ~15 morphotypes (genera) were identified (Table 4), including Turritellidae (“cf. *Turritella* sp.”), Pediculariidae (cf. *Cypraedia* sp.), Seraphsidae?, Cassidae (cf. *Galeodea* sp.), Ranellidae?, Cymatiidae (cf. *Sassia* sp.), Ficidae?, Epitoniidae, and Vermitidae (Fig. 16). Although present, non-neogastropod caenogastropod taxa are never particularly abundant, with the exception of eight cf. *Galeodea* sp. in the 15.7–17.65 m bed and a nodule containing eight vermetids in the 80.0–80.35 m bed.

Bivalves are less diverse and less common than gastropods in the study area. However, at least 16 morphotypes within 11 families occur (Nuculanidae, Pectinidae, Spondyliidae?, Gryphaeidae, Cardiidae, Tellinidae, Corbulidae?, Pinnidae, Chamiidae, Ostreidae, and several unidentified taxa within the Heterodonta; Fig. 17, Table 5). Of these, pectins and ostreids are most commonly observed. However, gryphaeids are common in the upper part of the study interval, at the 80.0–80.35 m and 97.2–97.6 m beds. Minute ostreids (~4–8 mm in diameter) were noted cemented to the outer surface of several lithoclasts and numerous small solitary corals.

Decapod crustaceans.—Decapod crustaceans occur in horizons throughout the study interval and are particularly common in the 15.7–17.65 m and 97.2–97.6 m beds (Fig. 18). To date, we have recognized five taxa, remarkably all of them brachyurans, or true crabs. These include dromioidean sponge crabs (one taxon), raninoidean frog crabs (one taxon), goneplacoid crabs (two taxa), and portunoid swimming crabs (one taxon).

The brachyuran crabs are undeformed (non-flattened) and occur in every lithofacies in the study interval. They are particularly common in foraminiferal rudstone beds, nodular calcareous shale successions, and heterolithic silty shale successions with abundant iron carbonate concretions. The iron carbonate concretions often occur in linear branching networks, and well-preserved crabs were noted in many of the concretions (Fig. 12.1). These concretions are interpreted as early cemented burrow-infill, resulting in well-preserved, three-dimensional preservation of the crabs within. Notably, no axiidean ghost shrimp remains (e.g., claws) have been recognized from this

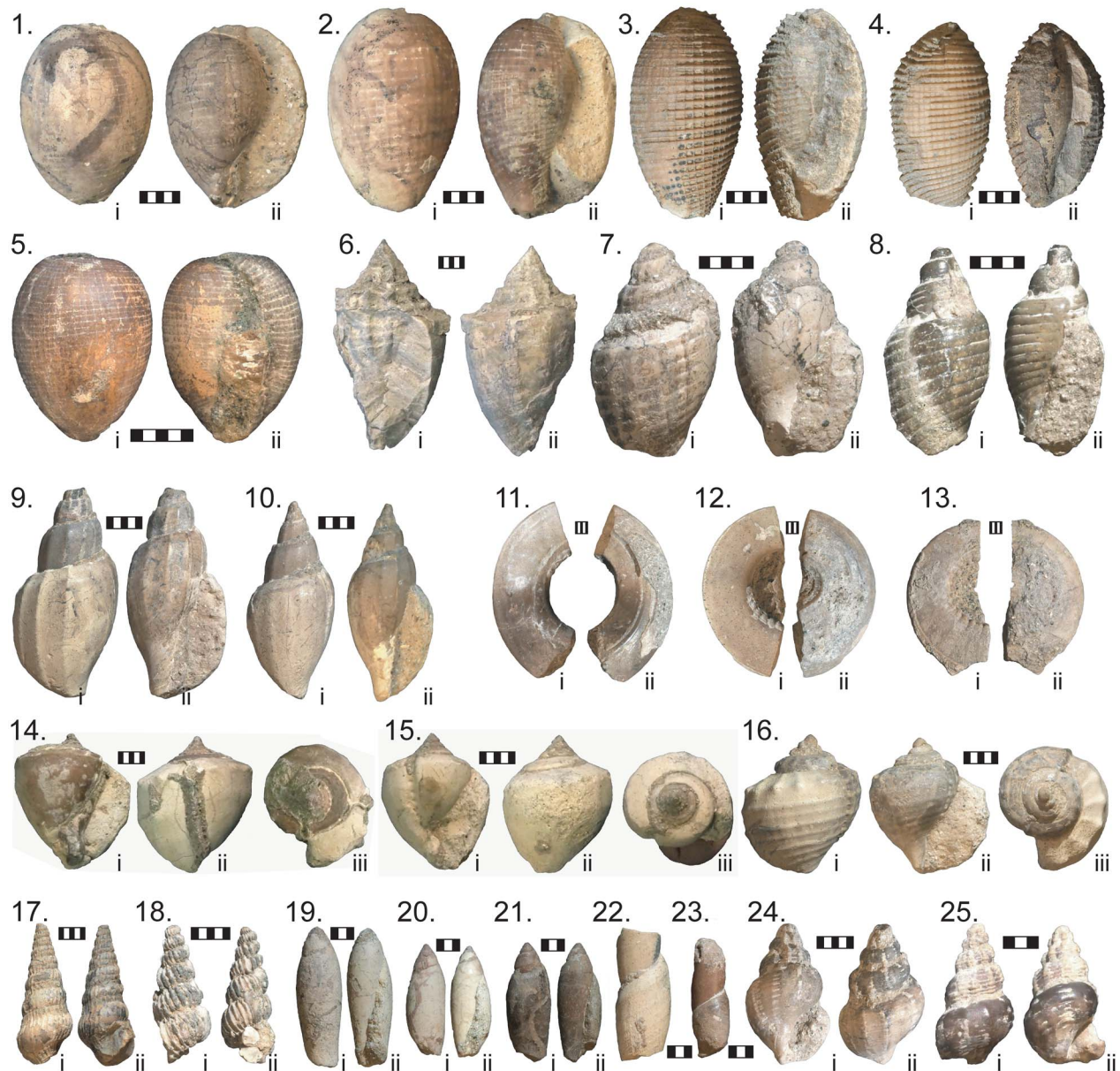


**Figure 16.** Gastropoda (exclusive of conids) of the Pagat Member, Satui region, Kalimantan. Unless indicated all specimens are from level 14-3b (15.7 m). Scale bar increments are millimeters. (1) *Cyprædia* sp. 1 dorsal (i) and ventral (ii) views, UA-P1806. (2) *Cyprædia* sp. 1, dorsal (i) and ventral (ii) views, UA-P1807. (3) *Cyprædia* sp. 2 from level 19-2B (97.5 m), dorsal (i) and ventral (ii) views, UA-P2039. (4) *Cyprædia* sp. 2 from level 19-2B, (97.5 m), dorsal (i) and ventral (ii) views, UA-P2038. (5) *Cyprædia* sp. 1 from level 19-2D (87 m), dorsal (i) and ventral (ii) views, UA-P2037. (6) Volutidae: *Athletinae*? from level 19-2B (97.5 m), ventral (i) and dorsal (ii) views, UA-P2089. (7) Volutidae: *Athletinae*? from level 14-6 (71.5 m), dorsal (i) and ventral (ii) views, UA-P1895. (8) Mitridae from level 14-3b (17.05 m), dorsal (i) and ventral (ii) views, UA-P1804. (9) Volutidae, *Fulgoraria* sp. 2 from level 14-3B (15.7 m), dorsal (i) and ventral (ii) views, UA-P1908. (10) Volutidae, *Fulgoraria* sp. 2, from level 14-3B (15.7 m), dorsal (i) and ventral (ii) views, UA-P1905. (11) Fragment of an Architectonicidae from level 14-3B (15.7 m), basal (i) and upper (ii) views, UA-P1805. (12) Fragment of an Architectonicidae from level 19-2C (80.5 m), basal (i) and upper (ii) views, UA-P2092. (13) Architectonicidae from level 19-2C (80.5 m), basal (i) and upper (ii) views, UA-P2092. (14) Cassidae: “*Galeodea*” sp. 1, from level 14-3B (15.7 m), ventral (i), dorsal (ii), and top (iii) views, UA-P1867. (15) Cassidae: “*Galeodea*” sp. 1, from level 14-3B (15.7 m), ventral (i), dorsal (ii), and top (iii) views, UA-P1863. (16) Cassidae: “*Galeodea*” sp. 2, from level 14-3B (15.7 m), dorsal (i), ventral (ii), and top (iii) views, UA-P1861. (17) Epitoniidae from level 19-2C (80.5 m), dorsal (i) and ventral (ii) views, UA-P2099. (18) Epitoniidae from level 14-3B (15.7 m), UA-P1899. (19) Seraphsidae from level 14-3B (15.7 m), dorsal (i) and ventral (ii) views, UA-P1802. (20) Seraphsidae from level 14-3B (15.7 m), dorsal (i) and ventral (ii) views, UA-P1800. (21) Seraphsidae from level 14-3B (15.7 m), dorsal (i) and ventral (ii) views, UA-P1801. dorsal (i) and ventral (ii) views. (22) Mitridae from level 14-3B (15.7 m), dorsal view, UA-P1786. (23) Mitridae from level 14-3B (15.7 m), dorsal view, UA-P1785. (24) Buccinoidea: Buccinidae from level 14-6 (71.5 m), ventral (i) and dorsal (ii) views, UA-P1953. (25) Muricidae from level 14-3B (15.7 m), dorsal (i) and ventral (ii) views, UA-P1797.

section yet, despite being among the most abundant decapod remains in this type of assemblage and often associated with burrow infills. The brachyuran crabs will be described in a subsequent taxonomy-focused manuscript and are not further discussed herein.

Hexacorallia.—Corals are represented by two zooxanthellate coral taxa and four azooxanthellate coral taxa (Fig. 19, Table 6). *Cycloseris* cf. *C. sinensis* Milne-Edwards and Haim, 1851, a zooxanthellate form is the most abundant coral in the study interval. *Cycloseris* is a small fungiid coral, common in

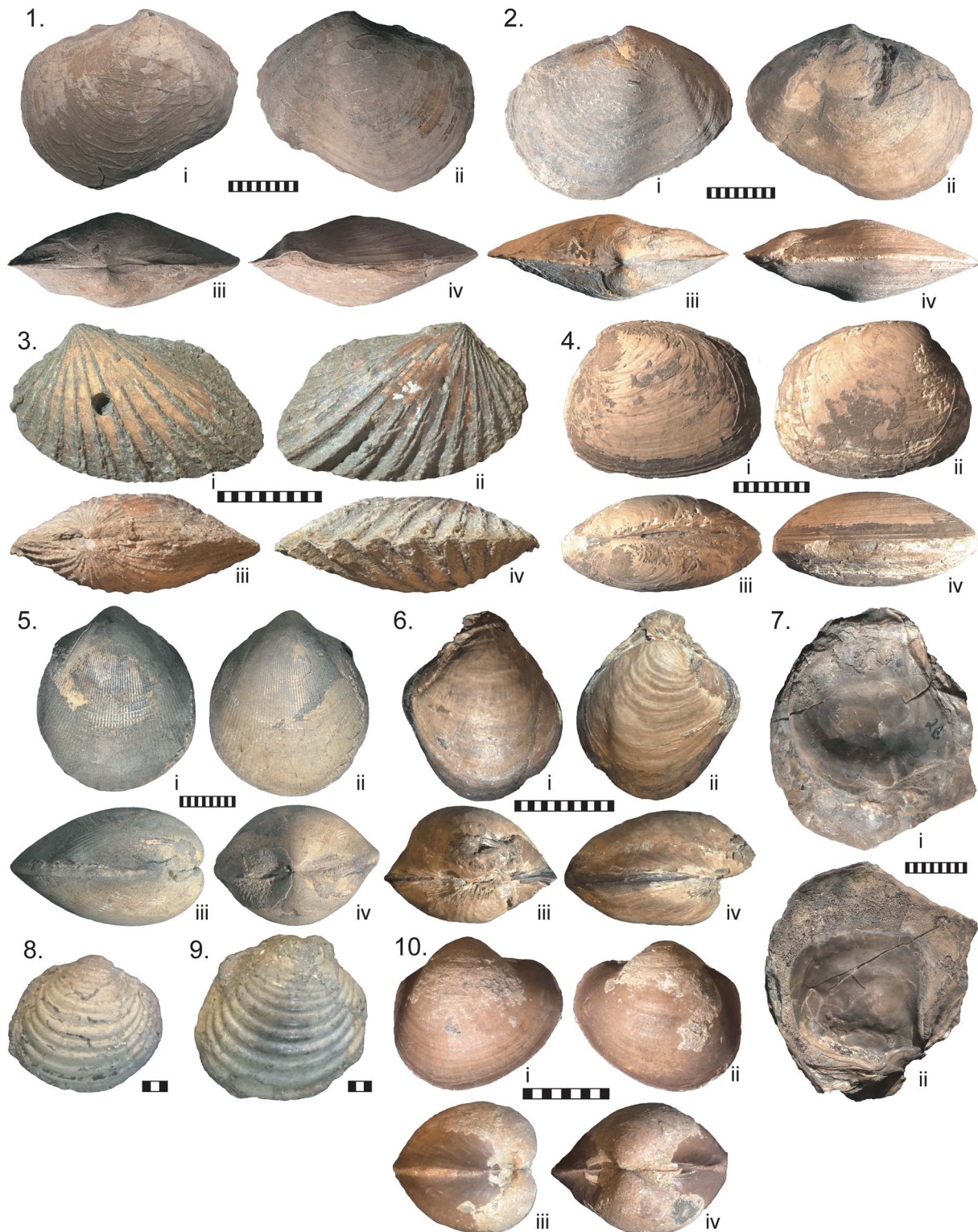


**Figure 17.** Bivalvia of the Pagat Member, Satui region, Kalimantan. Scale bar increments are millimeters. (1) cf. *Apolymetis* sp. (Cardiida: Tellinidae) from layer 19-2B (97.5 m), ventral (i), dorsal (ii), hinge (iii), and commissure (iv) views, UA-P 2027. (2) cf. *Apolymetis* sp. (Cardiida: Tellinidae) from layer 19-2B (97.5 m), dorsal (i), lateral (ii) iii, hinge (iii), and commissure (iv) views, UA-P2031. (3) cf. *Carditamera* sp. (Carditida: Carditidae) from layer 19-2C (80.5 m), *Oichnus simplex* boring on the dorsal side (i), ventral (ii), hinge (iii), and commissure (iv) views, UA-P2137. (4) Tellinid bivalve, layer 19-2C (80.5 m), ventral (i), dorsal (ii), hinge (iii), and commissure (iv) views, UA-P2140. (5) Heterodont bivalve from layer 19-2B (97.5 m), dorsal (i), ventral (ii), lateral (iii), and hinge (iv) views, UA-P2032. (6) Chamidae from layer 2B (97.5 m), dorsal (i), ventral (ii), hinge (iii), and lateral (iv) views, UA-P2051. (7) Ostreid from layer 2B (97.5 m), top side of ventral valve (i), base of ventral valve (ii), UA-P2024. (8) Heterodont bivalve (sp. 1) from layer 14-3b (17.05 m), ventral side, UA-P1817. (9) Heterodont bivalve (sp. 1) from layer 14-3b (17.05 m), dorsal side, UA-P1819. (10) Heterodont bivalve (sp. 3) from layer 14-3b (17.05 m), ventral (i), dorsal (ii), lateral (iii), and hinge (iv) views, UA-P1832.

**Table 4.** Gastropod distribution, Pagat Member, Tanjung Formation in the Asem Asem Basin, near Satui.

Taxonomic grouping	14-3	14-6	19-1	19-2	19-3	19-4
<b>Caenogastropoda (exclusive of Neogastropoda)</b>						
Cerithioidea: Turritellidae: “ <i>Turritella</i> ” juvenile	—	1	—	—	—	—
Cypraeoidea: Pediculariinae: “ <i>Cypraedia</i> ”	2	—	2	1	1	2
Stromboidea?: Seraphsidae?	4	1	2	—	—	—
Tonnoidea?	—	1	—	—	—	—
Tonnoidea: Cassidae: “ <i>Galeodea</i> ”? 1	7	—	—	—	—	—
Tonnoidea: Cassidae: “ <i>Galeodea</i> ”? 2	1	—	2	—	—	—
Tonnoidea: Ranellidae?	—	1	—	—	—	—
Tonnoidea: Ranellidae? (Cymatiidae): “ <i>Sassia</i> ” ?	—	1	—	—	—	—
Tonnoidea: Ranellidae?/Muricoidea: Muricidae?	3	—	—	—	—	—
Tonnoidea?: Ficidae?	—	3	—	—	—	—
Epitonioidae: Epitoniidae 1	—	1	—	—	—	—
Epitonioidae: Epitoniidae 2	—	1	—	—	—	—
Epitonioidae: Epitoniidae 3	1	—	5	—	—	—
Buccinoidea?: Buccinidae?	—	7	—	—	—	—
Vermetidae	—	—	8	2	4	—
<b>Neogastropoda</b>						
Muricoidea: Muricidae?	—	6	—	—	—	4
Muricoidea: Mitridae? 1	1	4	1	—	—	—
Muricoidea: Mitridae? 2	3	5	—	—	—	5
Muricoidea: Volutidae: Athletiniae? 1	5	6	—	—	—	—
Muricoidea: Volutidae: Athletiniae? 2	11	—	9	—	—	—
Muricoidea: Volutidae: Athletiniae? misc.	3	12	—	—	1	1
Muricoidea: Volutidae: Fulgorariinae? spp.	9	6	—	—	—	25
Muricoidea: Volutidae 1	4	10	—	—	—	—
Muricoidea: Volutidae? 2	—	1	—	—	1	—
Muricoidea: Volutidae? 3	2	—	—	—	—	—
Muricoidea: Volutidae? misc.	11	—	—	—	1	—
Conoidea: Conidae (s.s.): “ <i>Conus</i> ” 1	1	—	2	—	—	4
Conoidea: Conidae (s.s.): “ <i>Conus</i> ” 2	8	—	—	—	—	—
Conoidea: Conidae (s.s.): “ <i>Conus</i> ” 3	3	—	—	—	—	—
Conoidea: Conidae (s.s.): “ <i>Conus</i> ” 4	3	—	—	—	—	—
Conoidea: Conidae (s.s.): “ <i>Conus</i> ” misc.	13	4	—	—	—	7
Conoidea: Turridae (s.l.)	—	1	—	—	—	—
Neogastropoda indet. 1	1	1	—	—	—	—
Neogastropoda indet. 2	—	1	—	—	—	—
Neogastropoda indet. 3	2	4	—	—	—	—
Neogastropoda indet. 4	11	1	—	—	—	—
Neogastropoda indet. 5	—	1	—	—	—	—
Neogastropoda indet. 6	—	1	—	—	—	—
Neogastropoda indet. 7	1	—	—	—	—	—
Neogastropoda indet. 8	1	—	—	—	—	—
<b>Heterobranchia</b>						
Architectonicoidea: Architectonicidae	4	—	—	—	—	—
Gastropoda 1	—	1	—	—	—	—
Gastropoda 2	1	—	—	—	—	—
Gastropoda 3	—	—	13	—	—	—
Indeterminate gastropod fragments	—	14	—	—	—	—

**Table 5.** Bivalve distribution, Pagat Member, Tanjung Formation in the Asem Asem Basin, near Satui. The abbreviation ‘ab.’ denotes ‘abundant’.

Taxonomic grouping	14-3	14-6	19-1	19-2	19-3	19-4
Nuculanoidea?: Nuculanidae?	—	1	—	—	—	—
Pectinoidea: Pectinidae	4	—	4	4	—	—
Pectinoidea: Spondyliidae?	—	1	—	—	—	—
Ostreoidea: Gryphaeidae:	—	3	10	1	3	8
Pycnodonteinae	—	—	—	—	—	—
Ostreoidea: oyster attachments on corals	—	3	3	1	8	1
Ostreoidea: indeterminate fragments	ab.	ab.	ab.	ab.	ab.	ab.
Chamoidea: Chamidae	—	—	—	—	—	1
Carditioidea: Carditidae: “ <i>Carditamera</i> ”	2	—	2	—	—	—
Cardioidea: Cardiidae 1	1	—	—	1	—	3
Cardioidea: Cardiidae 2	1	—	1	—	—	1
Tellinoidea: Tellinidae: “ <i>Apolymetis</i> ”	4	—	—	—	—	10
Tellinoidea: Tellinidae	2	—	2	1	—	—
Myoidea?: Corbulidae?	—	1	—	—	—	—
Heterodonta 1	—	1	—	—	—	—
Heterodonta 2	4	—	—	—	—	—
Heterodonta 3	1	—	—	—	—	2
Heterodonta 4	—	—	1	—	—	—
Pinnoidae: Pinnidae: cf. <i>Pinna</i> sp.	—	—	—	—	—	1
Bivalve	—	—	6	—	—	2
Indeterminant bivalve fragments	—	21	2	—	27	—

the modern Indo-Pacific region. *Cycloseris* cf. *C. sinensis* in the study area form low, flat horns with broad calyces, 5 to 25 mm in diameter. *Trachyphyllia* sp. is a small (25 × 45 mm) merulinid coral. *Trachyphyllia* are free-living solitary and colonial corals also common in the modern Indo-Pacific region.

**Table 6.** Coral distribution, Pagat Member, Tanjung Formation in the Asem Asem Basin, near Satui.

Taxonomic grouping	14-3	14-6	19-1	19-2	19-3	19-4
Anthemiphyllidae: <i>Anthemiphyllia</i> sp.	8	—	15	—	4	—
Dendrophyllidae: <i>Balanophyllia</i> sp. 1	4	—	3	4	—	—
Dendrophyllidae: <i>Balanophyllia</i> sp. 2	2	—	—	—	—	—
Dendrophyllidae: <i>Balanophyllia</i> sp. 3	1	—	—	—	—	—
Dendrophyllidae: <i>Balanophyllia</i> sp. 4	5	—	—	—	—	—
Caryophyllidae: <i>Caryophyllia</i> sp.	76	25	34	7	31	7
Caryophyllidae: <i>Trochocyathus</i> sp.	—	1	—	—	—	—
Fungiidae: <i>Cycloseris</i> spp.	3	33	29	—	114	11
Merulinidae: <i>Trachyphyllia</i> sp.	—	—	1	—	—	—

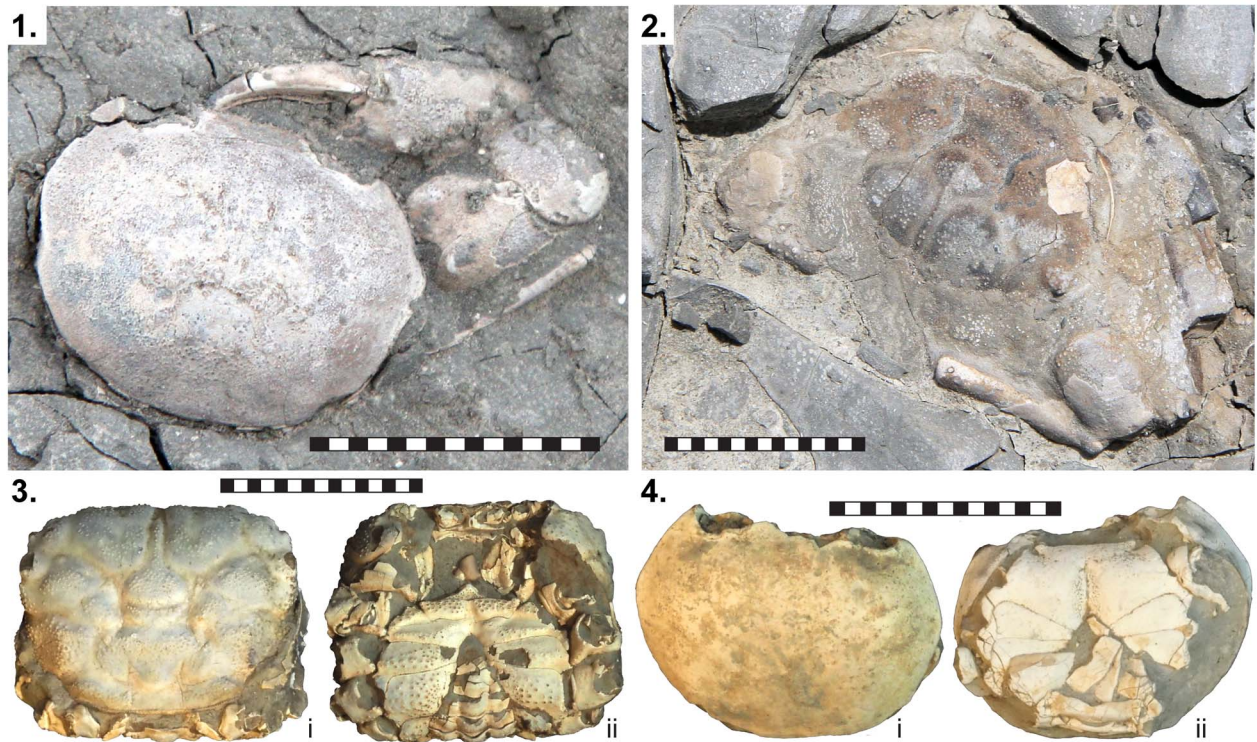


**Figure 18.** Brachyuran decapod crustaceans from the Pagat Member, Satui region, Kalimantan. Scale bar increments are millimeters. (1) Goneplacoid eubrachyuran crab specimen in dorsal view, in situ, with attached right claw and merus of pereopod, from shale succession below layer 14-4 (33.1 m), UA-P2195. (2) Goneplacoid eubrachyuran crab specimen in dorsal view, in situ, with attached right claw and proximal parts of left pereopods, from shale succession below layer 14-4 (33.1 m), UA-P2196. (3) Goneplacoid eubrachyuran crab carapace in dorsal (i) and ventral (ii) views, layer 19-2B (97.5 m), UA-P2164. (4) Tumidocarcinid (cf. *Lobonotus* sp.); carapace in dorsal (i) and ventral (ii) views, layer 19-2C (80.5 m), UA-P2161.

The four azooxanthellate forms include two small caryophyllids (*Caryophyllia* sp. and *Trochocyathus* sp.), a small anthemiphylliid (*Anthemiphyllia* sp.), and a small dendrophylliid (cf. *Balanophyllia* sp.). *Caryophyllia* from the Pagat Member are small horn-shaped corals up to 2 cm high and 1.3 cm in diameter (Fig. 19). *Trochocyathus* in the study area are small (0.5–1.1 cm diameter) horn-shaped disks. *Balanophyllia* in the study area form narrow ovoid horns up to 15 mm long and up to 7 mm in diameter.

*Anthemiphyllia* sp. occurs in small numbers in the 15.7–17.65 m bed, the 80.0–80.35 m bed, and the 93.3 to 93.6 m bed (Fig. 19). Four morphotypes of *Balanophyllia* are differentiated. All four occur in the 15.7–17.65 m bed, with morphotype A also occurring higher in the section, in the 80.0–80.35 m and in the 87.8–88.1 m beds. *Trochocyathus* and *Trachyphyllia* are uncommon, occurring only in the 71.4–71.9 m bed (Fig. 19). *Cycloseris* cf. *C. sinensis* and *Caryophyllia* sp. are the most abundant taxa, occurring throughout the study interval, with *Cycloseris* cf. *C. sinensis* more common lower in the section and *Caryophyllia* abundant in the 87.8–88.1 m bed (Fig. 19).

Echinoidea.—Echinoids are represented by partial tests of one spatangoid species and two cidaroid species, scattered interambulacral plates, and numerous cidaroid spines (Fig. 20). Two spatangoids and a partial test of the cidarid echinoid cf. *Goniocidaris* sp. were collected from the 15.7–17.65 m bed (Fig. 20.2 and 20.3). Neither of the spatangoids is sufficiently well preserved to confidently assign them to genera or species. Three interambulacral plates consistent with cf. *Porocidaris* sp. were also collected from the 80.1–80.35 m bed (Fig. 20.4).

In addition, cidarid spines exhibiting a variety of morphologies (Fig. 20.5–20.17) were present and abundant in all the fossiliferous rudstone beds. These include spines with smooth shafts, ridged shafts, abundant minute thorns, mamillated bumps, and flat-bladed or barbed/serrated branches (Fig. 20). Some morphologies are consistent with those described from well-preserved *Goniocidaris* spp. (Fig. 20.10–20.13) or *Porocidaris* spp. (Fig. 20.15–20.17), but the anatomy of Eocene cidarid spines is of limited taxonomic use beyond generic attribution.

As well as echinoid detritus, isolated asteroid skeletal elements were observed in all thin sections. These were differentiated from echinoid skeletal elements by their highly variable morphology and higher porosity.

Encrusting forms: serpulids, ostreids and Bryozoa.—A low-diversity assemblage of encrusting invertebrate taxa occurs in the Pagat Member at Satui (Fig. 21). These include coralline algae, ostreids, serpulid worm tubes (Serpulinae and Spirorbinae), and a variety of cheilostomate and cyclostomatid bryozoans. These encrusting taxa commonly occur attached to random bioclastic detritus and occur in all bioclastic rudstone and bioclastic grainstone beds in the study interval (Fig. 21). Larger bryozoan specimens commonly encrust multiple bioclasts.

Minute ostreids (25–150 mm<sup>2</sup>) are common, attached to the lateral surfaces of solitary azooxanthellate corals (particularly cf. *Caryophyllia* sp. and cf. *Cycloseris* sp.) (Fig. 21.10). The small size of these corals severely limits the size that attached

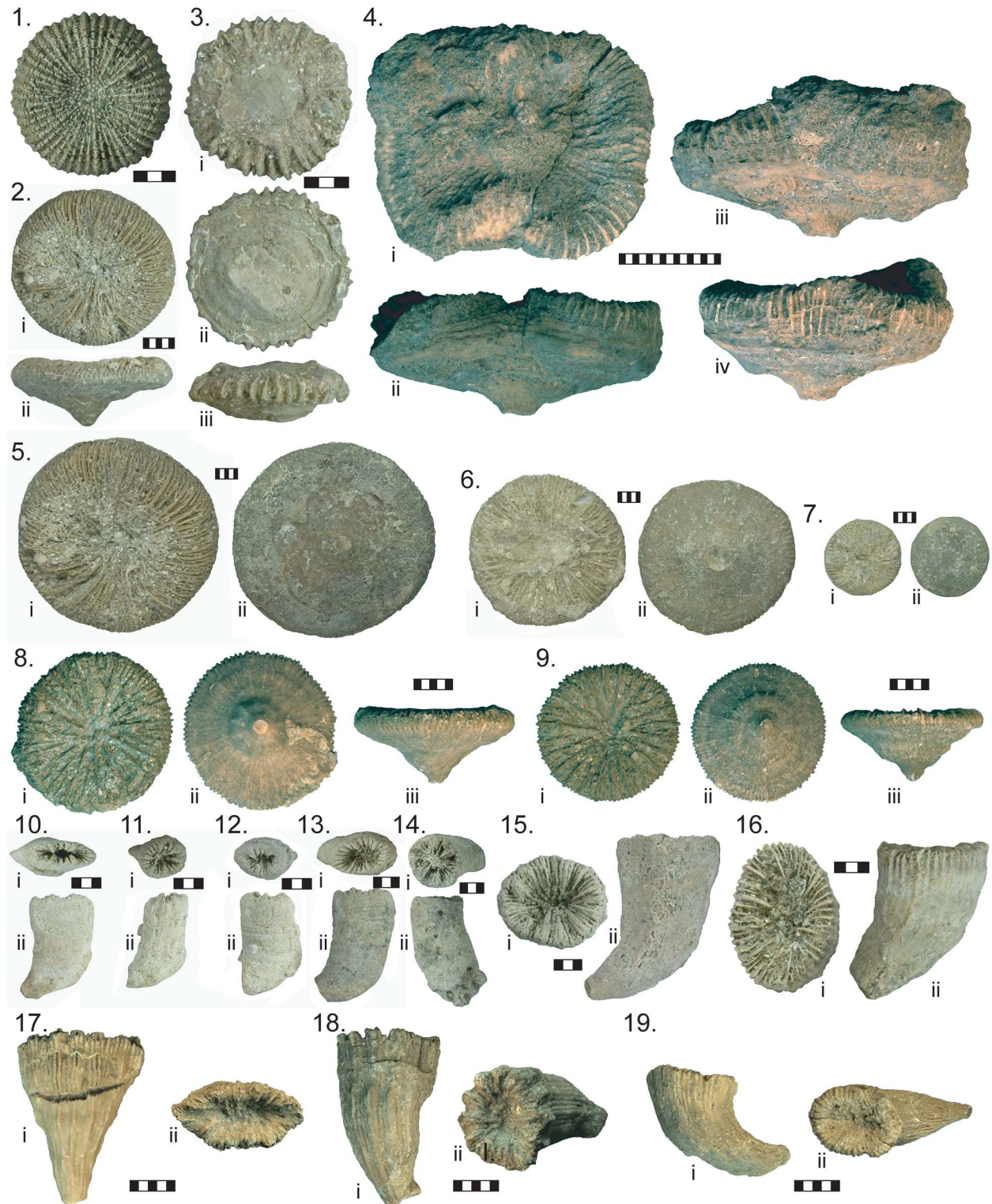


**Figure 19.** Corals of the Pagat Member, Satui region, Kalimantan. Scale bar increments are millimeters. (1) *Anthemiphyllia* cf. *A. dentata* (Alcock, 1902) from layer 14-3c (17.5 m), UA-P2165. (2) *Cycloseris* sp. from layer 14-6 (71.5 m), calicular (i) and lateral (ii) views, UA-P2166. (3) Coral from layer 14-3c (17.5 m), calicular (i), basal (ii), and lateral (iii) views, UA-P2167. (4) *Trachyphyllia* sp. from layer 19-2C (80.5 m), calicular (i) and lateral (ii–iv) views, UA-P2168. (5–7) Large, intermediate, and small *Cycloseris* sp. 1 from layer 14-6 (71.5 m), calicular (i) and basal (ii) views, UA-P2169, UA-P2170, and UA-P2171. (8, 9) *Cycloseris* sp. 2 from level 19-2C (80.5 m), calicular (i), basal (ii), and lateral (iii) views, UA-P2172 and UA-P2173. (10–14) *Balanophyllia* spp. from layer 14-3c (17.5 m), calicular (i) and lateral (ii) views, UA-P2174, UA-P2175, UA-P2176, UA-P2177, and UA-P2178. (15) *Caryophyllia* sp., layer 14-6 (71.5 m), calicular (i) and lateral (ii) views, UA-P2179. (16) *Caryophyllia* sp. from layer 14-6 (71.5 m), calicular (i) and lateral (ii) views, UA-P2180. (17–19) *Caryophyllia* sp. from layer 19-2A (93.5 m), lateral (i) and calicular (ii) views, UA-P2181, UA-P2182, and UA-P2183.

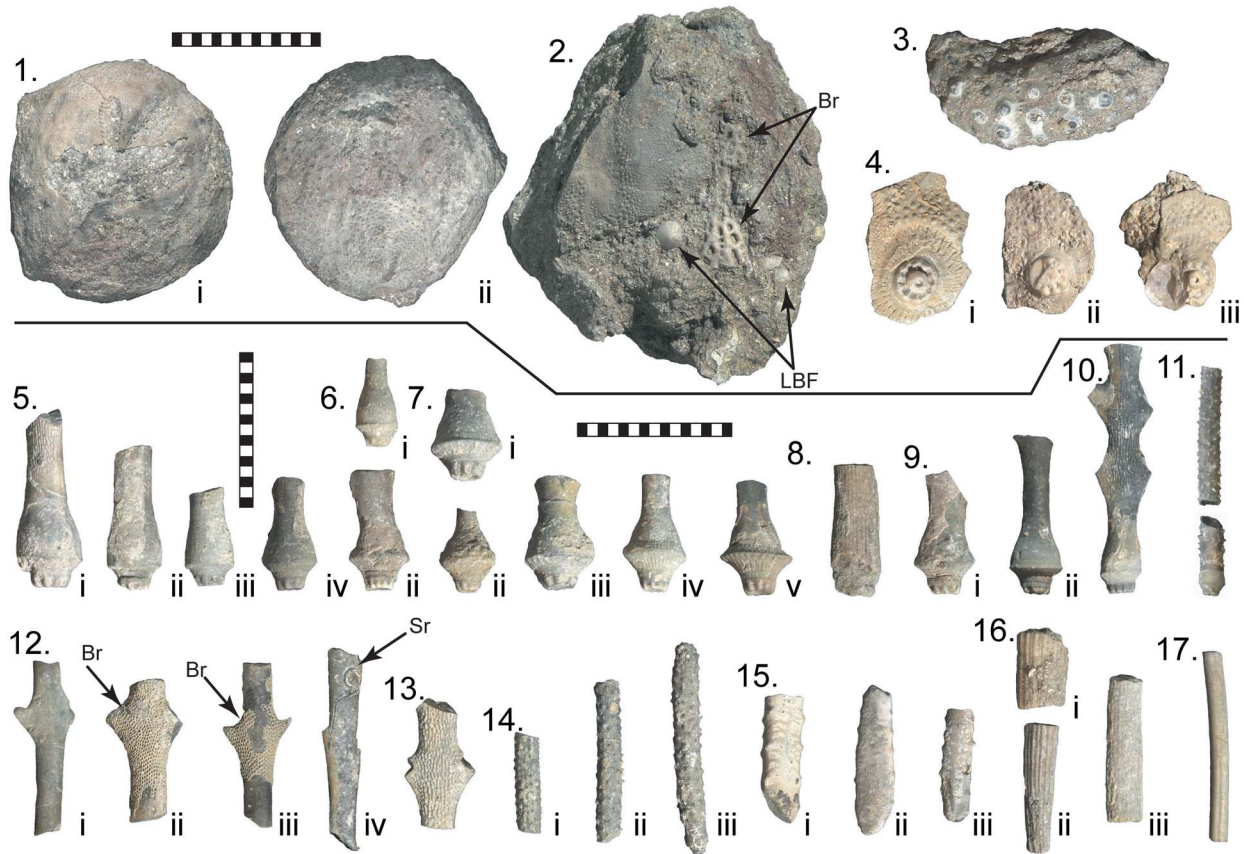


**Figure 20.** Echinoid fossils from the Pagat Member, Satui region, Kalimantan. Scale bar increments are millimeters. (1) Spatangoid echinoid from layer 14-3b (17.05 m), aboral (i) and oral (ii) surfaces, UA-P2141. (2) Fragment of the dorsal surface of a spatangoid echinoid within a matrix with fragments of fenestrated bryozoans (Br) and foraminifera (LBF), from layer 14-3c (17.65 m), UA-P2142. (3) Partial test of the cidarid echinoid *Goniocidarid* sp. from layer 14-3c (17.65 m), UA-P2143. (4) Three interambulacral plates from cf. *Porocidarid* sp. from layer 19-2C (80.1–80.5 m), UA-P2144. (5) Echinoid spine type 1 exhibiting a toothed base and tapered collar, (i) layer 19-2D (87.8–88.1 m), UA-P2145, (ii) layer 19-2C (80–80.35 m), UA-P2197, (iii) layer 19-2D (87.8–88.1 m), UA-P2198, and (iv) layer 19-2C (80–80.35 m), UA-P2199. (6) Echinoid spine type 2 with a toothed base and slender rimmed collar, (i) layer 19-2C (80–80.35 m), UA-P2146, and (ii) layer 19-2C (80–80.35 m), UA-P2200. (7) Echinoid spine type 3 with a toothed base, a ridged milled ring, and a wide, sharply rimmed collar, (i) layer 19-2D (87.8–88.1 m), UA-P2147, (ii) layer 19-2A (93.3–93.6 m), UA-P2201, (iii) layer 19-2D (87.8–88.1 m), UA-P2202, (iv) layer 19-2A (93.3–93.6 m), UA-P2203, and (v) layer 19-2A (93.3–93.6 m), UA-P2204. (8) Echinoid spine type 4 with a smooth base, a slender collar, and longitudinal ridges, layer 14-3 (15.7–17.65 m), UA-P2148. (9) Echinoid spine type 5 with a toothed base, wide, rimmed collar, and a flattened smooth barbed shaft, (i) layer 19-2C (80–80.35 m), UA-P2149, and (ii) layer 19-2C (80–80.35 m), UA-P2205. (10) Echinoid spine type 6 with a toothed base, slender collar, and a flattened crenulated barbed shaft, layer 19-2D (87.8–88.1 m), UA-P2150. (11) Echinoid spine type 7 with a slender collar and a distinctly thorny shaft, (i) layer 19-2D (87.8–88.1 m), UA-P2151, and (ii) layer 19-2D (87.8–88.1 m), UA-P2206. (12) Fragments of flattened crenulated barbed spine shafts, (i) layer 14-6 (71.4–71.9 m), UA-P2152, (ii) layer 14-3 (15.7–17.65 m), UA-P2207, (iii) layer 14-6 (71.4–71.9 m), UA-P2208, and (iv) layer 19-2D (87.8–88.1 m), UA-P2209. Note the bryozoans (Br) on ii and iii (arrows) and the spirorbid serpulid (Sr) on iv (arrow). (13) Fragment of flattened crenulated barbed spine shaft, layer 19-2D (87.8–88.1 m), UA-P2153. (14) Fragments of thorny spine shafts, (i) layer 14-6 (71.4–71.9 m), UA-P2154, (ii) layer 14-6 (71.4–71.9 m), UA-P2210, and (iii) layer 14-6 (71.4–71.9 m), UA-P2211. (15) Fragments of mamillated, bumpy spine shafts, (i) layer 19-2B (97.2–97.6 m), UA-P2155, (ii) layer 19-2B (97.2–97.6 m), UA-P2212, and (iii) layer 19-2B (97.2–97.6 m), UA-P2213. (16) Fragments of longitudinally ridged spine shafts, (i) layer 19-2A (93.3–93.6 m), UA-P2156, (ii) layer 19-2B (97.2–97.6 m), UA-P2214, and (iii) layer 19-2A (93.3–93.6 m), UA-P2215. (17) Fragment of slender, smooth spine shaft, layer 19-2A (93.3–93.6 m), UA-P2157.

ostreids can attain. Larger ostreids occurred resting on and attached to seafloor bioclastic detritus. Although large ostreids are common, they are underrepresented in the collected material because they commonly fragment and disaggregate shortly after exposure.

Small, simple serpulids (both Serpulinae and Spirorbinae) occur cemented to the external surface of small solitary corals (cf. *Caryophyllia* sp. and cf. *Cycloseris* sp.) (Fig. 21.10 and 20.13). These occur on approximately 35% of cf. *Caryophyllia* sp. and 25% of cf. *Cycloseris* sp. specimens collected in the study area. Serpulids were common on the lateral surfaces of both cf. *Caryophyllia* sp. and cf. *Cycloseris* sp. but also occur on the calicular surface of cf. *Caryophyllia* sp. Those on the lateral surfaces occurred in both aperture-up and aperture-down

orientations. Most colonized corals have single epibionts; however, several were characterized by multiple epibionts. In some of these latter examples, the epibionts colonized several sides of the coral, supporting the hypothesis that, in some cases, the coral was alive and in growth position when the epibionts colonized it or, alternatively, that the corals rolled after the initial colonization and were subsequently colonized by a latter generation of epibiont.

Echinoid spines are commonly encrusted by cyclostomate bryozoans, cheilostomate bryozoans, and, rarely, coiled serpulids (Spirorbinae) (Figs. 20.12 and 21.4). The bryozoans commonly completely encircle the spine shafts, which may indicate that the encrustation occurred while the echinoids were alive. Cyclostomate bryozoans also occur on some larger

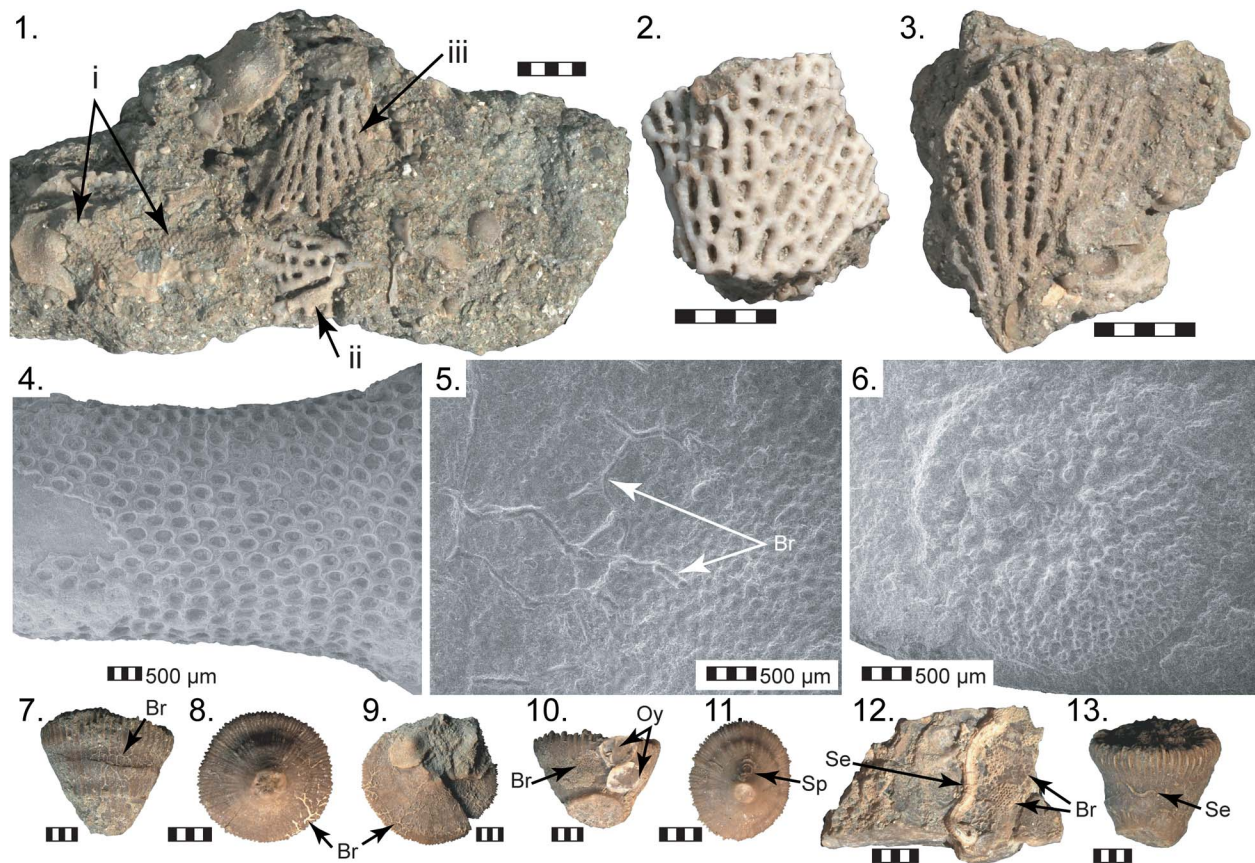


**Figure 21.** Bryozoa and other encrusting taxa in the Pagat Member, Satui region, Kalimantan. Scale bar increments are millimeters, with the exception of the scale bars in the SEM images which are in 100  $\mu\text{m}$  increments. Common encrusters include bryozoans (Br), oysters (Oy), spirorbiniid polychaetes (Sp), and serpulid polychaetes (Se). (1) Three groups of bryozoans including one morphospecies of cheilostomatid bryozoans attributed to cf. *Tubiporella* sp. (i) and two cyclostomates (ii, iii) in foraminiferal rudstone from level 19-2A (93.5 m), UA-P2158. (2, 3) Cyclostomata: Lichenoporidae on foraminiferal packstone, level 19-2A (93.5 m), UA-P2159, UA-P2160. (4) SEM of Cheilostomata: Calloporidae on an echinoid spine, level 14-3c (17.6 m), UA-P2185. (5) Branching, uniserial cyclostomate bryozoan on the surface of a larger benthic foraminifera, level 14-6 (71.5 m), UA-P2186. (6) Circular bryozoan patch on the surface of a larger benthic foraminifera, level 14-6 (71.5 m), UA-P2187. (7) Branching uniserial cyclostomate bryozoan on the lateral wall of a small *Caryophyllia*, level 19-2A (93.5 m), UA-P2188. (8) Branching uniserial cyclostomate bryozoans on the base of a small *Cycloseris*, layer 19-2C (80.5 m), UA-P2189. (9) Branching bryozoans on the base of a small *Cycloseris*, layer 19-2C (80.5 m), UA-P2190. (10) Two small oysters and a bryozoan patch on the wall of a small *Caryophyllia*, layer 19-2C (80.5 m), UA-P2191. (11) Spirorbiniid polychaete tube on the base of a small *Cycloseris*, layer 19-2C (80.5 m), UA-P2192. (12) Oyster fragment with multiple encrusters including two types of bryozoans and a serpulid polychaete tube, layer 19-2C (80.5 m), UA-P2193. (13) Serpulid polychaete tube on the wall of a small *Caryophyllia*, layer 19-2C (80.5 m), UA-P2194.

benthic foraminifera (Fig. 21.5 and 21.6) and on cf. *Caryophyllia* sp. (Fig. 21.7–21.10), particularly those collected from the 71.4–71.9 m bed. These commonly occur as chains of uniserial zoecia (cf. *Stomatopora* sp.) encrusted on the external surface of disc-shaped foraminifera.

In addition to small forms encrusting upon individual bioclasts, larger patches of bryozoans occur on and within the bioclastic detritus that formed the Pagat sea floor in the study area, primarily within bioclastic floatstone and rudstone facies (Fig. 21.1–21.3). Coralline algae (cf. *Lithoporella* sp.), which were identified in thin sections, occur in foraminiferal rudstone facies throughout the study interval, most commonly as isolated strands accreted to individual bioclasts or to bioclastic detritus.

## Discussion

*Age of the Pagat Member in the Asem Asem Basin.*—As discussed above, 10 of the 12 bioclastic floatstone and rudstone beds in the study interval contained identifiable larger benthic foraminifera (Figs. 4–6). These fossils constrain

the study interval to a late Eocene Tb age (SBZ 18–20/Priabonian), prior to the Eocene/Oligocene boundary. The Pagat Member in the Barito Basin to the north ranges in age from late Eocene into the early Oligocene (East Indian letter stages Tb–Td) based on planktonic foraminifera, larger benthic foraminifera, and palynological analyses (Witts et al., 2012b). The upper part of the Pagat was not accessible during field analyses in this project, and the Pagat–Beraï contact was not observed. At present, it is not demonstrable whether or not the Pagat Member in the Asem Asem Basin straddles the Eocene–Oligocene Boundary.

*Relative sea level and paleoenvironmental conditions.*—The Mangkook, Tambak, and Pagat members of the Tanjung Formation in southern Kalimantan record an overall deepening-upwards succession (Witts et al., 2012b). The Tanjung Formation grades from conglomerate and pebbly sandstone deposited in an alluvial braidplain setting (Witts et al., 2012b) through a heterolithic, interstratified mudstone, siltstone, very fine-grained sandstone, and coal succession

deposited in coastal floodplain, estuarine, and deltaic settings (Witts et al., 2012b; Zonneveld et al., 2024). The Tanjung Formation culminates in the interbedded siliciclastic and carbonate beds of the Pagat Member, which are the focus of the present study. Although these units occur in a vertical succession in the study area, they formed lateral components in a complex coastal depositional system (Siregar and Sunyaro, 1980; Kusuma and Darin, 1989; Satyana et al., 2001; Witts et al., 2012b; Zonneveld et al., 2012, 2024).

The Pagat Member in the Satui area is overwhelmingly dominated by variably silty/sandy calcareous mudstone. Coarser-grained horizons (interbedded silty shale/sandstone; bioclastic sandstone and bioclastic rudstone), which comprise approximately 9% of the vertical section, decrease in proportional abundance up-section (Fig. 4). Similarly, the proportion of siliciclastic sediment in coarser-grained intervals decreases up-section (Fig. 10). The retrogradational stratal stacking pattern, upwards decrease in the proportional abundance of clastic sediment (and concomitant increase in the proportional abundance of bioclasts), distribution of invertebrate fossil distribution patterns and trace fossil distribution patterns in the study interval are consistent with an overall transgressive cycle, consistent with interpretations of the Tanjung Formation in the Barito Basin to the north (Witts et al., 2012b). It is worth noting that inferences on bathymetry and stratigraphic architecture are made solely on the basis of lithology, trace fossil distribution, and body fossil content. Limitation of lithologic exposures to the mine area precludes correlation of any surface for more than ~4 km, and thus regionality of depositional units and important surfaces could not be assessed.

Glaucinite, which is common in the lower part of the study interval, forms under moderately reducing conditions via the degradation of other minerals, such as biotite, typically in the presence of decomposing organic detritus (Jeans et al., 2000; Deer et al., 2013). This is consistent with the inferred depositional setting of the Pagat Member, proximal to the Tambak coastal plain succession, which was characterized by extensive coal swamps and numerous sluggish meandering rivers and deltas (Spagnuolo et al., 2024; Zonneveld et al., 2024). Abundant glauconitic pellets and peloids in heterolithic silty shale, muddy sandstone, and bioclastic rudstone beds are consistent with deposition in a distal-shelf/mid-ramp, temperate, subtropical, or tropical shelf setting (Odin and Matter, 1981; Odin and Fullagar, 1988; Leithold, 1989; Bannerjee et al., 2012, 2016, 2018; Stassen et al., 2015). Siliciclastic sediment (clay, silt, and very fine-grained sand) was delivered to the coast by Tambak fluvial-deltaic and estuarine channel systems (Zonneveld et al., 2024). Sediment delivery was likely seasonal/episodic, allowing sufficient time for microbial degradation of organic matter and alteration of fecal material to glauconite (sensu Odin and Matter, 1981; López-Quirós et al., 2019).

Trace fossils provide clear constraints on the depositional environment of the lower part of the study interval. Heterolithic silty sand, glauconitic sandstone, and sandy bioclastic rudstone/grainstone beds are characterized by a diverse suite of trace fossils that represent a wide variety of behaviors, including shallow- and deep-tier infaunal deposit feeding as well as the domiciles of carnivores, detritivores, and suspension feeders (Table 4). This assemblage and its mix of ethologies is consistent with the

*Cruziana* ichnofacies, which most commonly occurs in successions emplaced in mid-ramp/mid to distal continental shelf settings below fairweather but above storm wave base (MacEachern et al., 2012; Pemberton et al., 2012).

Soft-bottom trace fossil assemblages in the shale-dominated upper part of the study interval are low in density and low in diversity, likely due to substrate constraints. Many taxa are unable to suspend themselves or move in soupy substrates, and for those that do, the preservation potential of the traces is quite low (Ekdale, 1985; Rine and Ginsburg, 1985; O'Brien, 1987). Overall, the proportion of endobenthos appears to have been much lower in finer-grained lithologies than in siliciclastic sandstone and bioclastic wackestone, packstone, and rudstone facies. The reduced proportion of coarse lithologies to shale and the low-diversity *Zoophycos* trace fossil assemblage are consistent with the interpretation of the study interval as an overall transgressive stratigraphic succession.

Many of the coarser beds/bedsets throughout the study interval are emplaced upon erosional discontinuity surfaces demarcated by moderate diversity *Glossifungites*, and less commonly, *Trypanites* trace fossil assemblages (Figs. 11 and 14). Substrate-controlled trace fossil assemblages are common in mixed siliciclastic–carbonate depositional systems (Zonneveld et al., 2012, 2024; Schultz et al., 2016). This is due primarily to incipient and early cementation associated with hiatal and exhumed surfaces in mixed systems (Zonneveld et al., 2012, 2024; Schultz et al., 2016). Glaucinite commonly occurs above erosional surfaces in transgressive stratigraphic settings (Jeans et al., 2000; Clark and Robertson, 2005; Deer et al., 2013; Hegab et al., 2016). In the basal part of the study interval, glauconitic sediment is common in an interval characterized by numerous erosional surfaces (*Glossifungites* and *Trypanites* ichnofacies; Fig. 11). Glaucinite in the study interval is particularly common, in association with a foraminifera-rich burrow fill, within *Thalassinoides* and *Skolithos* burrows penetrating through compacted firmground and cemented hardground successions. Evidence of subaerial exposure is lacking. The sharp bedding contacts, truncated burrows, and burrow fills dominated by marine bioclasts suggest that these surfaces most likely represent storm-wave ravinement surfaces (e.g., Wanless et al., 1988; Tedesco and Wanless, 1991; Zonneveld et al., 2012; Reuter et al., 2013).

All bioclastic rudstone and bioclastic grainstone beds in the study interval are dominated by benthic foraminifera, although gastropods, bivalves, coralline algae, solitary corals, and disarticulated echinoid skeletal elements may also be abundant (Figs. 4–6). Larger benthic foraminifera (LBF) are particularly abundant and indicate deposition in the photic zone in neritic marine environments (Hallock, 1981; Racey, 2001; Beavington-Penney and Racey, 2004; Beavington-Penney et al., 2005; BouDagher-Fadel, 2008; BouDagher-Fadel and Price, 2010). The abundance and number of taxa of LBF in the rudstone beds are consistent with deposition in a tropical to sub-tropical shallow marine depositional setting (Hallock, 1981; Racey, 2001; Beavington-Penney and Racey, 2004; Beavington-Penney et al., 2005; BouDagher-Fadel and Price, 2010; Less et al., 2011; BouDagher-Fadel, 2018). The foraminifera fauna is consistent with other regional faunas and is part of the equatorial *Assilina–Pellatispira–Biplanispira* fauna that characterizes much of Island Southeast Asia during the Eocene (Lunt, 2003).

The co-occurrence of foraminifera, bryozoans, conoid, buccinoid, cypraeoid, muricoid, tonnoid gastropods, echinoids, and zooxanthellate and azooxanthellate solitary corals support the interpretation of an open marine depositional setting for the study interval (e.g., Cairns and Parker, 1992; Cairns and Zibrowius, 1997; Duda and Kohn, 2005; Cairns and Kitahara, 2012; Cairns, 2016; Galindo et al., 2016; Tracey et al., 2017; Astibia et al., 2018). The occurrence of coralline algae in the bioclastic rudstone beds further constrains the depositional setting to a proximal or mid-ramp setting shallower than ~200 m depth (Bosence, 1991; Aguirre et al., 2000).

*Paleoecological inferences based on the mollusk fauna.*—Overall, the fauna comprises typically tropical to subtropical elements (e.g., *Conus* sensu stricto), and all taxa reflect normal marine salinities. The bivalve fauna is sparse and moderately diverse but comprises carditids, cardiids, and tellinids, all of which are typical shelf taxa. It lacks abundant protobranchs and anomalodesmatans that might indicate deposition at bathyal or greater depths.

The gastropod fauna is dominated in both abundance and species richness by neogastropod caenogastropods and common tonnoids, although other ‘lower’ caenogastropods are rare. Overall, the fauna is clearly deeper than intertidal, but the rarity of Turridae (sensu lato) among the wide range of carnivorous gastropods present suggests depths that are shallower than bathyal (e.g., Roy, 2002; Brandt et al., 2009; Ludt and Rocha, 2015; Petuch and Berschauer, 2020). This is confirmed by the absence of deposit-feeding vetigastropods and the uncommon occurrence of heterobranchs. The absence of algal-feeding ‘mesogastropods’ may suggest deposition in deeper shelf depths (~60–100 m), which is not contradicted by the bathymetric ranges of recent cassids, pediculariids, epitoniids, ‘fulgorariine’ volutids, and architectonicids (Roy, 2002; Brandt et al., 2009; Ludt and Rocha, 2015; Petuch and Berschauer, 2020). When considered in association with other components of the fauna, such as zooxanthellate corals, and the occurrence of coralline algae in bioclastic packstone thin sections, it is likely that this fauna actually occurred in a shallower setting than its composition indicates, likely as a result of unfavorable muddy substrates throughout most of the Pagat coastline, with favorable conditions restricted to isolated patches of foraminiferal packstone/rudstone.

In terms of diet, the gastropod fauna consists almost entirely of predators (e.g., Kohn, 1959; Hughes and Hughes, 1971, 1981; Ingham and Zischke, 1977; Taylor and Reid, 1984; Hughes, 1986; Taylor and Morton, 1996; Duda et al., 2001; Walker, 2007; Tyler et al., 2018). This may indicate that a wide range of poorly represented, skeletonized, or unpreserved, soft-bodied benthos was present during the late Eocene at Satui. Modern pediculariids, epitoniids, and architectonicids are specialized predators (or ectoparasites) on a range of cnidarians, including scleractinian corals, octocorals, zoanthids, and sea anemones (e.g., Robertson, 1970; Cumming, 1997; Gittenberger and Hoeksema, 2013; Nützel, 2021). Although numerous small solitary corals occur within the fauna, these do not seem sufficient for the gastropod predator fauna preserved in the Satui Pagat fauna. Volutids are generalized carnivores or scavengers (Bigatti et al., 2009), cassids are echinoderm predators

(Hughes and Hughes, 1971, 1981; Hughes, 1986; Walker, 2007; Tyler et al., 2018), and conids feed primarily on mollusks and a range of ‘worms’ (Kohn, 1959, 1985).

*Community dynamics of the invertebrate fauna.*—Many of the corals and some of the mollusks host encrusting taxa, including serpulids, minute ostreids, and bryozoans, confirming euhaline depositional conditions. Rare corals exhibited boring trace fossils, such as *Oichnus* sp., and mollusk fossils exhibit a range of macroborings (*Entobia*, *Oichnus*, *Trypanites*, and *Rogerella*) and microborings. *Entobia* are attributed to the activities of filter-feeding sponges (Bromley, 1970; Bromley and D’Alessandro, 1987; Tapanila, 2006). *Oichnus* (= *Sedilichnus*) on pectinid shells (*O. paraboloides*) are typically attributed to the activities of predatory gastropods (Fretter and Graham, 1962; Zonneveld and Gingras, 2014), whereas the tracemaker of the tiny *Oichnus* on LBF remains unknown. *Rogerella* are attributed to acrothoracian barnacles (Donovan and Jagt, 2013), and *Trypanites* are attributed to the activity of marine worms (Bromley and D’Alessandro, 1987). Micro-traces, observed in thin section on bivalve and gastropod shells, commonly record shell alteration/degradation through the activity of bacteria and algae. *Gastrochaenolites*, which occur on some lithoclasts and several larger bivalves, results from the activities of boring bivalves (Kelly and Bromley, 1984; Taylor and Wilson, 2003).

Although borings were rare on azooxanthellate coral specimens, small, simple serpulids (Serpulinae) and tiny ostreids occur cemented to the external surface of small solitary corals (cf. *Caryophyllia* sp. and cf. *Cycloseris* sp.). These occur on approximately 35% of cf. *Caryophyllia* sp. and 25% of cf. *Cycloseris* sp. specimens collected in the study area. Serpulids were common on the lateral surfaces of both cf. *Caryophyllia* sp. and 25% of cf. *Cycloseris* sp. but also occur on the calicular surface of cf. *Caryophyllia* sp. Those on the lateral surfaces occurred in both aperture-up and aperture-down orientations. Most colonized corals have single epibionts; however, several were characterized by multiple epibionts. In some of these latter examples, the epibionts colonized several sides of the coral, supporting the hypothesis that, in some cases, the coral was alive and in growth position when the epibionts colonized it or, alternatively, that the corals rolled after the initial colonization and were subsequently colonized by a later epibiont generation. In contrast, serpulids with apertures that open in other directions (e.g., laterally or towards the base of the coral) were likely post-mortem encrustations.

Minute ostreids (25–150 mm<sup>2</sup>) are common, attached to the lateral surfaces of solitary azooxanthellate corals (particularly cf. *Caryophyllia* sp. and cf. *Cycloseris* sp.). The small size of these corals may have severely limited the size that attached ostreids could attain. Larger ostreids occurred resting on and attached to seafloor bioclastic detritus. Although large ostreids are common, they are underrepresented in the collected material because they commonly fragment and disaggregate shortly after exposure. All ostreid attachments and most encrusting bryozoans were observed on the lateral walls of cf. *Caryophyllia* sp. or on the basal surface of cf. *Cycloseris* sp. and are thus interpreted to reflect primarily post-mortem encrustations. Bioclastic detritus in modern tropical settings is characterized by a mix

of pre-mortem and post-mortem encrustations (Cairns, 2004; Hoeksema et al., 2011), consistent with our observations of the Satui Pagat fauna.

*Development of bioclastic mounds on a mud-dominated coast.*—Modern larger benthic foraminifera, which include members of the family Nummulitidae, host a variety of algal photosymbionts (Lee, 1998; Hallock, 2000; Hallock and Pomar, 2009; Prazeres and Renema, 2019), therefore this is inferred to hold true for all fossil taxa. Larger benthic foraminifera usually live in shallow reef and carbonate shelf environments (BouDagher-Fadel, 2018), but nummulitids occasionally can occur in basal euphotic environments (e.g., Goeting et al., 2022, and references therein). Nummulitids are most common in mesophotic to oligophotic settings with low nutrient input, can thrive in both reefal agitated waters as well as quieter settings below fair-weather wave-base and sporadically can range down to over 100 m water depth (Lee, 1998; Hallock, 2000; Beavington-Penney and Racey, 2004; Beavington-Penney et al., 2005; Vecchio and Hottinger, 2007; Hallock and Pomar, 2009; BouDagher-Fadel and Price, 2010; Less et al., 2011; BouDagher-Fadel, 2018; Hallock and Seddighi, 2022). The similarity and close relationship between modern LBF and many Cenozoic fossil forms suggest that they possessed similar algal symbionts (Lee, 1998; Hallock, 2000; Hallack and Pomar, 2009; Hallock and Seddighi, 2022).

Foraminiferal tests in the Pagat Member do not show significant abrasions or broken parts and do not seem to have imbricate textures. This points to quiet hydrodynamics at the sea floor (minimal to no transport distance), which is also consistent with the large variety of shapes and sizes observed in thin sections and with the sporadic abundance of porcelaneous smaller benthic foraminifera (Hohenegger and Briguglio, 2012; Seddighi et al., 2015; Briguglio et al., 2017; Olariu and Zeng, 2018; Roslim et al., 2019).

The abrupt basal contacts, commonly characterized by *Glossifungites* or *Trypanites* assemblages (Figs. 3, 7, 13.4, and 13.5), indicate that most of the mounds developed on local omission or erosional surfaces that are interpreted to be ravinement surfaces emplaced by regional storm waves. These surfaces were colonized by a variety of taxa that prefer stable (firm or hard) substrates, including those that bored into them (forming the *Glossifungites* and *Trypanites* communities) and those that colonized the stabilized surface forming the first components of the bioclastic mound (Fig. 22). Subsequent generations colonized the bioclastic detritus produced as earlier organisms died.

The bioclastic mounds would have generated some relief above the adjacent sea floor (Fig. 22) and provided ‘islands’ of firmer, more stable substrate that was conducive to colonization by a variety of epifaunal organisms including corals, bryozoans, and some of the bivalve and gastropod taxa (e.g., Driscoll and Brandon, 1973; Kidwell and Jablonski, 1983; Kidwell, 1991; Zonneveld et al., 1997; Zonneveld, 2001). The Pagat biostromes reflect initiation and accumulation via both allogenic and autogenic taphonomic feedback processes (sensu Kidwell and Jablonski, 1983; Kidwell, 1991). When recruitment rates were high, the biostromes were self-maintaining and sustained topographic relief above the adjacent mud-dominated shelf (Fig. 22). When the influx

of fine-grained sediment outpaced the accretion rate of the mounds, possibly during intervals of higher mud-laden fresh-water influx, the mounds were buried.

*Implications for the early development of the Central Indo-Pacific marine biodiversity hotspot.*—The study area occurs in the Indo-Australian Archipelago, an area of exceptional present-day species richness, often referred to as a biodiversity ‘hotspot’ (Renema et al., 2008; Lohman et al., 2011). The heart of this region comprises the “Coral Triangle,” a major portion of which is Indonesian territory. The Coral Triangle is characterized by 76% of the world’s coral species and over half of the world’s coral reefs (Stehli and Wells, 1971; Hoeksema, 2007; Allen, 2008; Veron et al., 2009; Asaad et al., 2018a, b), however the timing and nature of the origin of this marine biodiversity hotspot remain poorly understood and the subject of continued study (Renema et al., 2008; Halas and Winterbottom, 2009; Bellwood et al., 2012; Mihaljević et al., 2014, 2017; Yasuhara et al., 2022).

During the early and middle Eocene, global marine biodiversity hotspots developed in the northwestern and northeastern Tethys regions (Renema et al., 2008). These hotspots, predecessors to the modern Coral Triangle, were characterized by exceptionally high diversity of LBF, mollusks, mangroves, and corals (Kay, 1996; Wilson and Rosen, 1998; Elison et al., 1999; Morley, 2000; Wallace and Rosen, 2006; Renema, 2007; Renema et al., 2008; Król et al., 2016; Bosellini et al., 2022). However, following the Eocene–Oligocene transition, this diversity began to decrease through the Oligocene and into the Miocene (Renema, 2007; Yasuhara et al., 2022). As biodiversity declined in the Tethyan region, it increased in the Indo-Pacific, resulting in a biodiversity hotspot by the Miocene that persisted into the modern (Johnson et al., 2015a, b; Santodomingo et al., 2015a, b, 2016; Mihaljević et al., 2017; Yasuhara et al., 2022).

Wilson and Rosen (1998) referred to the paucity of Paleogene corals in the Indo-Pacific region as the “Paleogene gap.” Although there are some records of corals from the Eocene, they were mainly composed of a few taxa that did not build reefs. Instead, during this period, carbonate platforms were mainly built by larger benthic foraminifera (Wilson and Rosen, 1998). This is consistent with observations from the Pagat Member in the present study. Larger benthic foraminifera are diverse, abundant, and the dominant contributor to biostrome development, whereas the coral fauna comprises a low-diversity assemblage of free-living forms, none of which is ancestral to modern reef-building forms. The first occurrence of abundant and diverse coral assemblages in northern Borneo (Sabah, Malaysia) shrinks the gap and pushes the origin of the Coral Triangle to at least the early Oligocene (McMonagle et al., 2011; McMonagle, 2012).

Although devoid of reef-forming corals, the Satui Pagat invertebrate fauna provides invaluable data from the heart of the Indo Pacific region during the late Eocene because it comprises a moderately diverse tropical marine fauna consisting of ~40 mollusk genera, ~13 larger benthic foraminifera genera, 6 solitary coral genera, at least 4 crab genera, at least 3 echinoid genera, and a variety of bryozoans, serpulids, and

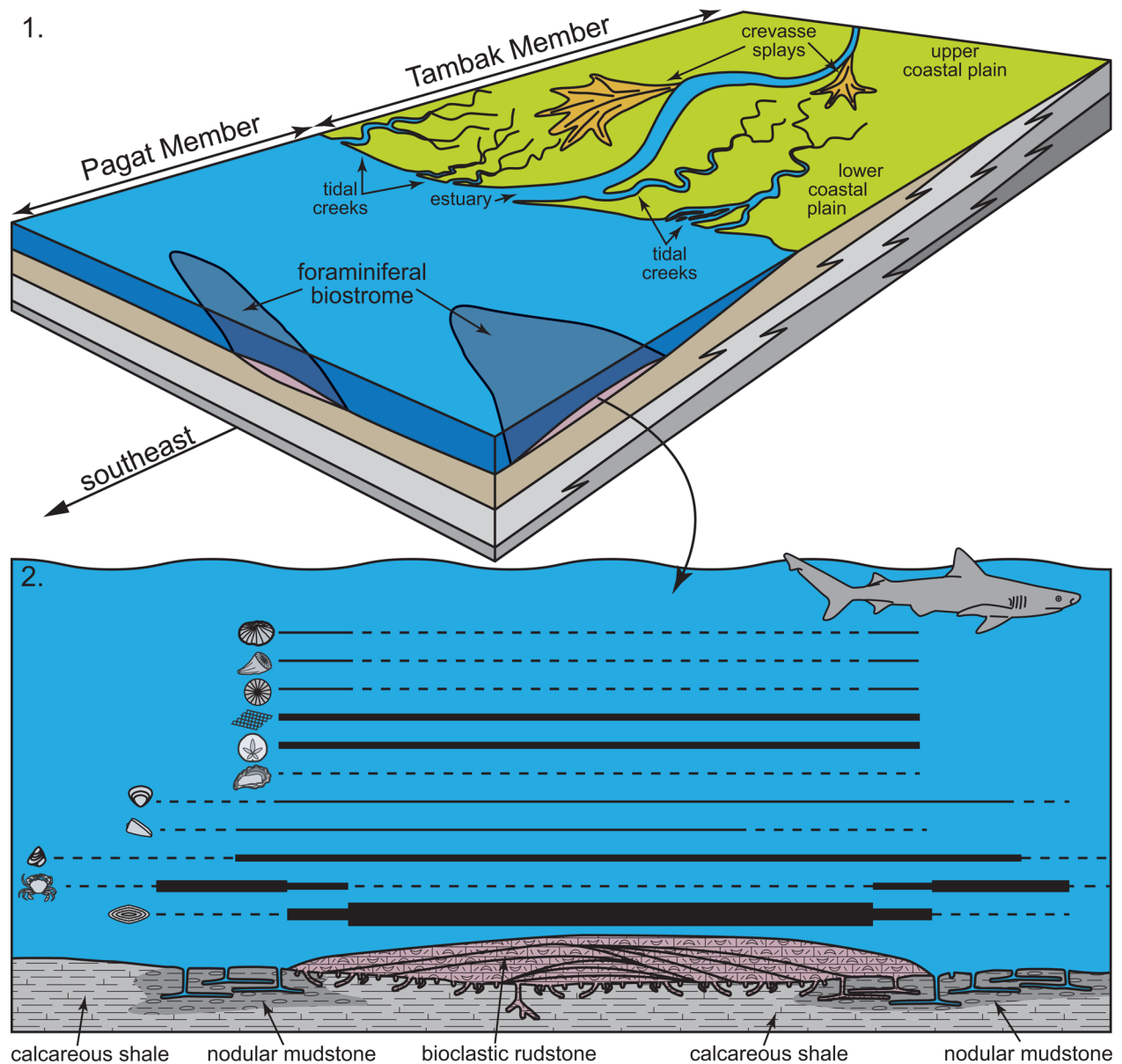


**Figure 22.** Interpreted depositional model of the upper Tambak and Pagat members in the Satui area, Kalimantan. (1) Schematic sketch showing the distribution of depositional subenvironments (based in part on Witts et al., 2012b). (2) Distribution of the main fossil groups in relationship to the foraminiferal biostromes in the Pagat Member. Key for symbols and lithology patterns provided in Figure 10.

chondrichthyans. As has been observed in other coeval localities (Wilson and Rosen, 1998; Renema et al., 2008), diversity of gastropods and bivalves is moderate. Although coral diversity is low, consisting of four azooxanthellate genera and two zooxanthellate genera (none of which are reef-forming taxa), larger benthic foraminifera are relatively diverse (up to 10 genera occurring in the uppermost beds) (Fig. 4).

When compared with the middle Eocene summary of other Indo-West Pacific sites by Renema et al. (2008), the Pagat LBF generic richness is much higher and is more similar to values reported from the Arabian Peninsula or from Miocene Indo-

West Pacific (IWP) assemblages. However, when compared with late Eocene numbers of LBF genera shown in the more recent review by Yasuhara et al. (2022) based on Renema (2007), Pagat values are similar, with ~8–13 genera, and much lower than those in the Tethyan hotspot (> 20 genera). The Melinau Limestone is a LBF-rich limestone in Sarawak and, like the Pagat Member, spans the Eocene/Oligocene boundary. The uppermost Eocene strata contain nummulitids, ortho-phragmines, and pellatispirids with more minor components, including *Halkyardia* and *Fabiania* and a total of 10 genera (Adams, 1965; Cotton et al., 2014). Although the overall

richness is higher than that of the middle Eocene for the region (Renema et al., 2008), it remains lower than that of the Miocene, when the IWP biodiversity hotspot came into existence. However, the overall richness does indicate that there may be an increasing number of taxa from the middle Eocene onwards. This study, therefore, highlights the relative knowledge gap regarding Paleogene larger benthic foraminifera in the region, which needs to be addressed in the future to better understand biodiversity hotspot dynamics.

Five of the solitary coral taxa in the study area have long temporal ranges, with *Caryophyllia*, *Balanophyllia*, and *Trachyphyllia* known from the early Cenozoic to the modern, and *Trochocyathus* and *Cycloseris* known from the Middle Jurassic to the modern (Wells, 1976; Bryan et al., 1997; Keller et al., 2009; Os'kina et al., 2010). *Anthemiphyllia* was previously known from the Eocene to the modern (Wells, 1976). The four azooxanthellate taxa have broad ranges in depth preference and include both unattached and attached forms (Cairns and Zibrowius, 1997; Cairns, 2004; Cairns and Kitahara, 2012). The zooxanthellate forms (*Cycloseris* and *Trachyphyllia*) occur in warm, shallow-water settings within the photic zone, where they occupy diverse depositional settings, from reef slope to shallow-water muddy siliciclastic shelves (Fisk, 1983; Best and Hoeksema, 1987; Foster et al., 1988; Klaus et al., 2011). *Cycloseris* occurs in proximal settings ranging from back-reef lagoons to lower reef slope settings and in proximal offshore settings up to ~85 m depth (Hoeksema and Achituv, 1993). *Caryophyllia*, *Cycloseris*, and *Balanophyllia* have been reported from other mixed siliciclastic–carbonate ramp/shelf successions (e.g., Durham, 1942; Smith and Johnson, 1958; Choi and Song, 2014; Távora et al., 2016).

The Satui Pagat coral fauna comprises a low-density, low-diversity assemblage dominated by solitary forms with wide temperature, turbidity, and depth tolerances (Ma, 1957; Wells, 1976; Perrin et al., 1995). This may reflect, at least in part, the occurrence of the Pagat biostromes in a setting with high siliciclastic input. The two zooxanthellate coral taxa (*Cycloseris* and *Trachyphyllia*) prefer shallow, warm, clear-water depositional settings (Best and Hoeksema, 1987; Klaus et al., 2011). Their occurrence suggests that clastic input along the Satui Pagat coastline was episodic and that a limited zooxanthellate coral fauna could thrive between sedimentation events.

The late Eocene to early Oligocene was a long interval of gradually rising sea level in Indonesia (Epting, 1980; Tomascik et al., 1997; Werdaya et al., 2013). In southern Borneo, this interval saw a segue from dominantly siliciclastic sedimentation to mixed siliciclastic–carbonate sedimentation and, eventually, the development of regional carbonate platforms (Epting, 1980; Tomascik et al., 1997; Werdaya et al., 2013). In the southern half of the Barito Basin and in the Asem Asem Basin, this transition interval is recorded by the Pagat Member and the overlying Berai Formation, a unit dominated by carbonate mudstone, packstone, grainstone, and rudstone deposited in a shallow platform setting (Werdaya et al., 2013). Although corals do occur in the Berai Formation, this unit has only been described from subsurface well logs and cores, and the fauna remains undefined. The Berai Formation ranges from the lower Oligocene through the early Miocene,

temporally equivalent to muddy carbonate strata of the Kinabatangan and Gomantong formations in Sabah (Malaysia) in northern Borneo (McMonagle et al., 2011), which is approximately coeval with the occurrence of the Arabian hotspot (Renema et al., 2008).

## Conclusions

The late Eocene Pagat Member of the Tanjung Formation records the transition from a siliciclastic, low-relief coastal plain succession to a heterolithic, mixed siliciclastic–carbonate shallow marine depositional system. The Pagat Member comprises an overall fining-upwards succession, with interbedded, heterolithic glauconitic silty/muddy sandstone transitioning upwards into calcareous shale punctuated by lenses of bioclastic packstone, grainstone, and rudstone.

The lower part of the study interval consists of heterolithic interbedded siliciclastic sandstone, glauconitic shale, thin beds of bioclastic wackestone, and bioclastic packstone. This grades upwards into a thick, calcareous shale succession. A diverse trace fossil assemblage, which occurs primarily in the muddy/glauconitic sandstone and bioclastic packstone/rudstone lithofacies, constrains the depositional setting to a mid-ramp/middle to distal continental shelf settings below fairweather but above storm wave base. The calcareous shale successions are characterized by a sparsely distributed, low-diversity assemblage.

The Pagat shale is punctuated by numerous, laterally restricted (approximately < 5 to >100 meters) lenses of foraminiferal packstone and foraminiferal rudstone lenses that range in thickness from a few mm to over a meter. These lenses are interpreted herein as low-relief foraminiferal biostromes. Many of the biostromes rest upon *Glossifungites* and/or *Trypanites* demarcated discontinuity surfaces, which are interpreted as storm-wave ravinement surfaces. These surfaces provided firm to hard surfaces in a depositional setting otherwise dominated by soupy substrates. The biostromes were initiated when invertebrate taxa that preferred firm or hard substrates, such as larger benthic foraminifera, solitary corals, oysters, and serpulids, colonized these stable substrates and expanded as older fossils died, with their shells providing additional substrate for subsequent generations.

The biostromes formed loci of exceptional marine biodiversity on the muddy Pagat coastline. Invertebrate taxa within and adjacent to the biostromes include 13 genera of larger benthic foraminifera, ~40 mollusk taxa, at least 5 genera and species of brachyuran crabs, 6 coral genera (*Anthemiphyllia*, *Balanophyllia*, *Caryophyllia*, *Cycloseris*, *Trachyphyllia*, and *Trochocyathus*), as well as a variety of bryozoans, serpulids, echinoids, and asterozoans.

The Satui Pagat coral fauna consists of a low-density, low-diversity assemblage dominated by forms with wide temperature, turbidity, and depth tolerances. This is interpreted to reflect common, albeit episodic, siliciclastic input on the Pagat muddy coast. The Pagat Member was deposited during an interval that witnessed a transition from primarily clastic-dominated deposition in southern Borneo to dominantly carbonate deposition.

Although Indonesia occurs at the heart of the Coral Triangle and comprises a major proportion of it, the timing and nature of the origin of the marine biodiversity hotspot remain poorly understood. High foraminiferal and molluscan diversity,

coupled with modest coral diversity, supports the hypothesis that the origin of the diverse tropical invertebrate faunas that characterize the modern Indo-Australian region may have occurred in the latest Eocene/earliest Oligocene.

## Acknowledgments

This project was initiated by Gregg F. Gunnell and Russ Ciochon. During the course of the project, Gregg passed away. Gregg collected many of the fossils discussed herein and contributed substantively to discussions on the significance of the fauna. Gregg was a mentor, advisor, compatriot, co-conspirator, colleague, and friend. He is missed every single day. We are grateful for the time we spent with Gregg, his wry sense of humor, and the myriad field projects that many of us were able to share with him.

We are grateful to Marcelle BouDagher-Fadel, who patiently provided her expertise on Paleogene foraminifera. Unfortunately, Marcelle passed away shortly before completion of this manuscript. We are grateful for her efforts and her willingness to share her taxonomic and paleoecological knowledge. All identifications of foraminifera discussed herein were provided by Marcelle. The other authors are forever grateful to Laura and Antonino for stepping in to clarify biostratigraphic and nomenclatural issues after Marcelle passed away.

We thank E. Di Martino for discussion and identification of Pagat bryozoans. We are grateful to Arutmin, Bayan Resources, and Wahana Baratama Mining for providing access to outcrop in the Haneman opencast mine. We appreciate the efforts of reviewer S. Dominici, an anonymous reviewer, Associate Editor S. Schneider, and Editor E. Currano, who have provided numerous helpful comments and suggestions.

This project was funded by National Geographic grants to G.F. Gunnell, R. Ciochon, and J.-P. Zonneveld, two NSERC Discovery Grants to JPZ, and National Science Foundation grant EAR-1925755 to PW. We are grateful to these organizations for continuing to fund science and our discovery of the world we live in.

## Declaration of competing interests

The authors declare no competing interests.

## References

- Adams, C.G., 1965, The foraminifera and stratigraphy of the Melinau Limestone, Sarawak, and its importance in Tertiary correlation: *Quarterly Journal of the Geological Society*, v. 121, p. 283–338.
- Adams, C.G., 1970, A reconsideration of the East Indian letter classification of the Tertiary: *Bulletins of the British Museum (Natural History)*, v. 19, p. 1–137.
- Aguirre, J., Riding, R., and Braga, J.C., 2000, Diversity of coralline red algae: origination and extinction patterns from the Early Cretaceous to the Pleistocene: *Paleobiology*, v. 26, p. 651–667.
- Alcock, A., 1902, Diagnoses and descriptions of new species of corals from the “Siboga-Expedition”. *Tijdschrift der Nederlandse Dierkundige Vereeniging* (ser. 2), v. 7, p. 89–115.
- Allen, G.R., 2008, Conservation hotspots of biodiversity and endemism for Indo-Pacific coral reef fishes: aquatic conservation: *Marine and Freshwater Ecosystems*, v. 18, p. 551–556.
- Asaad, I., Lundquist, C.J., Erdmann, M.V., and Costello, M.J., 2018a, Delineating priority areas for marine biodiversity conservation in the Coral Triangle: *Biological Conservation*, v. 222, p. 198–211.
- Asaad, I., Lundquist, C.J., Erdmann, M.V., Van Hooidek, R., and Costello, M.J., 2018b, Designating spatial priorities for marine biodiversity conservation in the Coral Triangle: *Frontiers in Marine Science*, v. 5, 400, <https://doi.org/10.3389/fmars.2018.00400>.
- Astibia, H., Merle, D., Pacaud, J.-M., Elorza, J., and Payros, A., 2018, Gastropods and bivalves from the Eocene marly formations of the Pamplona Basin and surrounding areas (Navarre, western Pyrenees): *Geodiversitas*, v. 40, p. 211–257.
- Bannerjee, S., Chatteraj, S.L., Saraswati, P.K., Dasgupta, S. and Sarkar, U., 2012, Substrate control on formation and maturation of glauconites in the Middle Eocene Harudi Formation, western Kutch, India: *Marine and Petroleum Geology*, v. 30, p. 144–160.
- Bannerjee, S., Bansal, U., and Thorat, A.V., 2016, A review on palaeogeographic implications and temporal variation in glaucony composition: *Journal of Paleogeography*, v. 5, p. 43–71.
- Bannerjee, S., Khanolkar, S., and Saraswati, P.K., 2018, Facies and depositional settings of the Middle Eocene–Oligocene carbonates in Kutch: *Geodinamica Acta*, v. 30, p. 119–136.
- Beavington-Penney, S.J., and Racey, A., 2004, Ecology of extant nummulitids and other larger benthic foraminifera: applications in palaeoenvironmental analysis: *Earth Science Reviews*, v. 67, p. 219–265.
- Beavington-Penney, S.J., Wright, V.P., and Racey, A., 2005, Sediment production and dispersal of foraminifera-dominated early Tertiary ramps: the Eocene El Garia Formation, Tunisia: *Sedimentology*, v. 52, p. 537–569.
- Bellwood, D.R., Renema W., and Rosen, B.R., 2012, Biodiversity hotspots, evolution and coral reef biogeography: a review, in *Gower, D.J., Johnson, K.G., Richardson, J.E., Rosen, B.R., Rüber, L., and Williams, S.T., eds., Biotic Evolution and Environmental Change in Southeast Asia: The Systematics Association Special Volume Series*, 82, p. 216–245.
- Bengtson, P., 1988, Open nomenclature: *Palaeontology*, v. 31, p. 223–227.
- Best, M.B., and Hoeksema, B.W., 1987, New observations on scleractinian corals from Indonesia: 1. Free-living species belonging to the Favina: *Zoologische Mededelingen*, v. 61, p. 387–403.
- Bigatti, G., Sanchez, C.J.M., Miloslavich, P., and Penchaszadeh, P.E., 2009, Feeding behaviour of *Adelomelon ancilla* (Lightfoot, 1786): a predatory neogastropod (Gastropoda: Volutidae) in Patagonian benthic communities: *The Nautilus*, v. 123, p. 159–165.
- Bosence, D.W.J., 1991, Coralline algae: mineralization, taxonomy and palaeoecology, in *Riding, R., ed., Calcareous Algae and Stromatolites*: Berlin, Springer Verlag, p. 98–113.
- Bosellini, F.R., Benedetti, A., Budd, A.F., and Papazzoni, C.A., 2022, A coral hotspot from a hot past: the EECO and post-EECO rich reef coral fauna from Friuli (Eocene, NE Italy): *Palaeogeography, Palaeoclimatology, Palaeoecology*, v. 607, 111284, <https://doi.org/10.1016/j.palaeo.2022.111284>.
- BouDagher-Fadel, M.K., 2008, Evolution and Geological Significance of Larger Benthic Foraminifera. *Developments in Palaeontology and Stratigraphy* 21: Amsterdam, Elsevier, 702 p.
- BouDagher-Fadel, M.K., 2018, Evolution and Geological Significance of Larger Benthic Foraminifera: London, UCL Press, 693 p.
- BouDagher-Fadel, M.K., and Price, G.D., 2010, Evolution and paleogeographic distribution of the lepidocyclinids: *Journal of Foraminiferal Research*, v. 41, p. 79–108.
- Brandt, A., Linse, K., and Schüller, M., 2009, Bathymetric distribution patterns of Southern Ocean macrofaunal taxa: Bivalvia, Gastropoda, Isopoda and Polychaeta: *Deep Sea Research Part 1: Oceanographic Research Papers*, v. 56, p. 2013–2025.
- Briguglio, A., Seddighi, M., Papazzoni, C.A., and Hohenecker, J., 2017, Shear versus settling velocity of recent and fossil larger foraminifera: new insights on nummulite banks: *Palaos*, v. 32, p. 321–329.
- Bromley, R.G., 1970, Borings as trace fossils and *Entobia cretacea* Portlock, as an example: *Geological Journal, Special Issue*, v. 3, p. 49–90.
- Bromley, R.G., 1981, Concepts in ichnology illustrated by small round holes in shells: *Acta Geologica Hispanica*, v. 16, p. 55–64.
- Bromley, R.G., and Asgaard, U., 1979, Triassic freshwater ichnocoenoses from Carlsberg Fjord, East Greenland: *Palaeogeography, Palaeoclimatology, Palaeoecology*, v. 28, p. 39–80.
- Bromley, R.G., and Asgaard, U., 1993, Two bioerosion ichnofacies produced by early and later burial associated with sea-level change: *Geologische Rundschau*, v. 82, p. 872–874.
- Bromley, R.G., and D’Alessandro, A., 1987, Bioerosion of the Plio-Pleistocene transgression of southern Italy: *Rivista Italiana di Paleontologia e Stratigrafia*, v. 93, p. 379–442.
- Bromley, R.G., and Uchman, A., 2003, Trace fossils from the Lower and Middle Jurassic marginal-marine deposits of the Sorthat Formation, Bornholm, Denmark: *Bulletin of the Geological Society of Denmark*, v. 50, p. 185–208.
- Bruguère, J.G., 1792, Camerine, in *Bruguère, J.G., Encyclopédie Méthodique: Histoire Naturelle des Vers*. Tome Premier: Paris, Chez Panckoucke, p. 395–400.
- Bryan, J.R., Carter, B.C., Flugeman Jr, R.J., Krumm, D.K., and Stemann, T.A., 1997, The Salt Mountain Limestone of Alabama: *Tulane Studies in Geology and Paleontology*, v. 30, p. 2–60.

- Cairns, S.D., 2004, A new shallow-water species of *Javania* (Scleractinia, Flabellidae) from Indonesia: The Raffles Bulletin of Zoology, v. 52, p. 7–10.
- Cairns, S.D., 2016, A key to the genera and species of the transversely-dividing Flabellidae (Anthozoa, Scleractinia, Flabellidae), with a guide to the literature, and the description of two new species: Zookeys, v. 562, p. 1–48.
- Cairns, S.D., and Kitahara, M.V., 2012, An illustrated key to the genera and subgenera of the Recent azooxanthellate Scleractinia (Cnidaria, Anthozoa), with an attached glossary: Zookeys, v. 227, p. 1–47.
- Cairns, S.D., and Parker, S.A., 1992, Review of the Recent Scleractinia (stony corals) of South Australia, Victoria and Tasmania: Record of the South Australian Museum, Monograph Series, v. 3, 82 p.
- Cairns, S.D., and Zibrowius, H., 1997, Cnidaria Anthozoa: Azooxanthellate Scleractinia from the Philippine and Indonesian regions, in Crosnier, A., and Bouchet, P., eds., Resultats des Campagnes Musorstom, Volume 16: Memoires du Museum National d'Histoire Naturelle, v. 172, p. 27–243.
- Choi, E., and Song, J.I., 2014, Four new records of two genera *Balanophyllia* and *Cladopsammia* (Anthozoa: Hexacorallia: Scleractinia: Dendrophyllidae) from Korea: Animal Systematics, Evolution and Diversity, v. 30, p. 183–190.
- Clark, M., and Robertson, A., 2005, Uppermost Cretaceous–lower Tertiary Ulukisla Basin, south-central Turkey: sedimentary evolution of part of a unified basin complex within an evolving Neotethyan suture zone: Sedimentary Geology, v. 173, p. 15–51.
- Cotton, L.J., and Pearson, P.N., 2011, Extinction of larger benthic foraminifera at the Eocene/Oligocene boundary: Palaeogeography, Palaeoclimatology, Palaeoecology, v. 311, p. 281–296.
- Cotton, L.J., Pearson, P.N., and Renema, W., 2014, Stable isotope stratigraphy and larger benthic foraminiferal extinctions in the Melinau Limestone, Sarawak: Journal of Asian Earth Sciences, v. 79, p. 65–71.
- Cumming, R.L., 1997, Oculids (Gastropoda) associated with gorgonians (Anthozoa: Gorgonoidea) at Cape D'Aguiar, Hong Kong: species, hosts, distributions and feeding ecology, in Morton, B., ed., The Marine Flora and Fauna of Hong Kong and Southern China IV: Proceedings of the Eighth International Marine Biological Workshop, Hong Kong, April 1995, p. 285–302.
- de Gibert, J.M., Domènech, R., and Martinell, J., 2007, Bioerosion in shell beds from the Pliocene Roussillon Basin, France: implications for the (macro) bioerosion ichnofacies model: Acta Palaeontologica Polonica, v. 52, p. 783–798.
- de Gibert, J.M., Domènech, R., and Martinell, J., 2012, Chapter 15. Rocky shorelines, in Knaust, D., and Bromley, R.G., eds., Trace Fossils as Indicators of Sedimentary Environments: Developments in Sedimentology, v. 64, p. 441–462.
- Deer, W.A., Howie, R.A., and Zussman, J., 2013, An Introduction to the Rock-forming Minerals, 3<sup>rd</sup> Edition: London, The Mineralogical Society, 506 p.
- Donovan, S.K., and Jagt, J.W.M., 2013, *Rogerella* isp., infesting the pore pairs of *Hemipneustes striatoradiatus* (Leske) (Echinoidea: Upper Cretaceous, Belgium): Ichnos, v. 20, p. 153–156.
- Driscoll, E.G., and Brandon, D.E., 1973, Mollusc–sediment relationships in north-western Buzzards Bay, Massachusetts, USA: Malacologia, v. 12, p. 13–46.
- Duda, T.F., and Kohn, A.J., 2005, Species-level phylogeography and evolutionary history of the hyperdiverse marine gastropod genus *Conus*: Molecular Phylogenetics and Evolution, v. 34, p. 257–272.
- Duda, T.F., Kohn, A.J., and Palumbi, S.R., 2001, Origins of diverse feeding ecologies within *Conus*, a genus of venomous marine gastropods: Biological Journal of the Linnean Society, v. 73, p. 391–409.
- Durham, J.W., 1942, Eocene and Oligocene coral faunas of Washington: Journal of Paleontology, v. 16, p. 84–104.
- Dworschak, P.C., and Rodrigues, S.A., 1997, A modern analogue for the trace fossil *Gyrolithes*: burrows of the thalassinidean shrimp *Axianassa australis*: Lethaia, v. 30, p. 41–52.
- Ekdale, A.A., 1985, Paleocology of the marine endobenthos: Palaeogeography, Palaeoclimatology, Palaeoecology, v. 50, p. 63–81.
- Elison, A.M., Farnsworth, E.J., and Merkt, R.E., 1999, Origins of mangrove ecosystems and the mangrove biodiversity anomaly: Global Ecology and Biogeography, v. 8, p. 95–115.
- Epting, M., 1980, Sedimentology of the Miocene carbonate buildups, central Luconia, offshore Sarawak: Geological Society of Malaysia Bulletin, v. 12, p. 17–30.
- Fernández, D.E., and Pazos, P.J., 2012, Ichnology of marginal marine facies of the Agrio Formation (Lower Cretaceous, Neuquén Basin, Argentina) at its type locality: Ameghiniana, v. 49, p. 505–524.
- Fisk, D.A., 1983, Free-living corals: distributions according to plant cover, sediments, hydrodynamics, depth and biological factors: Marine Biology, v. 74, p. 287–294.
- Foster, A.B., Johnson, K.G., and Schultz, L.L., 1988, Allometric shape change and heterochrony in the free-living coral *Trachyphyllia bilobata* (Duncan): Coral Reefs, v. 7, p. 37–44.
- Fretter, V., and Graham, A., 1962, British Prosobranch Molluscs: Their Functional Anatomy and Ecology: London, Ray Society, 755 p.
- Frey, R.W., and Seilacher, A., 1980, Uniformity in marine invertebrate ichnology: Lethaia, v. 13, p. 183–207.
- Furlong, C.M., Gingras, M.K., and Zonneveld, J.-P., 2015, *Trypanites*-type ichnofacies at the Bay of Fundy, Nova Scotia, Canada: Palaios, v. 30, p. 258–271.
- Furlong, C.M., Schultz, S.K., Gingras, M.K., and Zonneveld, J.-P., 2016, Oregon Sea Stack: ecological diversity of a modern *Trypanites* ichnofacies: Ichnos, v. 23, p. 77–98.
- Galindo, L.A., Puillandre, N., Utge, J., Lozouet, P., and Bouchet, P., 2016, The phylogeny and systematics of the Nassariidae revisited (Gastropoda, Buccinoidea): Molecular Phylogenetics and Evolution, v. 99, p. 337–353.
- Gingras, M.K., Pemberton, S.G., Saunders, T.D.A., and Clifton, H.E., 1999, The ichnology of Modern and Pleistocene brackish-water deposits at Willapa Bay, Washington: variability in estuarine settings: Palaios, v. 14, p. 352–374.
- Gingras, M.K., Pemberton, S.G., and Saunders, T.D.A., 2000, Firmness profiles associated with tidal-creek deposits: the temporal significance of *Glossifungites* assemblages: Journal of Sedimentary Research, v. 70, p. 1017–1025.
- Gingras, M.K., Dashtgard, S.E., MacEachern, J.A., and Pemberton, S.G., 2008, Biology of shallow marine ichnology: a model perspective: Aquatic Biology, v. 2, p. 255–268.
- Gittenberger, A., and Hoeksema, B.W., 2013, Habitat preferences of coral-associated wentletrap snails (Gastropoda: Epitoniidae): Contributions to Zoology, v. 82, p. 1–25.
- Goeting, S., Cosović, V., Benedetti, A., Fiorini, F., Kocsis, L., Roslim, A., and Briguglio, A., 2022, Diversity and depth distribution of modern benthic foraminifera offshore Brunei Darussalam: Journal of Foraminiferal Research, v. 52(3), p. 160–178.
- Halas, D., and Winterbottom, R., 2009, A phylogenetic test of multiple proposals for the origins of the East Indies coral reef biota: Journal of Biogeography, v. 36, p. 1847–1860.
- Hallock, P., 1981, Production of carbonate sediments by selected large benthic foraminifera on two Pacific coral reefs: Journal of Sedimentary Petrology, v. 51, p. 467–474.
- Hallock, P., 2000, Larger foraminifera as indicators of coral-reef vitality: Environmental Micropaleontology, v. 15, p. 121–150.
- Hallock, P., and Pomar, L., 2009, Cenozoic evolution of larger benthic foraminifera: paleoceanographic evidence for changing habitats, in Rigel, B., and Dodge, R.E., eds., Proceedings of the 11th International Coral Reef Symposium, Ft. Lauderdale, Florida, 7–11 July 2008, p. 16–20.
- Hallock, P., and Seddighi, M., 2022, Why did some larger benthic foraminifera become so large and flat?: Sedimentology, v. 69, p. 74–87.
- Hanken, N.-M., Uchman, A., Nielsen, J. K., Olausson, S., Eggebø, T., and Steinsland, R., 2016, Late Ordovician trace fossils from offshore to shallow water mixed siliciclastic and carbonate facies in the Ringerike area, Oslo Region, Norway: Ichnos, v. 23, p. 189–221.
- Hegab, O.A., Serry, M.A., Anan, T.I., and Abd El-Wahed, A.G., 2016, Facies analysis, glauconite distribution and sequence stratigraphy of the middle Eocene Qarara Formation, El-Minya area, Egypt: Egyptian Journal of Basic and Applied Sciences, v. 3, p. 71–84.
- Hidayat, R., Husein, S., and Surjono, S.S., 2012, Regional depositional model of South Makassar Basin depocentre, Makassar Strait, based on seismic facies: Journal of SE Asian Applied Geology, v. 41, p. 42–52.
- Hoeksema, B.W., 2007, Delineation of the Indo-Malayan centre of maximum marine biodiversity: the coral triangle, in Renema, W., ed., Biogeography, Time and Place: Distributions, Barriers, and Islands: Dordrecht, The Netherlands, Springer, p. 117–178.
- Hoeksema B.W., and Achituv Y., 1993, First Indonesian record of *Fungiacava eilatensis* Goreau et al., 1968 (Bivalvia: Mytilidae), endo-symbiont of *Fungia* spp. (Scleractinia: Fungiidae): Basteria, v. 57, p. 131–138.
- Hoeksema, B.W., van der Land, J., van der Meij, S.E.T., van Ofwegen, L.P., Reijnen, B.T., van Soest, R.W.M., and de Voogd, N.J., 2011, Unforeseen importance of historical collections as baselines to determine biotic change of coral reefs: the Saba Bank case: Marine Ecology, v. 32, p. 135–141.
- Hohenegger, J., and Briguglio, A., 2012, Axially oriented sections of nummulitids: a tool to interpret larger benthic foraminiferal deposits: Journal of Foraminiferal Research, v. 42, p. 134–142.
- Hughes, R.N., 1986, Laboratory observations on the feeding behavior, reproduction and morphology of *Galeodea echinophora* (Gastropoda: Cassidae): Zoological Journal of the Linnean Society, v. 86, p. 355–365.
- Hughes, R.N., and Hughes, H.P.I., 1971, A study of the gastropod *Cassis tuberosa* (L.) preying upon sea urchins: Journal of Experimental Marine Biology and Ecology, v. 7, p. 215–315.
- Hughes, R.N., and Hughes, H.P.I., 1981, Morphological and behavioural aspects of feeding in the Cassidae (Tonnacea, Mesogastropoda): Malacologia, v. 20, p. 385–402.
- Ingham, R.E., and Zischke, J.A., 1977, Prey preferences of carnivorous intertidal snails in the Florida Keys: The Veliger, v. 20, p. 49–51.

- Jeans, C.V., Wray, R.J., Merriman, R.J., and Fisher, M.J., 2000, Volcanogenic clays in Jurassic and Cretaceous strata of England and the North Sea Basin: *Clay Minerals*, v. 35, p. 25–55.
- Johnson, K.G., Renema, W., and Santodomingo, N., 2014, Oligocene and Miocene history of reef corals and coral reefs in Eastern Borneo (East Kalimantan, Indonesia and Sabah, Malaysia): *The Paleontological Society Special Publications*, v. 13, p. 22–21.
- Johnson, K.G., Hasibuan, F., Todd, J.A., and Müller, W., 2015a, Biotic and environmental origins of the Southeast Asian biodiversity hotspot: *Palaaios*, v. 30, p. 1–6.
- Johnson, K.G., Renema, W., Rosen, B.R., and Santodomingo, N., 2015b, Old data for old questions: what can the historical collections really tell us about the Neogene origins of reef-coral diversity in the Coral Triangle?: *Palaaios*, v. 30, p. 94–108.
- Kay, E.A., 1996, Origin and evolutionary radiation of the Mollusca, in Taylor, J.D., ed., *Origin and Evolutionary Radiation of the Mollusca*: New York, Oxford University Press, p. 211–220.
- Keller, N.B., Os'kina, N.S., and Nikolaev, S.D., 2009, A new approach in determining the age of deep-water species of Scleractinia using temperature ranges of their habitation: *Doklady Earth Sciences*, v. 425, p. 264–268.
- Kelly, S.R.A., Bromley, R.G., 1984, Ichnological nomenclature of clavate borings: *Palaeontology*, v. 27, p. 793–807.
- Kessler, F.L., and Jong, J., 2017, Carbonate banks and ramps on the northern shore of Paleogene and early Neogene Borneo: observations and implications on stratigraphy and tectonic evolution: *Bulletin of the Geological Society of Malaysia*, v. 63, p. 1–26.
- Kidwell, S.M., 1991, Taphonomic feedback (live/dead Interactions) in the genesis of bioclastic beds: keys to reconstructing sedimentary dynamics, in Einsele, G., Ricken, W., and Seilacher, A., eds., *Cycles and Events in Stratigraphy*: Berlin, Springer-Verlag, p. 268–282.
- Kidwell, S.M., and Jablonski, D., 1983, Taphonomic feedback: ecological consequences of shell accumulation, in Tevesz, M.J.S., and McCall, P.L., eds., *Biotic Interactions in Recent and Fossil Benthic Communities*: New York, Plenum, p. 195–248.
- Klaus, J.S., Lutz, B.P., McNeill, D.F., Budd, A.F., Johnson, K.G., and Ishman, S.E., 2011, Rise and fall of Pliocene free-living corals in the Caribbean: *Geology*, v. 39, p. 375–378.
- Knaust, D., 2004, Cambro-Ordovician trace fossils from the SW-Norwegian Caledonides: *Geological Journal*, v. 39, p. 1–24.
- Knaust, D., 2013, The ichnogenus *Rhizocorallium*: classification, trace-makers, palaeoenvironments and evolution: *Earth-Science Reviews*, v. 126, p. 1–47.
- Kohn, A.J., 1959, The Ecology of *Conus* in Hawaii: *Ecological Monographs*, v. 29, p. 47–90.
- Kohn, A.J., 1985, Evolutionary ecology of *Conus* on Indo-Pacific coral reefs: Proceedings of the Fifth International Coral Reef Congress, Tahiti, 27 May–1 June 1985, v. 4, p. 139–144.
- Król, J.J., Kolodziej, B., and Bucur, I.I., 2016, Coral reefs near the Eocene–Oligocene boundary in the northern Transylvanian Basin, Romania: composition and palaeoenvironmental interpretation: *Geological Journal*, v. 53, p. 565–579.
- Kusuma, I., and Darin, T., 1989, The hydrocarbon potential of the lower Tanjung Formation, Barito Basin, S.E. Kalimantan: Proceedings of the Eighteenth Annual Convention of the Indonesian Petroleum Association, IPA 89-11.09, <https://doi.org/10.29118/ipa.2166.107.138>.
- Kusworo, A., Reich, S., Wesselingh, F.P., Santodomingo, N., Johnson, K.G., Todd, J.A., and Renema, W., 2015, Diversity and paleoecology of Miocene coral-associated mollusks from East Kalimantan (Indonesia): *Palaaios*, v. 30, p. 116–127.
- Lamarck, J.B.A.M., 1801, *Système des Animaux sans Vertèbres ou tableau general des classes, des orders et des genres de ces animaux*: Paris, Chez Deterville, 432 p.
- Lambers, P., and Boekschoten, G.J., 1986, On fossil and recent borings produced by acrothoracic cirripeds: *Geologie en Mijnbouw*, v. 65, p. 257–268.
- Lee, J.J., 1998, “Living sands”—larger foraminifera and their endosymbiotic algae: *Symbiosis*, v. 25, p. 71–100.
- Leithold, E.L., 1989, Depositional processes on an ancient and modern muddy shelf, northern California: *Sedimentology*, v. 36, p. 179–202.
- Less, G., Ozcan, E., and Okay, A.I., 2011, Stratigraphy and larger Foraminifera of the middle Eocene to lower Oligocene shallow-marine units in the northern and eastern parts of the Thrace Basin, NW Turkey: *Turkish Journal of Earth Sciences*, v. 20, p. 793–845.
- Lohman, D.J., de Bruyn, M., Page, T., von Rintelen, K., Hall, R., Ng, P.K.L., Shih, H.-T., Carvalho, G.R., and von Rintelen, T., 2011, Biogeography of the Indo-Australian Archipelago: *Annual Review of Ecology, Evolution, and Systematics*, v. 42, p. 205–226.
- López-Quirós, A., Escutia, C., Sánchez-Navas, A., Nieto, F., García-Casco, A., Martín-Algarra, A., Evangelinos, D., and Salabarnada, A., 2019, Glaucony authigenesis, maturity and alteration in the Weddell Sea: an indicator of paleoenvironmental conditions before the onset of Antarctic glaciation: *Scientific Reports*, v. 9, 13580, <https://doi.org/10.1038/s41598-019-51017-1>.
- Ludt, W.B., and Rocha, L.A., 2015, Shifting seas: the impacts of Pleistocene sea-level fluctuations on the evolution of tropical marine taxa: *Journal of Biogeography*, v. 42, p. 25–38.
- Lunt, P., 2003, Biogeography of some Eocene larger Foraminifera, and their application in distinguishing geological plates: *Palaeontologica Electronica*, v. 6, 22, [https://palaeo-electronica.org/2003\\_2/geo/issue2\\_03.htm](https://palaeo-electronica.org/2003_2/geo/issue2_03.htm).
- Lunt, P., and Luan, X., 2022, SE Asian Cenozoic larger Foraminifera: taxonomic questions, apparent radiation and abrupt extinctions: *Journal of Earth Science*, v. 33, p. 1378–1399.
- Ma, T.Y.H., 1957, The effect of warm and cold currents in the southern-western Pacific on the growth rate of reef corals: *Oceanographia Sinica*, v. 5, p. 1–34.
- MacEachern, J.A., Raychaudhuri, I., and Pemberton, S.G., 1992, Stratigraphic applications of the Glossifungites Ichnofacies: delineating discontinuities in the rock record, in Pemberton, S.G., ed., *Applications of Ichnology to Petroleum Exploration: SEPM Core Workshop Notes 17*, p. 169–198.
- MacEachern, J.A., Bann K.L., Gingras, M.K., Zonneveld, J.-P., Dashtgard, S.E., and Pemberton, S.G., 2012, Chapter 4, The ichnofacies paradigm, in Knaust, D., and Bromley, R.G., eds., *Trace Fossils as Indicators of Sedimentary Environments: Developments in Sedimentology*, v. 64, p. 103–138.
- Marshall, N., Novak, V., Cibaj, I., Krijgsman, W., Renema, W., Young, J., Fraser, N., Limbong, A., and Morley, R.J., 2015, Dating Borneo's deltaic deluge: middle Miocene progradation of the Mahakam Delta: *Palaaios*, v. 30, p. 7–25.
- Mayoral, E., and Muñiz, F., 1996, La ichnofacies de *Gnathichnus* en la sector suroccidental de la Cuenca del Guadalquivir (Lepe, Huelva, España): *Coleoquios de Paleontología*, v. 48, p. 71–82.
- McMonagle, L.B., 2012, *A diverse assemblage of corals from the late Oligocene of Eastern Sabah, Borneo: pre-Miocene origins of the Indo-West Pacific marine biodiversity hotspot* [M.S. thesis]: Durham, UK, Durham University.
- McMonagle, L.B., Lunt, P., Wilson, M.E.J., Johnson, K.G., Manning, C., and Young, J., 2011, A re-assessment of age dating of fossiliferous limestones in eastern Sabah, Borneo: implications for understanding the origins of the Indo-Pacific marine biodiversity hotspot: *Palaeogeography, Palaeoclimatology, Palaeoecology*, v. 305, p. 28–42.
- Mihaljević, M., Renema, W., Welsh, K., and Pandolfi, J.M., 2014, Eocene–Miocene shallow-water carbonate platforms and increased habitat diversity in Sarawak, Malaysia: *Palaaios*, v. 29, p. 378–391.
- Mihaljević, M., Korpanty, C., Renema, W., Welsh, K., and Pandolfi, J.M., 2017, Identifying patterns and drivers of coral diversity in the central Indo-Pacific marine biodiversity hotspot: *Paleobiology*, v. 43, p. 343–364.
- Milne-Edwards, H., and Haime, J., 1851, Recherches sur les polypiers. Mémoire 6. Monographie des Fongides. *Annales des Sciences Naturelles, Zoologie*, ser. 3, v. 15, p. 73–144.
- Molina, E., Torres-Silva, A.I., Corić, S., and Briguglio, A., 2016, Integrated biostratigraphy across the Eocene/Oligocene boundary at Noroña, Cuba, and the question of the extinction of orthophragminids: *Newsletters on Stratigraphy*, v. 49, p. 27–40.
- Morley, R.J., 2000, *Origin and Evolution of Tropical Rain Forests*: New York, Wiley, 384 p.
- Moss, S.J., and Chambers, J.L.C., 1999, Tertiary facies architecture in the Kutai Basin, Kalimantan, Indonesia: *Journal of Asian Earth Sciences*, v. 17, p. 157–181.
- Müller, A.H., 1977, Zur ichnologie der subherzynen Oberkreide (Campan): *Zeitschrift für Geologische Wissenschaften*, Berlin, v. 5, p. 881–897.
- Neto de Carvalho, C., Rodrigues, N.P.C., Viegas, P.A., Baucon, A., and Santos, V.F., 2010, Patterns of occurrence and distribution of crustacean ichnofossils in the Lower Jurassic–Upper Cretaceous of Atlantic occidental margin basins, Portugal: *Acta Geologica Polonica*, v. 60, p. 19–28.
- Nützel, A., 2021, Chapter 6: Gastropods as parasites and carnivorous grazers: a major guild in marine ecosystems, in De Baets, K., and Huntley, J.W., eds., *The Evolution and Fossil Record of Parasitism: Springer Topics in Geobiology*, v. 49, p. 209–229.
- O'Brien, N., 1987, The effects of bioturbation on the fabric of shale: *Journal of Sedimentary Petrology*, v. 57, p. 449–455.
- Odin, G.S., and Fullagar, P.D., 1988, Chapter C4. Geological significance of the Glaucony Facies, in Odin, G.S., ed., *Green Marine Clays: Elsevier Developments in Sedimentology*, v. 45, p. 295–332.
- Odin, G.S., and Matter, A., 1981, De glauconiarum origine: *Sedimentology*, v. 28, p. 611–641.
- Olariu, M.I., and Zeng, H., 2018, Prograding muddy shelves in the Paleogene Wilcox deltas, South Texas Gulf Coast: *Marine and Petroleum Geology*, v. 91, p. 71–88.
- Os'kina, N.S., Keller, N.B., and Nikolaev, S.D., 2010, The assessment of the age of scleractinian coral species (Anthozoa: Scleractinia) based on the temperature ranges of their habitat: *Oceanology*, v. 50, p. 975–983.

- Panggabean, H., 1991, *Tertiary source rocks, coals and reservoir potential in the Asem–Asem and Barito basins, southeast Kalimantan, Indonesia* [Ph.D. dissertation]: Wollongong, Australia, University of Wollongong.
- Pemberton, S.G., and Frey, R.W., 1984, Ichnology of storm-influenced shallow marine sequence: Cardium Formation (Upper Cretaceous) at Seebe, Alberta, in Stott, D.F., and Glass, D.L., eds., *The Mesozoic of Middle North America*: Canadian Society of Petroleum Geologists, Memoir 9, p. 281–304.
- Pemberton, S.G., Kobluk, D.R., Yeo, R.K., and Risk, M.J., 1980, The boring *Trypanites* at the Silurian–Devonian disconformity in southern Ontario: *Journal of Paleontology*, v. 54, p. 1258–1266.
- Pemberton, S.G., Frey, R.W., Ranger, M.J., and MacEachern, J., 1992, The conceptual framework of ichnology, in Pemberton, S.G., ed., *Applications of Ichnology to Petroleum Exploration: A Core Workshop: SEPM Core Workshop 17*, Tulsa, Oklahoma, SEPM, p. 1–32.
- Pemberton, S.G., MacEachern, J.A., Dashtgard, S.E., Bann, K.L., Gingras, M.K., and Zonneveld, J.-P., 2012, Chapter 19. Shorefaces, in Knaust, D., and Bromley, R.G., eds., *Trace Fossils as Indicators of Sedimentary Environments: Developments in Sedimentology*, v. 64, p. 563–603.
- Perrin, C., Bosence, D., and Rosen, B., 1995, Quantitative approaches to palaeozonation and palaeobathymetry of corals and coralline algae in Cenozoic reefs, in Bosence, D.W.J., and Allison, P.A., eds., *Marine Palaeoenvironmental Analysis from Fossils: Geological Society Special Publication*, v. 83, p. 181–229.
- Petuch, E.J., and Berschauer, D.P., 2020, *Tropical Marine Mollusks: An Illustrated Biogeographical Guide*: Boca Raton, Florida, CRC Press, 373 p.
- Prazeres, M., and Renema, W., 2019, Evolutionary significance of the microbial assemblages of large benthic Foraminifera: *Biological Review*, v. 94, p. 828–848.
- Racey, A., 2001, A review of Eocene nummulite accumulations structure, formation and reservoir potential: *Journal of Petroleum Geology*, v. 24, p. 79–100.
- Renema, W., 2007, Fauna development of larger benthic foraminifera in the Cenozoic of southeast Asia, in Renema, W., ed., *Biogeography, Time and Place: Distributions, Barriers and Islands*: Dordrecht, The Netherlands, Springer, p. 179–215.
- Renema, W., Racey, A., and Lunt, P., 2002, Paleogene nummulitid foraminifera from the Indonesian Archipelago: a review: *Cainozoic Research*, v. 2, p. 23–78.
- Renema, W., Bellwood, D.R., Braga, J.C., Bromfield, K., Hall, R., et al., 2008, Hopping hotspots: global shifts in marine biodiversity: *Science*, v. 321, p. 654–657.
- Renema, W., Warter, V., Novak, V., Young, J.R., Marshall, N., and Hasibuan, F., 2015, Ages of Miocene fossil localities in the northern Kutai Basin (East Kalimantan, Indonesia): *Palaios*, v. 30, p. 26–39.
- Reuter, M., Piller, W.E., Harzhauser, M., and Kroh, A., 2013, Cyclone trends constrain monsoon variability during late Oligocene sea level highstands (Kachch Basin, NW India): *Climate of the Past*, v. 9, p. 2101–2115.
- Rine, J.M., and Ginsburg, R.N., 1985, Depositional facies of a mud shoreface in Suriname, South America—a mud analogue to sandy, shallow-marine deposits: *Journal of Sedimentary Petrology*, v. 55, p. 633–652.
- Robertson, R., 1970, Review of the predators and parasites of stony corals, with special reference to symbiotic prosobranch gastropods: *Pacific Science*, v. 24, p. 43–54.
- Rosler, A., Pretkovic, V., Novak, V., Renema, W., and Braga J.C., 2015, Coralline algae from the Miocene Mahakam delta (East Kalimantan, Southeast Asia): *Palaios*, v. 30, p. 83–93.
- Roslim, A., Briguglio, A., Kocsis, L., Ćorić, S., and Gebhardt, H., 2019, Large rotaliid foraminifera as biostratigraphic and palaeoenvironmental indicators in northwest Borneo: an example from a Late Miocene section in Brunei Darussalam: *Journal of Asian Earth Sciences*, v. 170, p. 20–28.
- Roveda V., 1959, *Nummulites retiatius* nouvelle espèce de Nummulite réticulée de Abruzzes (Italie): *Revue de Micropaléontologie*, v. 1, p. 201–207.
- Roy, K., 2002, Bathymetry and body size in marine gastropods: a shallow water perspective: *Marine Ecology Progress Series*, v. 237, p. 143–149.
- Saller, A.H., and Vijaya, S., 2002, Depositional and diagenetic history of the Kerendan carbonate platform, Oligocene, central Kalimantan, Indonesia: *Journal of Petroleum Geology*, v. 25, p. 125–150.
- Santodomingo, N., Wallace, C.C., and Johnson, K.G., 2015a, Fossils reveal a high diversity of the staghorn coral genera *Acropora* and *Isopora* (Scleractinia: Acroporidae) in the Neogene of Indonesia: *Zoological Journal of the Linnean Society*, v. 175, p. 677–763.
- Santodomingo, N., Novak, V., Petković, V., Marshall, N., Di Martino, E., et al., 2015b, A diverse patch reef from turbid habitats in the Middle Miocene (East Kalimantan, Indonesia): *Palaios*, v. 30, p. 128–149.
- Santodomingo, N., Renema, W., and Johnson, K.G., 2016, Understanding the murky history of the Coral Triangle: Miocene corals and reef habitats in East Kalimantan (Indonesia): *Coral Reefs*, v. 35, p. 765–781.
- Sapiie, B., Pamumpuni, A., and Hadiana, M., 2011, Balancing cross-section and sandbox modeling of Satui fold-thrust-belt, Asem–Asem Basin, South Kalimantan: *Proceedings of the Thirty-Second Annual Convention and Exhibition, Indonesian Petroleum Association, IPA08-G-151*, <https://doi.org/10.29118/IPA.2427.08.G.151>.
- Satyana, A.H., 1995, Paleogene unconformities in the Barito Basin, southeast Kalimantan: a concept for the solution of the ‘Barito dilemma’ and a key to the search for Paleogene structures: *Proceedings of the Indonesian Petroleum Association 24th Annual Convention*, Jakarta, p. 263–375.
- Satyana, A.H., 2002, Oligo-Miocene reefs: East Java’s giant fields: *Proceedings of the Giant Field and New Exploration Concepts Seminar, Indonesian Association of Geologists IAGI, Jakarta*, 17 October 2002, 12 p.
- Satyana, A.H., and Armandita, C., 2008, On the origin of the Meratus Uplift, Southeast Kalimantan—tectonic and gravity constraints: a model for exhumation of collisional orogen in Indonesia: *Proceedings of the Thirty-third Annual Convention of the Indonesian Association of Geophysicists (HAGI)*, Bandung, November 3–5, 2008.
- Satyana, A.H., and Silitonga, P.D., 1994, Tectonic reversal in East Barito Basin, South Kalimantan: consideration of the types of inversion structures and petroleum system significance: *Proceedings of the Twenty-third Annual Convention of the Indonesian Petroleum Association, IPA94-1.1-027*, p. 57–74, <https://doi.org/10.29118/ipa.623.57.74>.
- Satyana, A.H., Eka, M.M.P., and Imron, M., 2001, Eocene coals of the Barito Basin, Southeast Kalimantan: sequence stratigraphic framework and potential for sources of oil: *Berita Sedimentologi*, v. 17, p. 1–15.
- Schultz, S.K., Furlong, C.M., and Zonneveld, J.-P., 2016, The co-occurrence of *Trypanites* and *Glossifungites* substrate-controlled trace fossil assemblages in a mixed siliciclastic–carbonate depositional system: Baldonnel Formation, Williston Lake, B.C. Canada: *Journal of Sedimentary Research*, v. 86, p. 879–893.
- Seddighi, M., Briguglio, A., Hohenegger, J., and Papazzoni, C.A., 2015, New results on the hydrodynamic behaviour of fossil *Nummulites* tests from two nummulite banks from the Bartonian and Priabonian of northern Italy: *Bolletino della Società Paleontologica Italiana*, v. 54, p. 103–116.
- Seike, K., and Nara, M., 2007, Occurrence of bioglyphs on *Ocypode* crab burrows in a modern sandy beach and its palaeoenvironmental implications: *Palaeogeography, Palaeoclimatology, Palaeoecology*, v. 252, p. 458–463.
- Seilacher, A., 1964, Biogenic sedimentary structures, in Imbrie, J., and Newell, N., eds., *Approaches to Paleocology*: New York, Wiley, p. 296–316.
- Serra-Kiel, J., Hottinger, L., Caus, E., Drobne, K., Ferrández, C., et al., 1998, Larger benthic foraminiferal biostratigraphy of the Tethyan Paleocene and Eocene: *Bulletin de la Société Géologique de France*, v. 169, p. 281–299.
- Sikumbang, N., 1986, *Geology and tectonics of pre-Tertiary rocks in the Meratus Mountains, southeast Kalimantan, Indonesia* [Ph.D. dissertation]: London, University of London.
- Siregar, M.S., and Sunaryo, R., 1980, Depositional environment and hydrocarbon prospects, Tanjung Formation, Barito Basin, Kalimantan: *Proceedings of the Indonesian Petroleum Association, Ninth Annual Convention*, p. 379–400, <https://doi.org/10.29118/ipa.1950.379.400>.
- Smith, L.N., and Johnson, H.S., 1958, South Carolina Coastal Plain: *Carolina Geological Society*, November 1–2, 1958, Guidebook, 14 p.
- Spagnuolo, E.J., Wilf, P., Zonneveld, J.-P., Shaw, D., Aswan, Rizal, Y., Zaim, Y., Bloch, J.I., and Ciochon, R.L., 2024, Giant seeds of an extant Australasian legume lineage discovered in Eocene Borneo (South Kalimantan, Indonesia): *International Journal of Plant Sciences*, v. 185, p. 482–502.
- Stassen, P., Thomas, E., and Speijer, R.P., 2015, Paleocene–Eocene Thermal Maximum environmental change in the New Jersey coastal plain: benthic foraminiferal biotic events: *Marine Micropaleontology*, v. 115, p. 1–23.
- Stehli, F.G., and Wells, J.W., 1971, Diversity and age patterns in hermatypic corals: *Systematic Zoology*, v. 20, p. 115–126.
- Tapanila, L., 2006, Devonian *Entobia* borings from Nevada, with a revision of *Topsentopsis*: *Journal of Paleontology*, v. 80, p. 760–767.
- Távora, V.A., Dias, J.J., and Fernandes, A.C.S., 2016, New records and re-descriptions of Brazilian Scleractinia corals (Itamaracá, Maria Farinha and Pirabas formations): *Paleontología Mexicana*, v. 5, p. 71–86.
- Taylor J.D., and Morton, B., 1996, The diets of predatory gastropods in the Cape D’Aguilar marine reserve, Hong Kong: *Asian Marine Biology*, v. 13, p. 141–166.
- Taylor, J.D., and Reid, D.G., 1984, The abundance and trophic classification of molluscs upon coral reefs in the Sudanese Red Sea: *Journal of Natural History*, v. 18, p. 175–209.
- Taylor, P.D., and Wilson, M.A., 2003, Palaeoecology and evolution of marine hard substrate communities: *Earth-Science Reviews*, v. 62, p. 1–103.
- Tedesco, L.P., and Wanless, H.R., 1991, Generation of sedimentary fabrics and facies by repetitive excavation and storm infilling of burrow networks, Holocene of South Florida and Caicos Platform, B.W.I.: *Palaios*, v. 6, p. 326–343.
- Tomascik, T., Mah, A.J., Nontji, A., and Moosa, M.K., 1997, *The Ecology of the Indonesian Seas: Part One*. Oxford, UK, Oxford University Press, 642 p.

- Tracey, S., Craig, B., Belliard, L., and Gain, O., 2017, One, four or forty species? – early Conidae (Mollusca, Gastropoda) that led to a radiation and biodiversity peak in the late Lutetian of the Cotentin, NW France: *Carnets de Voyages Paléontologiques dans le Bassin Anglo-Parisien*, v. 3, p. 1–38.
- Tyler, C.L., Dexter, T.A., Portell, R.W., and Kowalewski, M., 2018, Predation-facilitated preservation of echinoids in a tropical marine environment: *Palaios*, v. 33, p. 478–486.
- van Bemmelen, R.W., 1949, *The Geology of Indonesia*: The Hague, Government Printing Office, 732 p.
- van de Weerd, A., and Armin, R.A., 1992, Origin and evolution of the Tertiary hydrocarbon bearing basins in Kalimantan (Borneo), Indonesia: *American Association of Petroleum Geologists Bulletin*, v. 76, p. 1778–1803.
- Vecchio, E., and Hottinger, L., 2007, Agglutinated conical Foraminifera from the lower-middle Eocene of the Trentinara Formation (southern Italy): *Facies*, v. 53, p. 509–533.
- Veron, J.E.N., Devantier, L.M., Turak, E., Green, A.L., Kininmonth, S., Stafford-Smith, M., and Peterson, N., 2009, Delineating the coral triangle: *Galaxea, Journal of Coral Reef Studies*, v. 11, p. 91–100.
- Wallace, C.C., and Rosen, B.R., 2006, Diverse staghorn corals (*Acropora*) in high-latitude Eocene assemblages: implications for the evolution of modern diversity patterns of reef corals: *Proceedings of the Royal Society B*, v. 273, p. 975–982.
- Wakita, K., 2000, Cretaceous accretionary–collision complexes in central Indonesia: *Journal of Asian Earth Sciences*, v. 19, p. 739–749.
- Wakita, K., Miyazaki, K., Zulkarnain, I., Sopaheluwakan, J., and Sanyoto, P., 1998, Tectonic implications of new age data for the Meratus complex of South Kalimantan, Indonesia: *Island Arc*, v. 7, p. 202–222.
- Wanless, H.R., Tedesco, L.P., and Tyrrell, K.M., 1988, Production of subtidal tubular and surficial tempestites by Hurricane Kate, Caicos Platform, British West Indies: *Journal of Sedimentary Petrology*, v. 58, p. 739–750.
- Wells, J.W., 1976, Eocene corals from Eua, Tonga: U.S. Geological Survey Professional Paper, 640-G, 25 p.
- Werdaya, A.A., Wulansari, M., and Billing, I., 2013, Gross depositional environment model of the Berai Carbonate Formation and its implication for reservoir prospectivity, Barito Basin, South Kalimantan, Indonesia: *Proceedings of the Thirty-seventh Annual Convention & Exhibition, 15–17 May 2013, Jakarta, Indonesia, Indonesian Petroleum Association, IPA13-G-001*.
- Walker, S.E., 2007, Chapter 18: Traces of gastropod predation on molluscan prey in tropical reef environments, *in* Miller, W., ed., *Trace Fossils: Concepts, Problems, Prospects*: Amsterdam, Elsevier, p. 324–344.
- Wilson, M.E.J., 2015, Oligo-Miocene variability in carbonate producers and platforms of the Coral Triangle biodiversity hotspot: habitat mosaics and marine biodiversity: *Palaios*, v. 30, p. 150–168.
- Wilson, M.E.J., and Lokier, S.W., 2002, Siliciclastic and volcanoclastic influences on equatorial carbonates: insights from the Neogene of Indonesia: *Sedimentology*, v. 49, p. 583–601.
- Wilson, M.E.J., and Rosen, B.R., 1998, Implications of paucity of coral in the Paleogene of SE Asia: plate tectonics or centre of origin? *in* Hall, R., and Holloway, J.D., eds., *Biogeography and Geological Evolution of SE Asia*: Leiden, Netherlands, Backhuys Publishers, p. 165–195.
- Wilson, M.E.J., Chambers, J.L.C., Evans, M.J., Moss, S.J., and Nas, D.S., 1999, Cenozoic carbonates in Borneo: case studies from northeast Kalimantan: *Journal of Asian Earth Sciences*, v. 17, p. 183–201.
- Witts, D., Hall, R., Morley, R., and BouDagher-Fadel, M.K., 2012a, Stratigraphy and sediment provenance, Barito Basin, southeast Kalimantan: *Proceedings of the Thirty-fifth Annual Convention and Exhibition, May 2011, Indonesian Petroleum Association, IPA11-G-054*.
- Witts, D., Hall, R., Nichols, G., and Morley, R., 2012b, A new depositional model for the Tanjung Formation, Barito Basin, SE Kalimantan, Indonesia: *Journal of Asian Earth Sciences*, v. 56, p. 77–104.
- Witts, D., Davies, L., and Morley, R., 2014, Uplift of the Meratus complex: sedimentology, biostratigraphy, provenance and structure. *Proceedings of the Thirty-eighth Annual Convention and Exhibition, Indonesian Petroleum Association, IPA14-G-082*.
- Yasuhara, M., Huang, H.H.M., Reuter, M., Tian, S.Y., Cybulski, J.D., et al., 2022, Hotspots of Cenozoic tropical marine biodiversity, *in* Hawkins, S.J., Allcock, A.L., Bates, A.E., Byrne, M., Evans, A.J., et al., eds., *Oceanography and Marine Biology: An Annual Review*: v. 60, p. 243–300, <https://doi.org/10.1201/9781003288602-5>.
- Zonneveld, J.-P., 2001, Middle Triassic biostromes from the Liard Formation, British Columbia, Canada: oldest examples from the Mesozoic of NW Pangaea: *Sedimentary Geology*, v. 145, p. 317–341.
- Zonneveld, J.-P., and Gingras, M.K., 2014, *Sedilichnus*, *Oichnus*, *Fossichnus* and *Tremichnus*: small round holes in shells revisited: *Journal of Paleontology*, v. 88, p. 895–905.
- Zonneveld, J.-P., Moslow, T.F., and Henderson, C.M., 1997, Lithofacies associations and depositional environments in a mixed siliciclastic–carbonate coastal depositional system, upper Liard Formation, Triassic, northeastern British Columbia: *Bulletin of Canadian Petroleum Geology*, v. 45, p. 553–575.
- Zonneveld, J.-P., Gingras, M.K., Beatty, T.W., Bottjer, D.J., Chaplin, J.R., et al., 2012, Chapter 26. Mixed siliciclastic–carbonate systems, *in* Knaust, D., and Bromley, R.G., eds., *Trace Fossils as Indicators of Sedimentary Environments: Developments in Sedimentology*, v. 64, p. 807–833.
- Zonneveld, J.-P., Zaim, UY., Rizal, Y., Aswan, Boyer, D.M., Ciochon, R.L., Smith, T., Head, J., Wilf, P., and Bloch, J.I., 2024, Avian foraging on an intertidal mudflat succession in the Eocene Tanjung Formation, Asem Asem Basin, South Kalimantan, Indonesia: *Palaios*, v. 39, p. 67–96.

Accepted: 9 February 2024